In vitro characterization of telmisartan-derived compounds for selective peroxisome-proliferator activated receptor gamma (PPARγ) modulation

Dissertation to obtain the academic degree

Doctor rerum naturalium (Dr. rer. nat.)

submitted to the

Department of Biology, Chemistry and Pharmacy of Freie Universität Berlin

by

LENA HERBST

from Zittau

Houston/TX/USA 2012

This doctoral dissertation was supervised by Prof. Dr. Ulrich Kintscher and performed at the Center for Cardiovascular Research, University Hospital Charité in Berlin/Germany and completed at the Center for Nuclear Receptors and Cell Signaling, University of Houston in Houston/Texas/USA.

1. Evaluator: Prof. Dr. Ulrich Kintscher

2. Evaluator: Prof. Dr. Matthias Melzig

Disputation 08.06.2012

Table of contents

Page

Abstract

The peroxisome proliferator-activated receptor gamma (PPARγ) is the 'master regulator' of adipogenesis and adipocyte gene expression, and represents an effective pharmacological target for the treatment of insulin resistance and type 2 diabetes mellitus. Activation and modulation of its function plays an important role on overall treatment effectiveness and the side effect profile. Full PPARγ agonists, known as thiazolidinediones (TZDs) are currently used in the clinic. Unfortunately, they are associated with diverse side effects, like weight gain and an increased risk for cardiovascular events. To circumvent these side effects associated with the full agonism, intensive investigation was performed during the last years to create drugs which exhibit a combination of partial activation and selective receptor modulation.

Besides its blood pressure lowering property, the AT_1-receptor blocker telmisartan was shown to be a partial agonist of PPARγ with beneficial metabolic effects *in vitro* and *in vivo*. In previous work of our group, comprehensive structure-activity relationship studies were analyzed to reveal the importance of different parts of the telmisartan structure and various moieties. These studies were the foundation for the here presented thesis, investigating the biochemical and biological effects of the most promising structures. Telmisartan-derived PPARγ agonists (agonists 1, 2 and 3) with partial and full agonism were selected and analyzed for differential cofactor interaction, differential gene expression and glucose uptake. The degree of PPARγ activity was characterized by a differentiation assay performed with 3T3-L1 cells and by a PPARγ transactivation assay using Cos-7 cells transiently transfected with pGal4-hPPARγDEF, pGal5-TK-pGL3 and pRL-CMV. Interaction with the coactivators SRC1, PGC-1α and TRAP220, and the corepressor NCoR1 were determined using TR-FRET assays. Furthermore, microarray and qPCR analyses were performed to elucidate the gene expression profile of 3T3-L1 cells after stimulation with telmisartan-derived compounds. Moreover, glucose uptake was measured in mature adipocytes differentiated from 3T3-L1 cells after incubation with the indicated compounds and ^{3}H-labeled deoxy-glucose. Telmisartan-derived PPARγ agonists demonstrated a distinct cofactor interaction and mRNA expression profile from their corresponding control substances pioglitazone and telmisartan.

In addition, compounds with new modifications on the telmisartan structure were characterized for their PPARγ activation potential and cofactor interaction. These compounds contain a benzimidazole (agonists 4-5 and 4-6), benzothiophene (agonists 5-5 and 5-6) or benzofuran (agonists 6-5 and 6-6) moiety either at position 5 or 6 of the benzimidazole core structure. The shift of the benzofuran or benzothiophene moiety from position 5 to position 6 increased both, potency and efficacy, and also increased cofactor recruitment/ release. Conclusively, all new agonists demonstrated *in vitro* characteristics of SPPARγMs, and therefore, present promising results for future *in vivo* experiments.

Zusammenfassung

Der Peroxisomen-Proliferator-aktivierte Rezeptor gamma (PPARγ) ist der „*master regulator*“ der Fettzelldifferenzierung und Adipozytengenexpression, und repräsentiert ein effektives pharmakologisches Ziel für die Behandlung von Insulinresistenz und Diabetes Typ 2. Die Aktivierung und Modellierung der Rezeptorfunktion spielt eine bedeutende Rolle in der Gesamteffizienz der Behandlung und dem Nebenwirkungsprofil. Die volle Aktivierung von PPARγ durch Thiazolidindione (TZDs), welche in der Klinik eingesetzt werden, ist mit verschiedenen Nebenwirkungen, wie Gewichtszunahme und einem erhöhtem Risiko für Herz-Kreislauf Erkrankungen, verbunden. In den letzten Jahren wurde intensive Forschung durchgeführt, um Medikamente mit verbesserter Wirkung und Verträglichkeit herzustellen, welche PPARγ partiell und selektiv aktivieren und modulieren.

Neben seiner blutdrucksenkenden Wirkung ist der AT_1-Rezeptorblocker Telmisartan auch ein partieller Agonist für PPARγ mit vielversprechenden metabolischen Eigenschaften *in vitro* und *in vivo*. In vorhergehenden Arbeiten unserer Gruppe wurden umfangreiche Studien zur Struktur-Wirkbeziehung durchgeführt, um die Bedeutung der Struktureinheiten von Telmisartan und unterschiedlicher Seitengruppen im Hinblick auf ihre PPARγ aktivierenden Effekte aufzudecken. Diese Studien lieferten die Grundlage für diese Arbeit, bei der biochemische und biologische Effekte der interessantesten Substanzen untersucht wurde. Zunächst wurden unterschiedliche telmisartanbasierte PPARγ Agonisten (Agonist 1, 2 und 3) ausgewählt und bezüglich selektiver Kofaktorwechselwirkungen, differentieller Genexpression und Glukoseaufnahme untersucht. Der Grad der PPARγ Aktivität wurde mit Hilfe eines Differenzierungsassays unter Verwendung von 3T3-L1 Zellen, und eines PPARγ Transaktivierungsassays mit Cos-7 Zellen, welche transient mit pGal4-hPPARgDEF, pGal5-TK-pGL3 und pRL-CMV transfiziert wurden, ermittelt. Wechselwirkungen mit den Koaktivatoren SRC1, PGC-1α und TRAP220, und dem Korepressor NCoR1 wurden mit TR-FRET untersucht. Microarray und qPCR Analysen wurden durchgeführt, um das Genexpressionsprofil von 3T3-L1 Zellen nach Stimulation mit telmisartanbasierten Substanzen zu ermitteln. Außerdem wurde die Glukoseaufnahme von ausgereiften Adipozyten der 3T3-L1 Zelllinie nach Inkubation mit den Substanzen und ^{3}H-markierter Deoxyglukose

gemessen. Die telmisartanbasierten Substanzen zeigten, im Vergleich zu den Kontrollen Pioglitazon und Telmisartan, abweichende Kofaktorwechselwirkungen und ein differenzielles mRNA-Expressionsprofil.

Desweiteren wurden Substanzen mit neuen Modifizierungen der Telmisartanstruktur bezüglich ihrer PPARγ-aktivierenden Eigenschaft und Kofaktorwechselwirkungen charakterisiert. Diese Substanzen haben eine Benzimidazol (Agonist 4-5 und 4-6), Benzothiophen (Agonist 5-5 und 5-6), oder Benzofuran (Agonist 6-5 und 6-6) Seitengruppe entweder an Position 5 oder Position 6 des Benzimidazolgrundkörpers. Die Verlagerung der Benzothiophen oder Benzofuran Seitengruppe von Position 5 nach Position 6 verstärkte sowohl Potenz und Effizienz, als auch Kofaktorrekrutierung. Alle neuen telmisartanbasierten Substanzen zeigten die *in vitro* Eigenschaften selektiver PPARγ Modulatoren, und sind daher vielversprechende Substanzen für zukünftige *in vivo*-Experimente.

Abbreviations

ACE	angiotensin-converting enzyme
ADD1/SREBP1c	adipocyte determination- and differentiation-dependent factor 1/ sterol-regulatory element binding protein 1c
AT_1	Angiotensin-II-Receptor-Subtype-1
ATP	adenosine triphosphate
AUC	area under the curve
C/EBPs	CCAAT-enhancer-binding proteins
CLOCK	Circadian Locomotor Output Cycles Kaput
CoRNR	corepressor/ nuclear receptor
DR-1	direct repeat 1
ER	endoplasmatic reticulum
FA	fatty acids
HFD	high fat diet
HIF-1α	hypoxia-inducible factor-1α
HODE	hydroxy-octadecadienoic acid
IGF-1	Insulin-like Growth Factor-1
IL-6	interleucin-6
IKK/NF-κB	IκB kinase/ nuclear factor-κB
iNOS	inducible nitric oxide synthase
JNK1	c-Jun N-terminal protein kinase 1
MA	microarray

NCoR	nuclear receptor corepressor
PPARs	peroxisome proliferator-activated receptors
SMRT	silencing mediator of retinoic acid and thyroid hormone receptor
TG	triglyceride
TNF-α	tumor necrosis factor- α

List of figures

List of tables

1 Introduction

1.1 Energy metabolism and glucose homeostasis

The ingestion of food provides the fundamental source of energy for basic cellular maintenance, physical activity and adaptive thermogenesis. To assure constant function of the cells, energy must be supplied to cells and tissues continuously. It can either be provided directly from ATP or indirectly from the cellular respiration of glucose, fatty acids, ketone bodies and other organic molecules. These molecules are ultimately obtained from food, or during fasting state, from the glycogen, fat and protein stored in the body. When cellular ATP concentrations rise because more energy is available than can be immediately used, ATP production is inhibited and glucose is converted into glycogen and fat. The major fuel depots are represented by the liver, adipose tissue and skeletal muscle [1]. In time of energy demand, stored substrates can be interconverted to meet the energy needs of the body (figure 1). If possible, the body tends to conserve its protein reserves and to draw on fat reserves preferentially, to keep muscle mass.

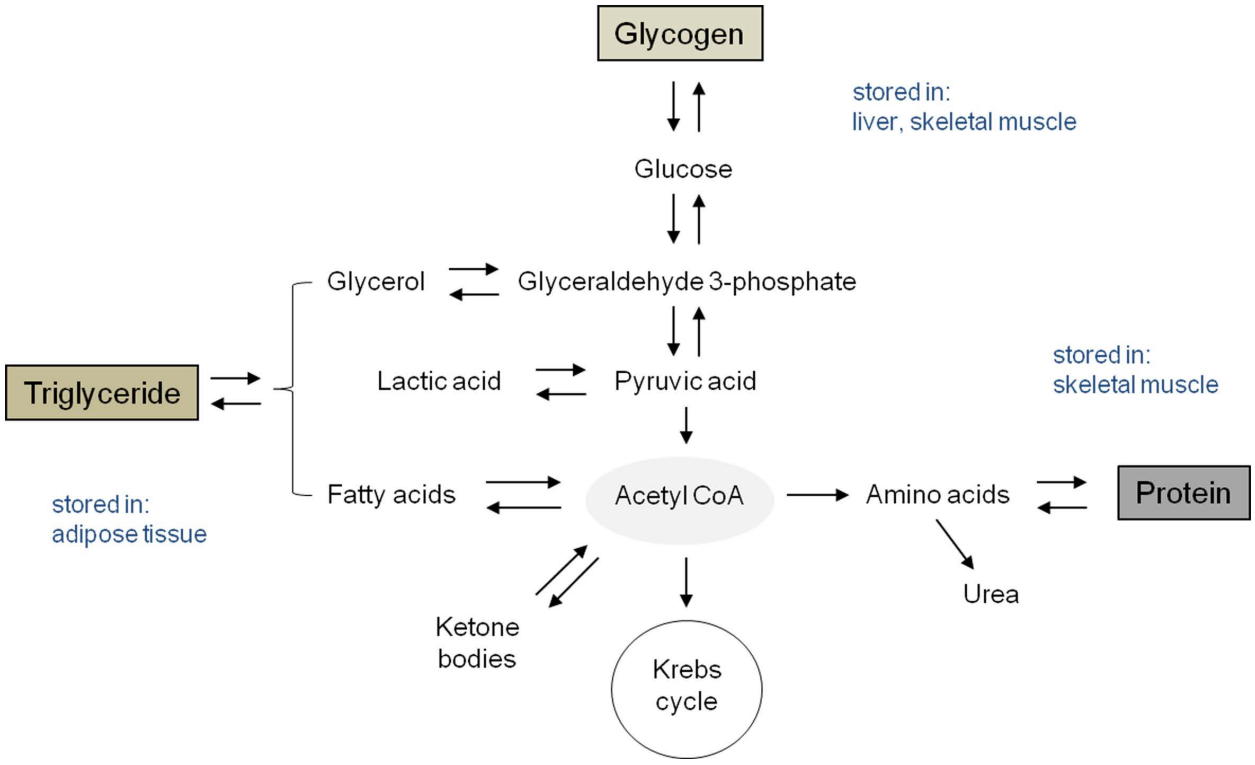

Figure 1: Interconversion of glycogen, fat and protein.

Fat represents the major form of energy storage in the body. Storage of fuel in form of triglycerides is advantageous over storage in form of glycogen, because triglycerides release four to five times more energy when oxidized than equivalent amounts of glycogen. Furthermore, lipids are stored very compactly to keep body weight in an adequate range. Most tissues can use fatty acids as their primary, if not sole, source of metabolic energy. Depending on differences in cellular enzyme content, organs differ in the metabolic fuels they prefer as substrates for energy production. Resting skeletal muscle for example, use fatty acids as their favored energy source. In contrast, the brain has an almost absolute requirement for glucose. [2].

Metabolic fuels are distributed among tissues via the bloodstream. Maintaining constant levels of circulating energy substrates is a sophisticated process regulated by the endocrine system. Insulin and glucagon, released by pancreatic cells, play a prominent role in metabolic homeostasis. The rise in blood glucose level after a meal stimulates beta cells to secrete insulin and inhibits the secretion of glucagon from alpha cells. Insulin decreases glucose production from the liver and increases glucose uptake as well as utilization and storage in fat and muscle tissue. Insulin also stimulates cell growth and differentiation, and promotes the storage of substrates in fat, liver and muscle by stimulating lipogenesis, glycogen and protein synthesis. Simultaneously, insulin inhibits catabolism of these molecules. On the other hand, glucagon is the counter-regulating hormone to increase the blood glucose level, when it falls under the normal range of about 4 to 7 mmol/liter [3].

1.2 Adipose tissue

Adipose tissue plays a central role in whole body energy homeostasis and is an important endocrine organ [4]. Adipose tissue is specialized connective tissue that is widely distributed within the body. In humans, it is located around internal organs (visceral fat) and most prevalently, as deposits beneath the skin (subcutaneous fat). Adipose tissue is composed of several cell types, with the highest percentage of cells being adipocytes. Other cell types that contribute to the structural integrity include fibroblasts, macrophages and pre-adipocytes, which are not yet filled up with lipid [5].

Adipocytes are considered to originate from fibroblast-like precursor cells that differentiate into adipocytes under the appropriate stimulatory conditions [6, 7], described later. Some adipocytes appear during embryonic development, and their number increases greatly after birth. The size of adipose tissue mass is a function of both adipocyte number and size. An increase in adipose tissue mass can occur by hyperplastic growth, which is an increase in cell number and occurs primarily by mitotic division in precursor cells. Additionally, adipose tissue mass can also increase by hypertrophic growth, which is an increase in the size of adipocytes. This increase in size primarily takes place by lipid accumulation within the cell. Once new adipocytes are formed, they remain throughout life. Only a reduction in size is possible [1].

Adipose tissue contains many small blood vessels. This blood supply provides sufficient support for the active metabolism of adipocytes [8]. The primary role of adipocytes is to synthesize and store triglycerides during periods of caloric excess and to mobilize these energy depots in form of free fatty acids and glycerol during periods of nutritional deprivation. Adipose tissue produces and secretes adipocytokines acting on the central nervous system and peripheral tissues to modulate lipid and carbohydrate metabolism [9–11]. Adipocytokines include e.g. leptin, adiponectin, TNF-α and resistin which are involved in the regulation of feeding behavior, inflammation and energy metabolism [12], [13]. The differentiation of adipocytes is a complex process accompanied by coordinated changes in morphology, hormone sensitivity and gene expression. These changes are regulated by several transcription factors, activated at different stages of adipocyte differentiation, like C/EBPs, PPARγ and ADD1/SREBP1c. Not only adipogenic transcription factors but also hormones and other secreted proteins affect adipocyte differentiation. For example, insulin and IGF-1 are well known to play a key role in adipocyte differentiation *in vivo* and *in vitro* [14].

1.3 Obesity and related health conditions

1.3.1 Prevalence

During the last decades, a shift towards an increase in body weight has been reaching global epidemic proportions. The rising process reflects the profound changes in society and in behavioral patterns of communities over years. Economic growth, modernization, urbanization and globalization of food markets are just some of the forces thought to underlie the epidemic. Increased consumption of more energy-dense, nutrient-poor foods with high levels of sugar and saturated fats, combined with reduced physical activity, have led to obesity rates that have risen three-fold or more since 1980 in some areas of North America, the United Kingdom, Eastern Europe, the Middle East, the Pacific Islands, Australasia and China. The obesity epidemic is not restricted to industrialized societies. Moreover, its increase is often faster in developing countries than in the developed world. Often coexisting in developing countries with under-nutrition, obesity is a complex condition with serious social and psychological dimensions, affecting all ages and socioeconomic groups. Obesity was identified as a major contributor to the global burden of chronic disease and disability. The WHO reported 2003 more than one billion adults worldwide as overweight with at least 300 million of them as clinically obese [15, 16].

The prevalence of overweight and obesity is commonly assessed by using a measurement called the body mass index (BMI), defined as the weight in kilograms divided by the square of the height in meters (kg/m²). The WHO classifies people with a BMI over 25 kg/m² as overweight and people with a BMI over 30 kg/m² as obese.

During the past 22 years there has been a dramatic increase in obesity in the United States, shown in figure 2. In 2008, about 32.2% adult men and 35.5% adult women were considered to be obese in the US [17]. In 2010, data collected through the Behavioral Risk Factor Surveillance System by the Center for Disease Control and Prevention show 12 U.S. states (Alabama, Arkansas, Kentucky, Louisiana, Michigan, Mississippi, Missouri, Oklahoma, South Carolina, Tennessee, Texas, and West Virginia) with a prevalence of obesity of 30% or higher, and no state had a prevalence of less

than 20% [18]. Ten years before, all states showed a prevalence rate of less than 25%. Similar trends have been recognized for European countries [19, 20].

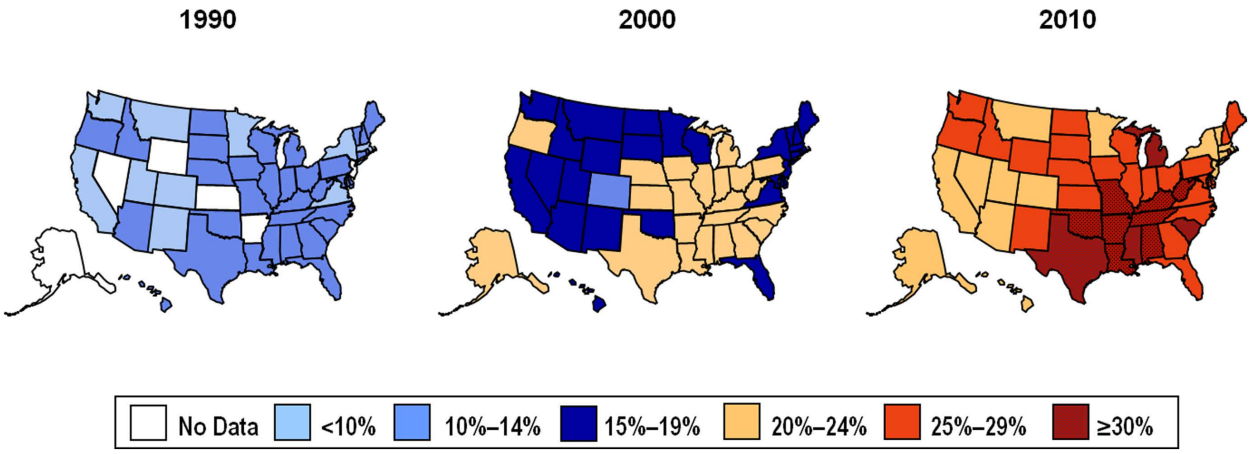

Figure 2: Obesity trends among U.S. adults from 1990 to 2010. Percent of obese with a BMI ≥ 30 [18].

Importantly, obesity seems to be a burden of much younger age, which is linked with a high number of obese children and adolescents. In 2010, the prevalence of obesity in children and adolescents in the US was 16.9% [21]. Hence, childhood obesity is already epidemic in some areas in the world and on the rise in others. Worldwide, about 17.6 million children under five were estimated to be already overweight in 2003 [16].

Only a comprehensive approach in public health policy can offer any realistic prospect of averting an accelerating epidemic health development [22].

1.3.2 Metabolic Syndrome

Obesity is the direct result of an imbalance between energy intake and energy expenditure. Although adipocytes are specifically designed to store energy and easily fill up with fat, the morphological changes associated with adipose tissue growth are not without consequences for the organism as a whole [23].

The excessive fat accumulation in adipose tissue, liver and other organs strongly predispose to the development of metabolic changes that increase overall morbidity risk. The non-fatal, but debilitating health problems associated with obesity include respiratory difficulties, chronic musculoskeletal problems, skin problems and infertility.

More life-threatening problems fall into four main areas:

- cardiovascular diseases (hypertension, myocardial infarction and stroke) [24],
- conditions associated with insulin resistance and diabetes mellitus type 2 [25],
- gallbladder disease [26],
- certain types of cancer, especially hormonally related and large-bowel cancers [27].

Visceral obesity, which is characterized by excess fat storage in and around the abdomen, is the primary cause for metabolic abnormalities. The expanded fat mass has an accelerated lipolytic activity, and releases increased amounts of free fatty acids (FFA) and pro-inflammatory cytokines (e.g. IL-6 and TNFα) into the circulation. Consequently, due to the missing suppressive effect of insulin hepatic gluconeogenesis becomes active. The resulting high blood glucose levels directly affect insulin release from ß-cells, leading finally to impaired insulin secretion, hyperglycemia, insulin resistance, and accumulation of triglycerides in peripheral tissue [28, 29]. In most cases, mild insulin resistance can be compensated by an increase in insulin secretion [30]. However, under consistent impaired glucose tolerance or aggravation, ß-cell dysfunction can occur and manifest into diabetes mellitus type 2 [31]. As mentioned before, adipocyte tissue not only expands in mass, but also in adipocyte size. The hypertrophic adipocytes create regional areas of microhypoxia which leads to the increased expression of HIF-1α and both, downstream activation of JNK1 and IKK/NF-κB pathways as well as ER stress in adipocytes. The subsequent inflammatory response includes increased cytokine and chemokine release and recruitment of macrophages, which themselves release pro-inflammatory cytokines and induce insulin resistance via paracrine and endocrine effects [32].

Furthermore, insulin contributes to the formation of hypertension by activating the sympathetic nervous system and inducing sodium reabsorption in the kidneys. High levels of circulating FA, pro-inflammatory and pro-thrombotic (e.g. PAI-1) adipocytokines, and low levels of HDL cholesterol increase the risk for cardiovascular diseases [28]. An overview of the pathophysiologic interaction between adipose tissue and other metabolic relevant tissues underlying the metabolic syndrome is presented in figure 3.

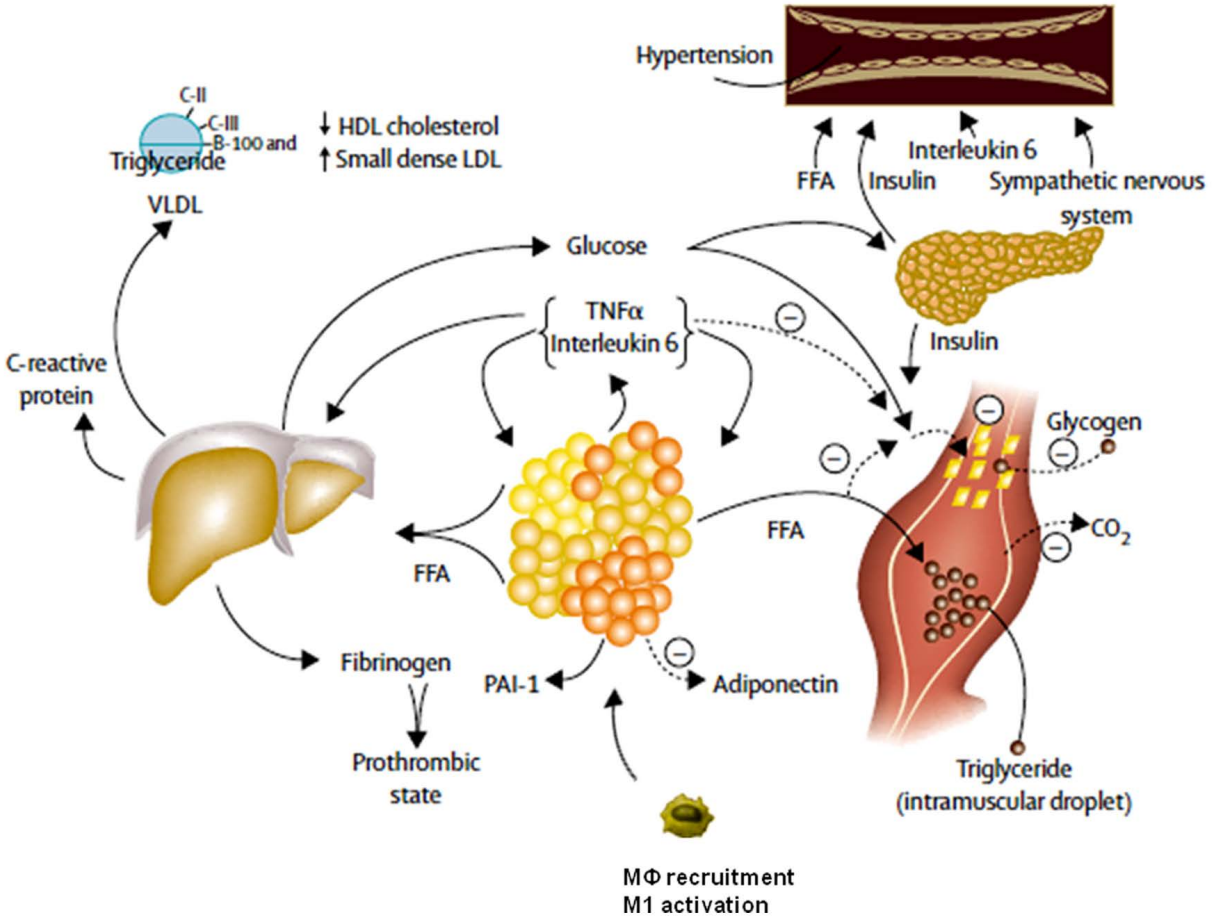

Figure 3: Pathophysiologic interaction responsible for manifestation of the metabolic syndrome [28 modified]. VLDL, very low-density lipid; HDL, high-density lipid; LDL, low-density lipid; FFA, free fatty acid; PAI-1, plasminogen activator inhibitor 1; MΦ, macrophage.

A combination of the above named medical conditions that come together in a single individual is termed metabolic syndrome or syndrome X. The criteria of diagnosis can be slightly different depending on the group of experts doing the defining.

The U.S. National Cholesterol Education Program's (NCEP) Adult Treatment Panel (ATP) III (2001), for example, requires at least three of the following criteria to set the diagnosis [33]:

- blood pressure ≥ 130/85 mmHg
- central obesity: waist circumference ≥ 102 cm (male), ≥ 88 cm (female)
- dyslipidaemia: TG ≥ 1.695 mmol/l (150 mg/dl)
- dyslipidaemia: HDL-Cholesterol < 40 mg/dl (male), < 50 mg/dl (female)
- fasting plasma glucose ≥ 6.1 mmol/l (110 mg/dl)

The World Health Organization criteria (1999) in contrast, require presence of diabetes mellitus, impaired glucose tolerance, impaired fasting glucose or insulin resistance, and two of the following criteria:

- blood pressure: ≥ 140/90 mmHg
- dyslipidaemia: TG ≥ 1.695 mmol/l and HDL-Cholesterol ≤ 0.9 mmol/l (male), ≤ 1.0 mmol/l (female)
- central obesity: waist:hip ratio > 0.90 (male); > 0.85 (female), and/or body mass index > 30 kg/m^2
- microalbuminuria: urinary albumin excretion ratio ≥ 20 mg/min or albumin:creatinine ratio ≥ 30 mg/g

This variability leads to confusion and absence of comparability between studies. Nevertheless, there is agreement that the metabolic syndrome is a major public health challenge worldwide and consistent evidence stresses the need for intervention [34].

1.3.3 Treatment

The metabolic syndrome represents a complex disease which acquires a multi-factorial therapy. Most important is the implementation of healthy lifestyle changes to reduce body weight. It should include a balanced diet and an increase in physical activity. Studies indicate that moderate weight losses (10%) and even short periods of exercise (30 minutes per day) already have enormous effects on glucose levels and lower cardiovascular risk factors, such as blood pressure and lipids [35, 36]. But, if lifestyle changes alone don't show beneficial improvement of the symptoms, a pharmacological therapy has to be applied [37].

Several drugs are available to specifically target selective conditions of the metabolic syndrome. For example, lipid resorption by the gastrointestinal tract can be prevented by lipase inhibitors (e.g. Orlistat) [38], statins (e.g. Simvastatin, Lovastatin) lower cholesterol levels [39], and administration of AT_1-receptor antagonists (e.g. Telmisartan, Losartan), ACE inhibitors (e.g. Ramipril, Captopril) or Calcium antagonists (e.g. Verapamil) lower blood pressure [40, 41]. However, the key strategy to treat the metabolic syndrome is the improvement of insulin sensitivity to prevent the manifestation of diabetes mellitus type 2. It can be achieved by treatment with Metformin which is used to block gluconeogenesis in the liver and triglyceride synthesis [42]. Another important group of drugs to increase insulin sensitivity are thiazolidonediones (TZDs: e.g. Pioglitazone, Rosiglitazone). They reveal their beneficial effect via activation of the nuclear receptor PPARγ [43].

Considering the high complexity of the metabolic syndrome and associated risk factors, a combination of different therapies is often necessary for the treatment [44]. Unfortunately, these combinational therapies are not able to achieve beneficial effects for all components of the metabolic syndrome and bear the risk for more side effects and negative drug-drug interaction. Hence, latest research focused on a more general approach to meet the requirement for appropriate intervention. Adipose tissue is in the center of these investigations.

1.4 Peroxisome Proliferator-Activated Receptors (PPARs)

1.4.1 PPAR family and structure

PPARs are ligand-activated transcription factors and belong to the superfamily of nuclear hormone receptors (NRs) [45]. Their name derived from the ability of chemical substances (e.g. fibrate hypolipidemic drugs and xenobiotics), later refered as peroxisome proliferators (PP), to increase the size and number of hepatic peroxisomes in rodents. Furthermore, these agents activated transcription of genes involved in peroxisomal ß-oxidation by the expression of a receptor, termed PPARα [46]. Subsequent cloning events identified more members of this family, but only activation of PPARα resulted in peroxisome proliferation in rodents [47].

There are three PPAR subtypes which are classified by the committee (V. Laudet, J. Auwerx, J.-A. Gustafsson, W. Wahli) for the nomenclature of NRs: NR1C1 [**PPARα**], NR1C2 [**PPARδ**/ PPARß] and NR1C3 [**PPARγ**] [48].

All PPARs share the molecular domain structure of most NRs. They are composed of an N-terminal domain (NTD) with ligand-independent activation function, a DNA-binding domain (DBD), a hinge region and a ligand-binding domain (LBD) with ligand-dependent activation function (figure 4). DNA-binding occurs through two highly conserved zinc fingers in the DBD, and requires dimerization with members of the retinoid X receptor (RXR) family. Heterodimerization between PPARs and RXRs is ligand-independent and relies on interfaces in the DBD and the LBD between the two receptors. Transactivation by the PPARs can be mediated through both the ligand-dependent AF2 region in the highly conserved LBD and through the ligand-independent AF1 region in the NTD. A very mutable hinge region connects DBD and LBD, and is responsible for protein flexibility [49, 50].

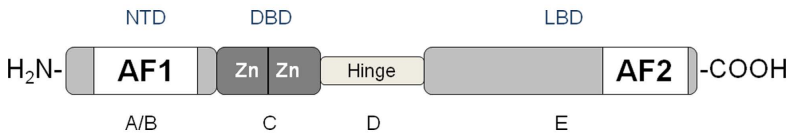

Figure 4: Domain structure of NRs [51 modified]. NTD, N-terminal domain; DBD, DNA-binding domain; LBD, ligand-binding domain; AF, activation function.

PPAR subtypes are located on different chromosomes. They are highly conserved between men and mouse, and their DBD and LBD protein sequences share a high degree of homology among the subtypes (figure 5) [52, 53].

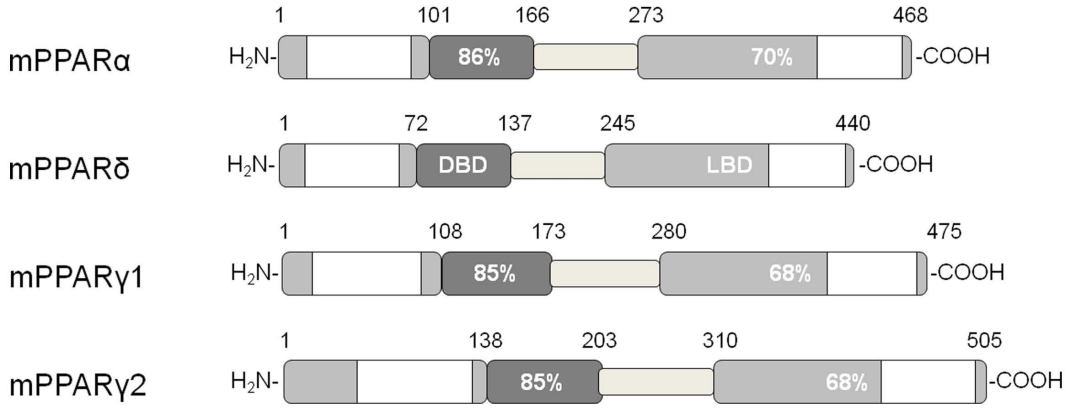

Figure 5: Domain structure of murine PPAR subtypes [53 modified]. Comparisons among the different domains are expressed as percent amino acid identity, using PPARδ as a reference. DBD, DNA-binding domain; LBD, ligand-binding domain.

In human and mouse, PPARγ exhibits three isoforms by alternate promoter usage and splicing. While PPARγ1 and PPARγ2 differ in additional 28 (mouse) and 30 (human) amino acids at the NTD of the PPARγ2 protein [54], PPARγ3 mRNA encodes the same protein like PPARγ1, but is controlled by an alternative promoter [55].

1.4.2 Mechanism

The PPAR:RXR heterodimer binds to specific target sites either within intragenic regions or the proximal promoter region of target genes [56]. The consensus binding motif is called peroxisome proliferator response element (PPRE) and represents a DR1 element consistent of two hexanucleotide direct repeats of the sequence 5'-AGGTCA-3' separated by a single nucleotide spacer [57, 58]. The orientation of the receptor binding is favored by the interaction between the hinge region of PPAR and the moderately conserved 5' flanking sequence of the PPRE [56]. An illustration of the binding mode is shown in figure 6.

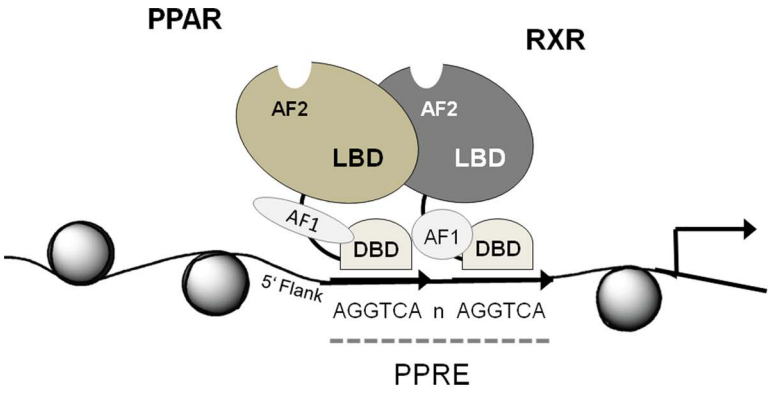

Figure 6: Mode of DNA-binding of the PPAR:RXR heterodimer to the PPRE. PPAR is occupying the 5' and RXR is occupying the 3' half-site of the PPRE. NTD, N-terminal domain; DBD, DNA-binding domain; LBD, ligand-binding domain; AF, activation function; PPRE, peroxisome proliferator response element.

The activity of the receptor complex is controlled by ligand binding and cofactor interactions, and can be further modulated by post translational modifications. PPARs are activated by fatty acids and fatty acid derivatives, whereas RXR is activated by fatty acids or 9-cis retinoic acid [59, 60]. Ligand binding to the AF2 domain of PPAR activates the receptor by inducing a conformational change of helix 12 of the LBD and generating a charge clamped hydrophobic cavity. In the inactive state, helix 12 enables interaction with conserved CoRNR-box motifs (LXXI/HIXXXI/L) of corepressors which inhibit transcriptional activity [61]. After ligand binding, corepressors dissociate from the LBD

and give room for the co-activator complex. Recruitment of the coactivator complex is mediated by a conserved LXXLL motif which is present in the majority of the coactivators [62].

The cofactor complex involves a large number of proteins with multiple enzymatic activities to control transcription. Mechanisms of action include: interaction with chromatin via histone acetyltransferases (HAT) or histone methyltransferases (HMT), recruitment of the polymerase machinery, and crosstalk with other transcription factors. Cofactors not only transactivate, but also transrepress the activity of target genes. Examples for cofactors which mediate PPAR's repressive activity are SMRT and NCoR. Both factors contain histone deacetylase (HDAC) activity to enforce a tight chromatin structure and therefore repress gene transcription [63]. The exchange of the corepressor complex with a coactivator complex is mediated by corepressor associated F-box/ WD-40 proteins (transducin ß-like 1 (TBL1) and TBL1-related protein 1 (TBLR1)) by ligand-dependent recruitment of the ubiquitin/ 19S proteasome system [64].

As mentioned before, PPARs can be activated ligand-dependent via the AF2 region, but also via the AF1 region [65]. However, conditions of non-stimulated activation are difficult to distinguish from binding and activation of endogenous ligands, since available concentrations of these ligands and there potency for PPAR activation are still unknown [66]. Nevertheless, presence of a PPAR ligand stabilizes the coactivator complex and thereby increases transactivation. A simplified overview of ligand-dependent and -independent PPAR activation is demonstrated in figure 7. Several members of different coactivator families are known to interact with PPARs [67]:

- Steroid receptor coactivator (SRC) family
  (HAT activity)
- Cyclic-AMP responsive element binding (CREB) protein (CBP)/ p300 family
  (HAT activity)
- PPARγ coactivator-1 (PGC-1) family
  (recruitment of proteins with HAT activity)
- Mediator complex
  (recruitment of RNA polymerase II machinery)

Due to a spatiotemporally orchestrated assembly of cofactors, the complex can act in a highly specific manner. Furthermore, post translational mechanisms, like phosphorylation, ubiquitination and sumoylation influence the function of PPARs [68].

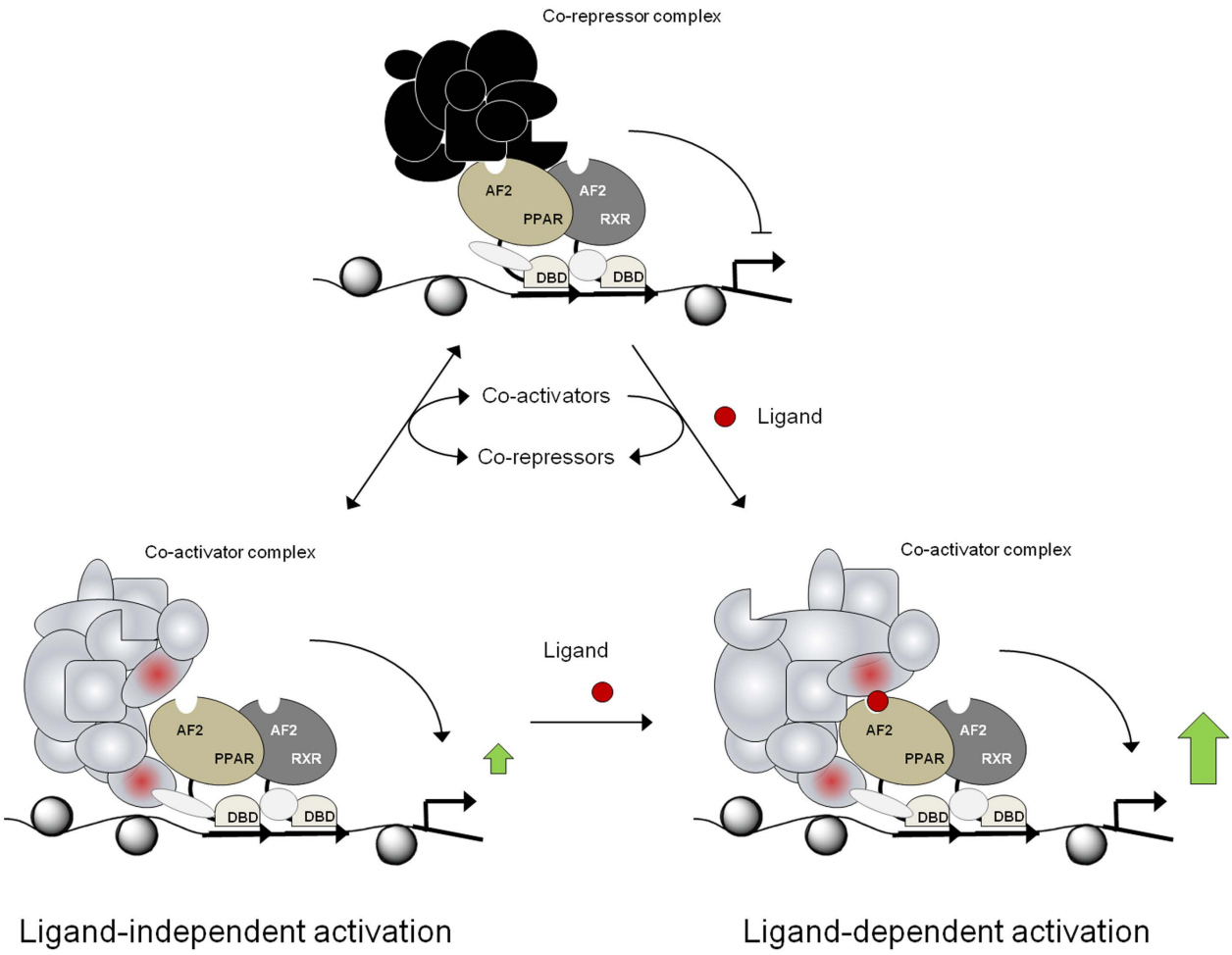

Figure 7: Ligand-dependent and -independent activation of PPAR target genes [66 modified]. The PPAR:RXR heterodimer can associate with corepressor and coactivator complexes. Binding of a ligand dramatically increases transactivation.

1.4.3 Function

PPARs are ‘lipid sensors’ and play key roles in the regulation of lipid metabolism, inflammation, development and differentiation [69]. The three PPAR subtypes share basic mechanistic functions due to an overlapping group of activating ligands, but also

have highly unique functions because of selective modulation by e.g. cofactors, as described above, and differential expression profiles [66, 69, 70].

PPARα is predominantly expressed in the liver, but can also be found to a lesser extent in kidney, heart and muscle [71]. In response to prolonged fasting, increased amounts of FAs are released from adipose tissue and transported into the liver, where they activate PPARα. Controlling FA oxidation and generating ketone bodies as an energy source for peripheral tissue is most crucial in PPARα function [72]. Furthermore, plasma triglyceride levels are decreased, and HDL levels are increased, resulting in improved insulin sensitivity [73]. Consequently, PPARα-null mice are unable to meet energy demands during fasting and develop hepatic steatosis, hypoglycemia and severe hypoketonemia [72]. PPARα regulates the peripheral circadian oscillator of the liver and itself is controlled by the core-circadian protein CLOCK [74, 75].

PPARδ is ubiquitously expressed, with highest levels in placenta and intestine [71]. It plays an important role as an activator of FA oxidation and energy homeostasis in skeletal muscle, heart, pancreatic ß-cells and adipose tissue [76, 77]. Moreover, PPARδ mediates glucose oxidation in the heart and glucose uptake and storage in the muscle. Activation with synthetic PPARδ ligands regulates glucose-stimulated insulin secretion in pancreatic ß-cells, suppresses macrophage derived inflammation [78], and increases formation of type 1 fibers in muscle tissue [79]. Furthermore, it is involved in wound healing by enhancing keratinocyte survival [80].

Highest levels of PPARγ are found in adipose tissue, where it is necessary for differentiation and function of white and brown adipocytes. PPARγ is directly involved in activation of the entire adipocyte gene program, and therefore termed as the ‘master regulator’ of adipogenesis [81, 82]. Ectopic expression of PPARγ in fibroblasts induces an adipocyte-specific gene expression that trigger morphological differentiation and lipid droplet formation, which involves a transcriptional cascade with members of the CAAT/ enhancer binding protein (C/EBP) family [83, 84]. Furthermore, PPARγ activation is associated with FA transport, and triglyceride synthesis and breakdown. Pertinent with that, there is a redistribution of fat mass, from visceral to healthier subcutaneous fat. Decreased production of adipocytokines, (like TNF-α and resistin), which cause insulin

resistance [85, 86], and increased expression of the anti-diabetic protein adiponectin, result in improved whole-body insulin sensitivity [87].

Homozygous PPARγ-null mice die during embryogenesis, due to placental insufficiency, but can be rescued by tetraploid chimeras with wild type placentas. However, rescued mutants still exhibit a lethal pathologic phenotype with hepatic steatosis and complete lack of adipose tissue [88]. Conditional PPARγ knock-out in the muscle causes secondary insulin resistance in liver and adipose tissue [89]. Hence, PPARγ plays an important role in maintaining glucose homeostasis. *In vitro*, embryonic fibroblasts derived from PPARγ-null fetuses fail to differentiate into adipocytes [90]. Consistent with these observations, dominant-negative PPARγ mutations in humans lead to partial lipodystrophy, hypertension and insulin resistance [91].

While PPARγ2 is exclusively expressed in white adipose tissue, PPARγ1 is more abundant and can also be found in small and large intestine, kidney, liver, spleen and muscle [92]. PPARγ1 promotes various anti-inflammatory capacities. It inhibits the expression of pro-inflammatory proteins, like iNOS, TNF-α, IL-6 and IL-1ß, and mediates the differentiation of alternatively activated macrophages, with preference for the IL-10 producing M2 type [93, 94].

Overall, PPARγ activation seems to have beneficial effects on the main features of the metabolic syndrome and therefore, is an area of active investigation with great effort during the last years.

1.5 PPARγ activation

1.5.1 Endogenous ligands

A variety of FAs (preferentially polyunsaturated FAs) and eicosanoids bind PPARγ. Examples are arachidonic acid derivatives, like 15-Deoxy-Δ 12,14-Prostaglandin J2 (PGJ_2), and linolic acid derivatives, like 9-HODE or 13-HODE [69, 95]. Most of these ligands bind PPARγ with low affinity and their concentration in target cells might be insufficient for activation of the receptor [96]. An alkyl phospholipid, which is an

oxidation product of LDL, was demonstrated to be a high affinity ligand for PPARγ and is discussed to play a role in PPARγ expression in atherosclerotic plaques [97]. Moreover, cellular 5-hydroxytryptamine (serotonin) metabolites were identified as natural ligands and able to activate PPARγ in adipocytes and macrophages [98]. Concerning the pivotal function of PPARγ during adipogenesis the presence of an unidentified ligand with high affinity is most likely [99]. The enzymes xanthine oxidoreductase and retinol saturase seem to be involved in the production of this endogenous ligand [100, 101]. However, the concrete underlying mechanism is not yet understood [59].

1.5.2 Synthetic ligands

TZDs, also known as glitazones, are synthetic ligands for PPARγ, introduced in the late 1990s. They demonstrate a class of drugs used for the treatment of diabetes mellitus type 2. TZDs exert beneficial effects on the lipid profile either by promoting triglyceride storage in adipose tissue, or by enhancing adiponectin production. Moreover, peripheral insulin resistance is reduced and pro-inflammatory cytokine levels decreased [102, 103]. There are different members of this class: troglitazone, rosiglitazone and pioglitazone, with slightly different characteristics.

Troglitazone (Rezulin®) became withdrawn from the market in the year 2000 due to severe hepatotoxicity [104]. Next generation glitazones were rosiglitazone (Avandia®) and pioglitazone (Actos®). They are either used in monotherapy or in combination with metformin or sulfonylurea. Rosiglitazone moderately decreases TG levels, while pioglitazone increases HDL levels [105]. However, glitazones are associated with certain side effects, like weight gain, fluid retention, edema formation, fractures, or an increased risk for myocardial infarction [106–108]. In 2011, rosiglitazone was withdrawn from the European market due to an increased risk of cardiovascular events, and put under selling restriction in the U.S. In the same year, Germany and France suspended the sale of pioglitazone, because of its association with bladder cancer during long-term treatment [109].

Several synthetic ligands for PPARγ have been developed within the last decade. Some examples are L-tyrosine derivatives [110], FMOC-L-Leucine [111], and indomethacin and other non-steroidal anti-inflammatory drugs [112].

1.5.3 Selective PPARγ Modulators (SPPARγMs)

Intensive investigation was performed in order to identify drugs with a better side effect profile. First strategies focused on the development of more potent and specific activators of PPARγ, to reduce unspecific interaction by decreasing the dose during treatment. Unfortunately, strong activation exacerbated unwanted side-effects [113]. In contrast, genetically reduced expression levels of the receptor improved insulin sensitivity. Heterozygous PPARγ-KO mice were shown to be more insulin sensitive than WT mice [114]. These observations guided the development of partial activators. They are characterized by a lower efficiency at saturating concentrations than a full agonist, like pioglitazone [115].

Further research on PPARγ agonists gained from parallel works performed on the estrogen receptor and its tissue-specific modulation. For example, the estrogen receptor ligand tamoxifen behaves like an agonist in bone and the cardiovascular system, but reveals antagonistic effects in breast tissue [116]. The principle of this mode of action is based on selective modulation of receptor conformation by natural or synthetic ligands, in general called ‘selective nuclear receptor modulators’. Depending on their chemical structure, these modulators induce a specific allosteric conformational change of the receptor resulting in selective recruitment of cofactors critical for the specific regulation of target gene transcription. The available set of cofactors varies by cell type and cell state and adds an additional regulatory level to the modulation of receptor activity [117, 118].

Hence, ideal modulators for PPARγ would be potent and highly efficacious inducers for anti-diabetic gene expression with low potency or low maximal activity of genes promoting adipose generation, loss of bone mineral density, fluid retention and congestive heart failure [119].

Newly synthesized drugs combine partial activation and selective modulation of PPARγ to achieve best therapeutic outcome (improving insulin sensitivity, decreasing dyslipidemia and inflammation), while preventing negative side effects.

FMOC-L-Leucine is a PPARγ agonist with very low potency, but similar efficacy than rosiglitazone. It induces selective co-factor recruitment, leading to reduced adipogenesis and improved glucose tolerance and insulin sensitivity in diet-induced glucose-intolerant mice and diabetic db/db mice [111].

In 2006, halofenate was demonstrated to be a SPPARγM with low affinity, and antagonizes rosiglitazone action. In insulin resistant ob/ob mice and obese zucker rats, halofenate reduces glucose and insulin levels comparable to rosiglitazone in absence of body weight increases. It mediates the displacement of corepressors (NCoR and SMRT), but recruits the coactivators p300, CBP and TRAP220 in a very weak manner compared to rosiglitazone [120]. In the 1970s, halofenate was tested in two clinical trials and found to lower triglyceride levels, but with weak effects on plasma glucose levels in diabetic patients [121, 122]. The (-) enantiomer of halofenate, MBX-102 (metaglidasen) improved metabolic outcome without weight gain and is currently in a clinical trial [123].

Another SPPARγM with selective cofactor recruitment is FK614. It favors the recruitment of PGC-1α over CBP and SRC1 when compared to rosiglitazone. Hyperglycemia, hypertriglyceridemia and insulin resistance and glucose tolerance are improved in diabetic animal models. Adipogenesis is not decreased [124–126]. FK614 advanced to phase II clinical trials, but was discontinued when no therapeutic effects were demonstrated.

The high numbers of compounds which are currently in development or in a preclinical stage [127] emphasize the significance of this research field.

Another group of compounds which are shown to be partial activators for PPARγ are angiotensin II type 1 (AT_1)-receptor blockers (ARBs) [128]. They are established and widely used for the treatment of high blood pressure [129]. In 2004, several ARBs were shown to exhibit partial PPARγ activating properties (telmisartan > irbesartan > losartan). The highest potency among the ARBs was demonstrated with telmisartan.

Furthermore, telmisartan induced a selective cofactor recruitment and gene expression pattern, distinct from pioglitazone, and therefore is considered to be a SPPARγM. *In vivo* experiments demonstrated that diet-induced obesity mice treated for 10 weeks with telmisartan have improved insulin sensitivity and glucose tolerance without gaining weight compared to the pioglitazone treated control group [130]. Several clinical studies support the conclusion that telmisartan has beneficial effects on glucose and lipid metabolism. Treatment of diabetic patients with telmisartan (40-80mg/day) for 6 months reduced serum glucose and triglyceride levels compared with baseline. Furthermore, telmisartan had an excellent tolerability profile [131]. Similar results were achieved in another clinical trial. There, patients were treated with telmisartan (80mg/day) for 3 months, and fasting plasma glucose and insulin resistance, as well as blood pressure were decreased [132]. Due to its anti-hypertensive characteristics and its anti-diabetic properties, telmisartan can act as bimodal drug and might be able to improve several conditions of the metabolic syndrome like insulin resistance, and might protect from cardiovascular events.

Because of these promising effects, our group decided to create more potent SPPARγMs based on the telmisartan structure.

During a first project period detailed structure-activity relationship (SAR) studies were performed to elucidate an essential structural scaffold for PPARγ activation [133], shown in figure 8.

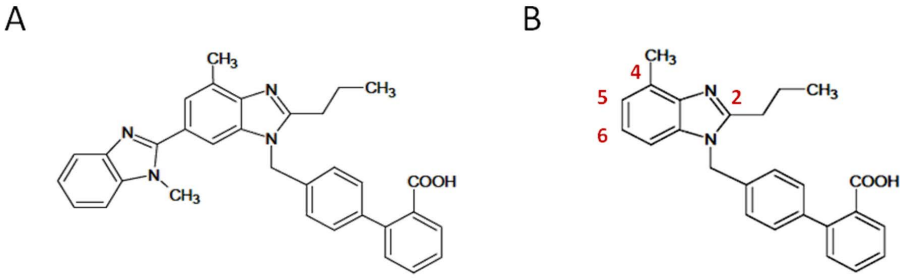

Figure 8: Telmisartan structure and minimum requirement for PPARγ activation. (A) Chemical structure of telmisartan; (B) Chemical structure of the 1-(biphenyl-4-ylmethyl)-1H-benzimidazole scaffold

Furthermore, structures with different modifications at position 2, 4, 5 and 6 of the core structure were synthesized and analyzed regarding their structure-activity relationship activating the PPARγ-LBD. Results demonstrated that the elongation of the alkyl chain at position 2 of the benzimidazole core, especially the length of the propyl chain, was important for potency and activation. Presence of the methyl group at position 4 induced partial activation [134]. And changes at positions 5 and 6 of the core scaffold were shown to have influence on efficacy [135].

1.6 Aim of this study

The purpose of this work for a second project period was to deepen the knowledge about the mode of action of modified telmisartan derivatives. Therefore, the following compounds with different PPARγ agonism:

- telmisartan and a partial agonist like telmisartan
- pioglitazone and a full agonist like pioglitazone
- an agonist with higher potency than pioglitazone

were selected and analyzed regarding differences in cofactor interaction, differential gene expression and glucose uptake.

Furthermore, the importance of position 5 and 6 of the telmisartan scaffold was further characterized. Newly designed compounds with specific moieties at position 5 or position 6 were analyzed regarding potency and efficacy for PPARγ transactivation, and correlation between PPARγ activation and cofactor recruitment.

Findings of this work should contribute to the current understanding of PPARγ modulation and the development of anti-diabetic drugs.

2 Material and Methods

2.1 Material

2.1.1 Compounds

Synthetic compounds were synthesized by M. Goebel at the Institute of Pharmacy, Freie Universität, Berlin/Germany. The chemical structure and molecular weight of the compounds and telmisartan is shown in figure 9.

The angiotensin-II receptor antagonist telmisartan provided the basic structure for the development of new compounds. Former PPARγ-telmisartan SAR-studies revealed the 1-(biphenyl-4-ylmethyl)-1H-benzimidazole as an essential core of telmisartan, which is necessary for minimum activation of PPARγ [133]. Based on these core structure (highlighted in blue, figure 1), 9 compounds with different moieties at position 2, 4, 5 and 6 were synthesized.

Telmisartan was purified and recrystallized from tablets (80mg) by M. Goebel [133]. Agonist 1 represents the core structure and contains, like telmisartan, a methyl group at position 4. This methyl group is not present in agonists 2 to agonists 6-6. Agonist 3, agonist 4-5 and agonist 4-6 have an elongation of the alkyl-chain at position 2. In both, agonist 2 and 3, the central benzimidazole of telmisartan was replaced with an 1H-naphto[2,3-d]imidazole.

Agonists 4 to 6 contain a benzimidazol moiety (agonists 4), a benzothiophene moiety (agonists 5) or a benzofuran moiety (agonists 6) either at position 5 or 6. All compounds were solved and diluted in DMSO.

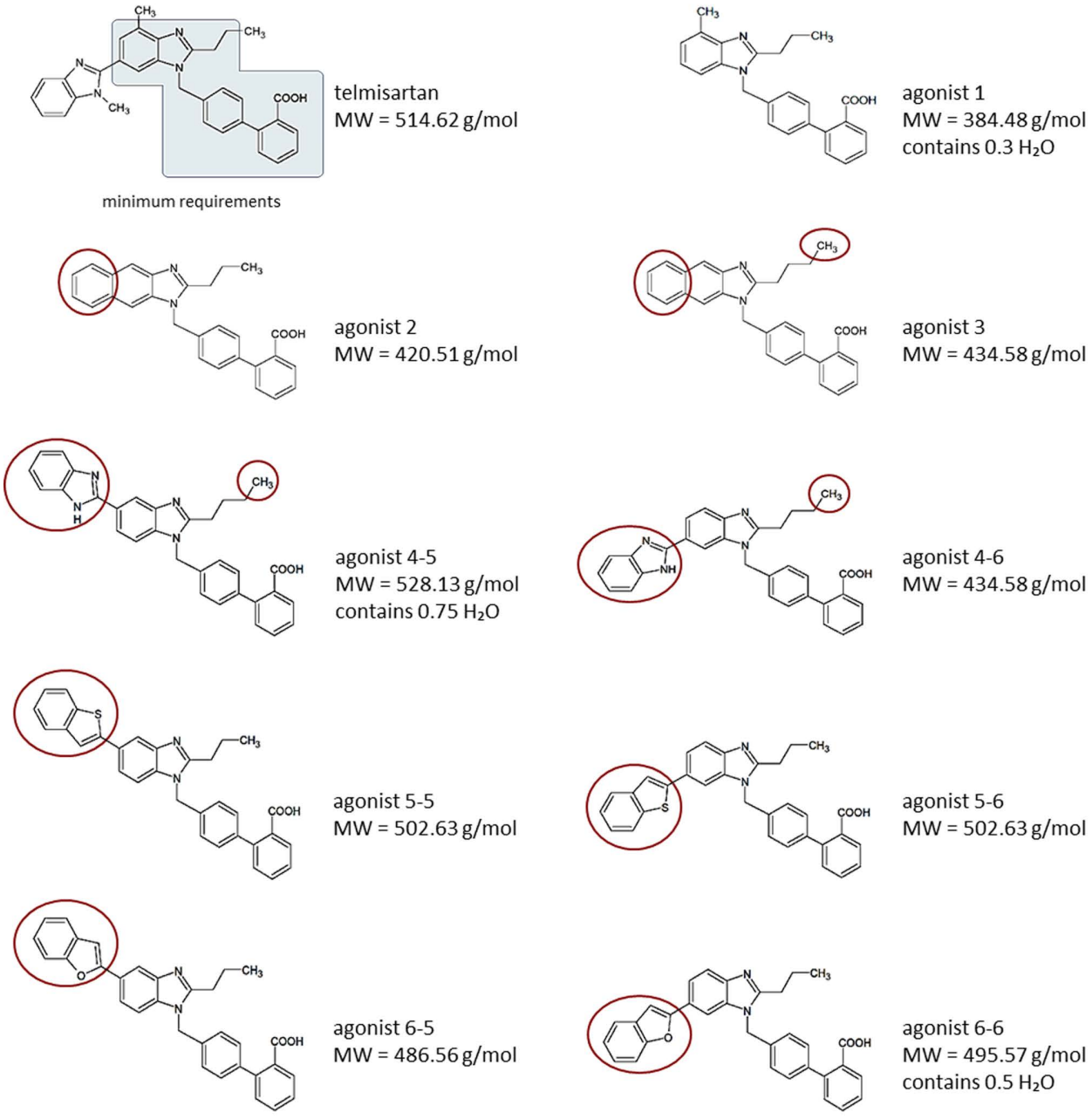

Figure 9: Chemical structures of analyzed compounds and telmisartan. The minimum requirement for PPARγ activation is highlighted in blue. Modifications of the telmisartan structure are highlighted in red.

2.1.2 Chemicals and substances

Ampicillin, Sigma-Aldrich, Hamburg, Germany

β-Mercaptoethanol, Sigma-Aldrich, Hamburg, Germany

Calcium chloride, Merck, Darmstadt, Germany

dNTPs (10mM), Promega, Mannheim, Germany

Dexamethason, Sigma-Aldrich, Hamburg, Germany

D-(+)-Glucose, Sigma-Aldrich, Hamburg, Germany

Dimethyl sulfoxide, ≥99.9%, Sigma-Aldrich, Hamburg, Germany

Dulbecco's Modified Eagle Medium (DMEM), 4.5 g/l glucose, GIBCO® Life Technologies, Karlsruhe, Germany

Ethanol, absolute, J.T. Baker,Griesheim, Germany

Fetal Bovine Serum, GIBCO® Life Technologies, Karlsruhe, Germany

^{3}H-labeld D-(+)-Glucose, GE Healthcare Europe GmbH, Munich, Germany

HEPES, Promega GmbH, Mannheim, Germany

Insulin, human, 10mg/ml, Sigma-Aldrich, Hamburg, Germany

Isobutylmethylxanthin, Sigma-Aldrich, Hamburg, Germany

Isopropanol, ≥99%, J.T. Baker,Griesheim, Germany

Kalium chloride, Merck, Darmstadt, Germany

LB Agar Miller(10g tryptone, 10 NaCl, 5g yeast extract, 15g agar), Becton Dickensen, Sparks, USA

LB Broth Miller (10g tryptone, 10 NaCl, 5g yeast extract), Becton Dickensen, Sparks, USA

Lipofectamine™ 2000, Invitrogen, Karlsruhe, Germany

M-MLV Reverse Transcriptase, Promega, Mannheim, Germany

M-MLV Reverse Transcriptase 5x Reaction Buffer, Promega, Mannheim, Germany

Magnesium chloride, Merck, Darmstadt, Germany

Magnesium sulfate, Merck, Darmstadt, Germany

Oil-Red O stain, BIOTREND Chemikalien GmbH, Köln, Germany

Opti-MEM® I, GIBCO® Life Technologies, Karlsruhe, Germany

OptiPhase Supermix Cocktail, PerkinElmer, Rodgau, Germany

PEG 6000/8000, Thermo Fisher Scientific, Rochester, USA

Penicillin/Streptomycin, Biochrom AG, Berlin, Germany

Pioglitazone, Enzo Life Sciences Inc., Farmingdale, USA

Phosphate buffered saline (PBS) 1x, GIBCO® Life Technologies, Karlsruhe, Germany

Power SYBR® Green PCR Master Mix, Life Technologies GmbH, Darmstadt, Germany

Random Primers, Promega, Mannheim, Germany

Recombinant Rnasin® Ribonuclease Inhibitor, Promega, Mannheim, Germany

Sodium chloride, Merck, Darmstadt, Germany

Sodium dihydrogen phosphit, Merck, Darmstadt, Germany

Sodium hydroxide, Merck, Darmstadt, Germany

Telmisartan, Boehringer Ingelheim GmbH, Ingelheim, Germany

Trypsin/EDTA, PAA Laboratories GmbH, Pasching, Austria

Ultra Pure Water, Biochrom AG, Berlin, Germany

2.1.3 Kits

Agilent RNA 6000 Nano Kit, Agilent Technologies, Waldbronn, Germany

Dual-Luciferase® Reporter Assay System, Promega GmbH, Mannheim, Germany

Illumina® TotalPrep™ RNA Amplification Kit, Applied Biosystems, Darmstadt, Germany

LanthaScreen™ Terbium Instrument Control Kit, Invitrogen, Karlsruhe, Germany

LanthaScreen™ TR-FRET PPAR gamma Coactivator Assay Kit, Invitrogen, Karlsruhe, Germany

MouseWG-6 v2.0 Expression BeadChip Kit, Illumina, Eindhoven, Netherlands

NucleoSpin® RNA II, MACHEREY-NAGEL GmbH & Co. KG, Düren, Germany

QIAGEN Plasmid Maxi Kit, QIAGEN GmbH, Hilden, Germany

2.1.4 Biological material

Chemically competent prokaryotic cells:

- E. coli Top10 (genotype: F- *mcr*A Δ(*mrr-hsd*RMS-*mcr*BC) φ80*lac*ZΔM15 Δ*lac*X74 *rec*A1 *ara*D139 Δ(*araleu*)7697 *gal*U *gal*K *rps*L (StrR) *end*A1 *nup*G), Invitrogen, Karlsruhe, Germany

Eukaryotic cell lines:

- 3T3-L1 (CL-173 Mouse embryonic fibroblast cell line), ATCC-LGC Standards GmbH, Wesel, Germany
- COS-7 (African green monkey kidney fibroblast-like cell line, SV40 transfected), Institute of Tumorpathology, University Hospital Charité-Berlin/Germany.

2.1.5 Plasmids

Plasmids were a kind gift of B. Staels/Institut Pasteur, Lille/France and contain a ampicillin resistance gene.

- pGal4-hPPARγDEF
- pGal5-TK-pGL3
- pRenilla-CMV

2.1.6 Cofactor peptides

Cofactor peptides are labeled with fluorescein and purchased from Invitrogen, Karlsruhe, Germany. Coactivators contain LXXLL-motif.

- NCoR1-DPASNLGLEDIIRKALMGSFDDK
- SRC1-GPQTPQAQQKSLLQQLLTE
- PGC-1α-EAEEPSLLKKLLLAPANTQ
- TRAP220-NTKNHPMLMNLLKDNPAQD

2.1.7 qPCR primers

Primers, shown in table 1, are specific for mouse genome and anneal at 60°C. They are exon-exon spanning to distinguish between amplification from remaining genomic DNA and RNA amplification. All primers were synthesized with the primer 3 program and blasted at *www.ncbi.nlm.nih.gov/BLAST* for unspecific binding within the mouse genome.

Table 1: Index of qPCR primers.

Gene	Sequence	Manufacturer
18S	forward 5'-CCT GAG AAA CGG CTA CCA CAT reverse 5'-TTC CAA TTA CAG GGC CTC GA	TIB MOLBIOL GmbH, Berlin, Germany
adiponectin	forward 5'-TCC GGG ACT CTA CTA CTT CTC TTA CCA C reverse 5'-GTC CCC ATC CCC ATA CAC C TG	Humboldt-University, Institut of Genetics, Berlin, Germany
ap2	forward 5'-TGG AAG ACA GCT CCT CCT CG reverse 5'-AAT CCC CAT TTA CGC TGA TGA TC	Sigma-Aldrich, Hamburg, Germany
CD36	forward 5'-GAT TAA TGG CAC AGA CGC AGC reverse 5'-TCC GAA CAC AGC GTA GAT AGA CC	Humboldt-University, Institut of Genetics, Berlin, Germany
PGC-1α	forward 5'-CAT TTG ATG CAC TGA CAG ATG GA reverse 5'-CCG TCA GGC ATG GAG GAA	Humboldt-University, Institut of Genetics, Berlin, Germany
PPARγ2	forward 5'-TGG GTG AAA CTC TGG GAG ATT C reverse 5'-GAG AGG TCC ACA GAG CTG ATT CC	Humboldt-University, Institut of Genetics, Berlin, Germany
resistin	forward 5'-TCA TTT CCC CTC CTT TTC CTT T reverse 5'-TGG GAC ACA GTG GCA TGC T	Humboldt-University, Institut of Genetics, Berlin, Germany

2.1.8 Equipment and consumables

-20°C freezer, Liebherr GmbH, Biberach an der Riss, Germany

-80°C freezer, Electrolux GmbH, Nürnberg, Germany

Adhesive transparent foil for PCR plates (QPCR), SARSTEDT AG & Co, Mümbrecht, Germany

Agilent 2100 Bioanalyzer, Agilent Technologies, Waldbronn, Germany

Analytical balance, Sartorius AG, Göttingen, Germany

Autoclave, Systec GmbH, Wettenberg, Germany

Bacterial incubator, ISS, Cookeville, USA

Centrifuges:

- Centrifuge 5810 R, Eppendorf AG, Hamburg, Germany
- Galaxy Mini centrifuge, Merck eurolab GmbH, Bruchsal, Germany
- Sorvall RC 5C Plus Centrifuge , Phoenix Equipment,Inc., Rochester, USA

Disposable plastic material:

- 6-well, 12-well and 96-well plates, SARSTEDT AG & Co, Mümbrecht, Germany
- 384 Well Low Volume Black Round Bottom Polystyrene NBS™ Microplate, CORNING B.V. Life Sciences, Amsterdam, Netherlands
- Cell culture flasks (T25, T75, T175), SARSTEDT AG & Co, Mümbrecht, Germany
- Cell scraper, SARSTEDT AG & Co, Mümbrecht, Germany
- Combitips plus® for Multipette® stream, several sizes, Eppendorf AG, Hamburg, Germany
- Cryo tubes, 2ml, Thermo Fisher Scientific, Rochester, USA
- Falcon tubes (15ml and 50ml), Becton Dickinson GmbH, Heidelberg, Germany
- Luminometer tubes, Sarstedt AG und Co., Nümbrecht Germany
- Petri dishes, Nunc GmbH & Co. KG, Langenselbold, Germany
- Real-time plates, SARSTEDT AG & Co, Mümbrecht, Germany

- Steril pipettes, SARSTEDT AG & Co., Nümbrecht Germany
- Scintillation vial (6ml), PerkinElmer, Rodgau, Germany
- Tips for micropipettes, several sizes, VWR International GmbH, Darmstadt, Germany
- Tubes (0,5ml; 1ml; 1,5ml; 2ml), SARSTEDT AG & Co, Mümbrecht, Germany

Drigalski-spatula, A. Hartenstein GmbH, Würzburg, Germany

Filter for PerkinElmer EnVision® Multilabel Plate Reader:

- Emission filter 1: wavelength 495nm/ bandwidth 10nm, PerkinElmer, Rodgau, Germany
- Emission filter 2: wavelength 520nm/ bandwidth 25nm, PerkinElmer, Rodgau, Germany
- Excitation filter: wavelength 340nm/ bandwidth 60nm, PerkinElmer, Rodgau, Germany

Freezing container, Nalgene® Mr. Frosty, Sigma-Aldrich, Hamburg, Germany

Fume hood, Köttermann, Uetze/Hänigsen, Germany

Gas burner, International Biological Laboratories, Haryana, India

Glass bottles, several sizes, VWR International GmbH, Darmstadt, Germany

Gloves:

- Latex examination gloves, Emerson & Co. S.r.L., Genoa, Italy
- Nitrile gloves, Ansell Healthcare, Brussels, Belgium

HERA cell 150 CO2 incubator, Thermo Fisher Scientific, Rochester, USA

Ice machine, Scotsman, Milan, Italy

LightCycler for Real-Time PCR Mx 3000 P, Stratagene, Amsterdam, Netherlands

NanoDrop Spectrophotometer 1000, PEQLAB Biotechnologie GmbH, Erlangen, Germany

Neubauer counting chamber, Marienfeld GmbH, Lauda-Königshofen, Germany

PerkinElmer EnVision® Multilabel Plate Reader, PerkinElmer, Rodgau, Germany

Phase contrast microscope and camera, Olympus GmbH, Hamburg, Germany

pH-meter, HANNA instruments, Kehl am Rhein, Germany

Pipettes:

- Micropipettes, several sizes, Gilson, Middleton, USA
- Pipette boy, Gilson, Middleton, USA
- Multipette® stream, Eppendorf AG, Hamburg, Germany

Pump for cell culture, KNF Laboport, Freiburg-Munzingen, Germany

Racks, several sizes, several companies

Refrigerators, Liebherr GmbH, Biberach an der Riss, Germany

Rocking platform, PerkinElmar GmbH, Rodgau – Jügesheim, Germany

Steril filter (0.2µm), Schleicher & Schuell, Dassel, Germany

Steril laminar flow chambers holten, Thermo Scientific, Ashville, USA

Sirius Luminometer, Berthold Detection Systems GmbH, Pforzheim, Germany

Thermo-mixer, Eppendorf AG, Hamburg, Germany

Vortex-mixer, Scientific Industries, Bohemia, USA

Wallac Model 1409 liquid scintillation counter, PerkinElmer, Rodgau, Germany

Water bath, GE Healthcare, Munich, Germany

2.1.9 Computer software and internet programs

Primer sequence program:

- Primer 3, Whitehead Institute for Biomedical Research, USA

Program to draw chemical structures:

- ACD/ChemSketch Version 12.01, Advanced Chemistry Development Inc., Toronto, Canada
- MarvinSketch 5.4.0.0, Chem Axon, Budapest, Hungary

Software for 2100 Agilent Bioanalyzer:

- 2100 Expert Software, Agilent Technologies, Waldbronn, Germany

Software for figures and statistics:

- GraphPad Prism 5.01, GraphPad Software, Inc., La Jolla, USA

Software for luminometer and spectrophotometer:

- FB12/Sirius PC Software, Montreal Biotech Inc., Dorval, Canada
- NanoDrop 1000 v.3.5.2, PEQLAB Biotech GmbH, Erlangen, Germany

Software for microarray and qPCR analysis:

- Cluster 3.0 and TreeView 1.60, University of California, Berkeley, USA
- GenomeStudio Gene Expression Module, Illumina, Eindhoven, Netherlands
- MxPro-Mx3000P v.4.10 Build 389, Stratagene, Amsterdam, Netherlands
- Partek Genomic Suite version 6.5., Partek Incorporated, St. Luis, USA
- R program version 2.14.1 containing lumi and limma packages, University of Auckland, Auckland, New Zealand

Software for PerkinElmer EnVision® Multilabel Plate Reader:

- Wallac EnVision® Manager software, PerkinElmer, Rodgau, Germany

2.2 Methods

2.2.1 Cell-lines

2.2.1.1 Culture and differentiation of 3T3-L1 cells

Adipocyte-differentiation experiments were performed with 3T3-L1 mouse embryonic fibroblasts purchased from the American Type Culture Collection. Cells were grown in Dulbecco's modified Eagle's medium (DMEM) with 10% fetal bovine serum (FBS) and 1% Penicillin-Streptomycin at 37°C and 5% CO_2. The special characteristic of this cell line is its potential to undergo adipogenesis after distinct hormonal stimulation. To keep the ability for differentiation, cells were passaged at 80-90% confluency until start of the experiment and not used higher than passage 12.

For each time point or treatment group, cells were seeded as triplicates into 6-well plates unless otherwise indicated. Two days after 3T3-L1 cells reached 100% confluency (day 0), adipogenesis was initiated by stimulation with culture medium containing 50mM Isobutylmethylxanthine, 2mM Dexamethasone and 10mg/ml Insulin for 3 days. Thereafter, medium was replaced with full supplemented DMEM with 10mg/ml Insulin and cells were incubated for another 3 days. Differentiation was accomplished after additional 3 days incubation with full supplemented DMEM.

To monitor morphological changes, pictures were taken at day 0, day 3, day 6 and day 9 during differentiation.

2.2.1.2 Culture of COS-7 cells

COS-7 cells were a kind gift of the Institute of Tumorpathology, University Hospital Charité-Berlin/ Germany. Medium- and culture conditions are the same like for 3T3-L1 cells. COS-7 cells were splitted at 90-100% confluency and used for experiments between passages 5 to 12.

2.2.1.3 Freezing and thawing of adherent cell-lines

After receiving cell-lines from a vendor or other institutes, cells were cultured to increase its biological mass and frozen as aliquots. Keeping cryo-stocks enables to work with low passages and provides backup in case of contamination. To prepare cells for freezing, the monolayer was rinsed once with warm 1x PBS to remove traces of FBS which would inhibit enzymatic action. Afterwards, cells were incubated with trypsin/ EDTA until they were detached from the plastic surface. To prevent any destruction of the cell surface, full supplemented medium was added immediately and cells were transferred to a falcon tube and centrifuged at 800rpm for 3min. Medium containing trypsin/EDTA was aspirated, cells were resuspended in 10% DMSO full supplemented medium and aliquoted in cryo-tubes. DMSO serves as anti-freezing agent and prevents rupture of the cells during a slow freezing process in freezing-containers in a -80°C freezer. After one day, tubes can be transferred to nitrogen for long-term storage.

Thawing has to be fast, to protect cells from toxic exposure to 10% DMSO. Hence, the cell suspension was warmed-up in a 37°C water-bath and transferred to a falcon tube. To adjust the osmotic pressure, full supplemented medium was added drop wise. Afterwards, cells were centrifuged at 800rpm for 3min, DMSO containing medium was aspirated and cells were resuspended with full supplemented medium.

2.2.2 Bacterial cells

2.2.2.1 Generation of chemically competent bacterial cells

Fresh overnight culture of chemically competent Top10 cells was used to inoculate 100ml of sterile LB broth and grown under constant shaking at 37°C. At an OD_{600} of approximately 0.4 to 0.6 the cell suspension was centrifuged at 4000rpm for 10min. The supernatant was discarded and the cell pellet was resuspended in 7.5ml TSB medium containing 5% DMSO, 10mM $MgSO_4$, 10mM $MgCl_2$ and 10% PEG 6000/8000 in LB broth. Cells were incubated on ice for 1h and afterwards aliquoted, frozen in nitrogen and stored at -80°C.

2.2.2.2 Transformation and plasmid extraction

Plasmids are retransformed into bacteria in order to amplify larger quantities of it. Therefore, chemically competent Top 10 cells were slowly thawed on ice and carefully mixed with 5-10ng pGal4-hPPARγDEF,pGal5-TK-pGL3 or pRenilla-CMV plasmid DNA, respectively. The suspension was kept on ice for 30min to get the DNA stick to the bacteria surface. During a heat-shock of 42°C for 1min, plasmid DNA is forced into the cells. Afterwards, tubes were put back on ice. Prewarmed SOC medium (2% w/v bacto-tryptone, 0.5% w/v bacto-yeast extract, 10mM NaCl, 2.5mM KCl, 10mM $MgCl_2$, 20mM glucose) was added and cell suspensions were shaken at 37°C. After 1h, cell suspensions were spread on LB agar plates containing 100mg/ml ampicillin and kept upside down at 37°C overnight. 5ml of LB broth were inoculated with a single colony of each transformation, respectively, and grown under constant shaking at 37°C overnight. At the next day, cell suspensions were transferred to 500ml of sterile LB broth each, containing 100mg/ml ampicillin and grown under constant shaking at 37°C to an OD_{600} of approximately 0.4 to 0.6. Then, plasmid DNA was extracted with a QIAGEN Plasmid Maxi Kit according to the instructions of the manufacturer. At the end, plasmid DNA was resolved in ultra pure water, concentrations were measured and plasmids were stored at -20°C.

2.2.3 Luciferase assay

2.2.3.1 Transient transfection and stimulation of COS-7 cells

Purpose of this assay is to determine PPARγ-activity after dose-dependent stimulation of COS-7 cells with different PPARγ agonists under the use of bioluminescence reporters.

In a pretest, plate size and cell number was established. Consequently, all experiments were performed in 96-well plates, due to saving material in a high throughput screening and a good growth behavior of COS-7 cells in 96-well plates. Optimized density of COS-7 cells was $1x10^5$ cells/ 96-well.

Cells were seeded and incubated at 37°C for 20h. Prior to transfection, medium was replaced with serum free medium, and cells were transfected with 0.25µl Lipofectamine 2000, 4.5ng pGal4-hPPARγDEF, 45ng pGal5-TK-pGL3 and 3ng pRenilla-CMV in 25µl Opti-MEM according to the Invitrogen transfection protocol. After 4h, full supplemented medium containing the synthesized compounds, pioglitazone, telmisartan and vehicle (DMSO) were added in a dose-dependent manner, and luciferase activity was measured after 36h.

2.2.3.2 Measurement of luciferase activity

Dual-luciferase reporter assay (Promega) was performed according the manufacturer's protocol. Briefly, cells were washed with 1x PBS. Buffer was removed and immediately replaced with 30µl 1x Passive Lysis Buffer (PLB) per well. After 15min shaking at RT on a rocking platform, plates were shock frozen at -80°C to complete lysis. In the meantime, Luciferase Assay Buffer and Stop&Glo Reagent were prepared as indicated in the protocol. Both reagents need to have the same temperature during the whole measurement according to prevent variances in the results. Cell debris would interfere with the measurement and had to be spinned down. With regard to transfection efficiency, appropriate amounts of PLB lysate were transferred to luminometer vials and measurement of firefly luciferase activity and renilla luciferase activity was performed with a single injector luminometer for 10sec respectively. Renilla luciferase was used for normalization and should be equal within triplicates. It is independent on firefly luciferase activity. Relative light units were determined by the ratio of firefly luciferase activity/ renilla luciferase activity.

Since firefly luciferase gene and PPARγ promoter are connected in pGal4-hPPARγDEF, firefly luciferase activity can be directly correlated with PPARγ activity.

2.2.4 Oil-Red O staining

Murine 3T3-L1 preadipocytes were maintained in DMEM with 10% fetal bovine serum and differentiated by a modified protocol as described before. Briefly, postconfluent preadipocytes were treated for 3 days with complete medium containing 1µM dexamethasone and 0.17µM insulin, but no IBMX. After medium change, cells were incubated with insulin (0.17µM) for further 3 days and with only complete medium for another 3 days. During the whole stimulation time, medium contained the synthesized compounds, pioglitazone, telmisartan or vehicle (DMSO) at 3 different concentrations (0.1µM, 1µM and 10µM), respectively. At day 9 of differentiation, cells were washed with 1x PBS and intracellular triglyceride content was stained with Oil-Red O. After 1h incubation at 37°C, cell layer was washed and plates were scanned for documentation.

Preparation of Oil-Red O solution:

For Oil-Red O stock solution, 0.7g Oil-Red O was solved in 200ml 100% 2-propanol and stirred at RT overnight. At the next day, the solution was filtered (0.2µm) and stored at 4°C. To prepare Oil-Red O working solution, 6 parts of stock solution were mixed with 4 parts of ultra pure water. The solution had to sit at RT for 20min and was filtered again (0.2µm), without aspirating the precipitate. The working solution had to be prepared freshly prior to use.

2.2.5 Time-Resolved Fluorescence Resonance Energy Transfer (TR-FRET)

TR-FRET is used to analyze protein-protein or DNA-DNA interaction. After labeling both items with a suitable pair of fluorophores, a donor-fluorophore can be excited and is capable of transferring energy to an acceptor-fluorophore. The intensity of that signal depends on the distance between donor and acceptor. The higher the signal, the stronger is the binding of both items.

In order to analyze the influence of dose-dependent PPARγ ligand binding on corepressor release and coactivator recruitment, cell free LanthaScreen TR-FRET PPARγ Coactivator Assay was used as described in the instructions of the manufacturer. It's a sensitive and robust technique using a delay of 100µsec after excitation (TR=time resolved) to overcome interference from background fluorescence, light scatter and other interfering sources. The assay principle is shown in figure 10.

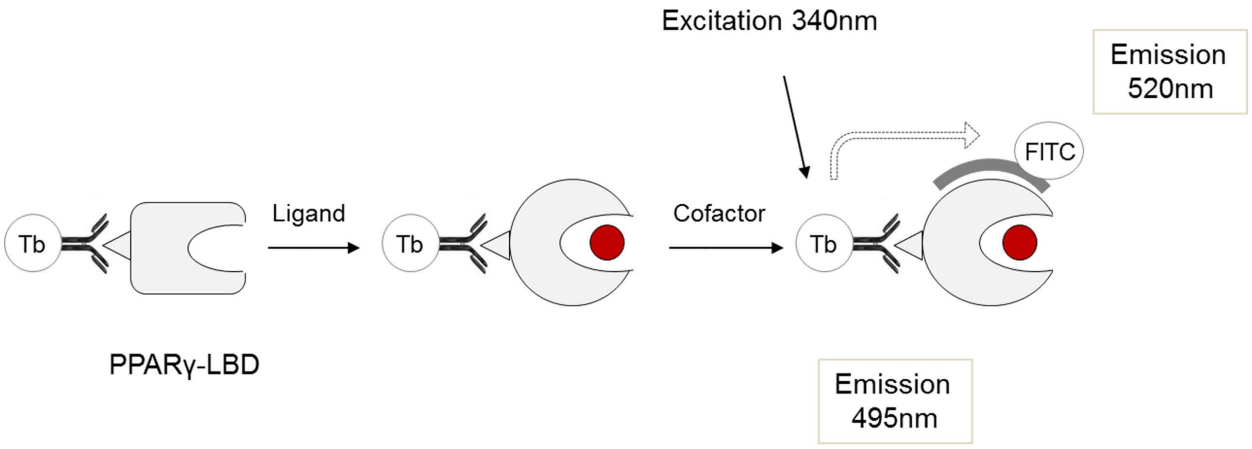

Figure 10: Principle of the PPARγ agonist dependent coactivator recruitment assay [136 modified]. Ligand binding induces a conformational change in helix 12 of the PPARγ-LBD (Tb labeled), causing an increase of the affinity of the LBD to a cofactor peptide (FITC labeled). Excitation of Tb induces an energy transfer to FITC, if both fluorophores are in close proximity. Tb=terbium, FITC=fluorescein

Briefly, recombinant PPARγ ligand-binding domain (LBD) is tagged with glutathione S-transferase (GST) and could be recognized by an anti-GST antibody. Dilution series

of the synthesized compounds, pioglitazone and telmisartan were produced in triplicates and mixed with PPARγ-LBD and anti-GST antibody in black 384 well-plates. Incubation time prior to measurement was 1h. Maximum concentration of pioglitazone represented the positive assay control and DMSO served as negative control. Binding of the agonist induced a conformational change of the PPARγ-LBD, resulting in an increased affinity for coactivator peptides. In this assay, cofactor peptides are labeled with fluorescein. Close proximity of terbium and fluorescein increased FRET-signal. Fluorescence intensities were measured with a filter-based EnVision plate reader and FRET-signal was calculated by the ratio of the emission signal at 520nm (fluorescein) and 495nm (terbium). Instrument settings consist with the specifications of the manufacturer for LanthaScreen assays and were tested with LanthaScreen Tb Instrument Control Kit as described in the manufacturer's instructions. The Z'-factor was calculated using the equation of Zhang et al. [137]. It indicates the robustness of an assay and is considered to be an excellent assay with values between 0.5 and 1, while a theoretical ideal assay is represented by 1. Calculated Z'-values of this experiment were between 0.5 and 0.7. Plate reader and software was kindly provided by the Department of Medicine/ Hepatology and Gastroenterology of the University Hospital Charité, Berlin/Germany.

2.2.6 Reverse transcription and qPCR

Quantitative real-time PCR is a sophisticated method to analyze gene expression. Cells were cultured and differentiated with PPARγ ligands as indicated above. Afterwards, cells were gently washed with ice-cold 1x PBS and directly lysed and homogenized. Extraction and purification of total RNA was accomplished using NucleoSpin® RNA II Kit according to the protocol provided by Macherey-Nagel. RNA concentration was determined with a spectrophotometer and samples were adjusted to 1µg/µl. Since RNA can be easily degraded by Rnases, cDNA was synthesized by reverse transcription using M-MLV reverse transcriptase, Rnasin and dNTPs from Promega according to the manufacturer's instructions. Next, cDNA was subjected to quantitative PCR amplification with gene-specific primers in the presence of a fluorescent dye (SYBR® Green, Applied Biosystems). Sample mix and thermal profile are shown in figure 11.

SYBR® Green	12,5µl
Primer_F (20µM)	0,25µl
Primer_R (20µM)	0,25µl
cDNA	~12ng
Ultra Pure Water	ad 25µl

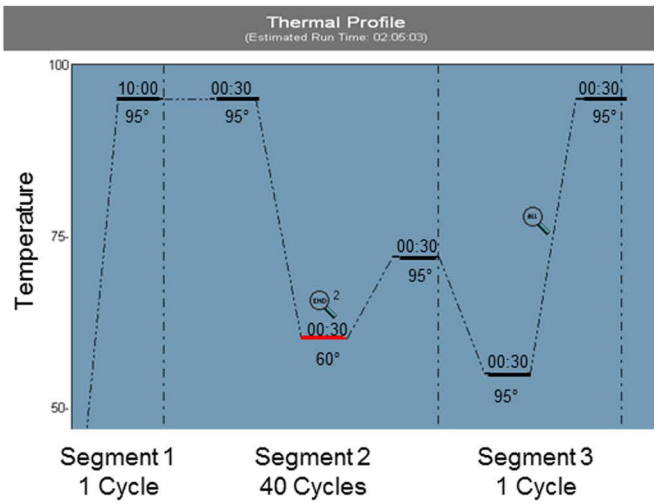

Figure 11: Sample mix and thermal profile for qPCR. Annealing temperature was adjusted depending on the primer sequence.

The measurement was performed with the LightCycler Mx 3000 P by Stratagene.

During adipogenesis, preadipocytes undergo dramatic morphologic and metabolic changes. Therefore, several genes (e.g. ß-actin, 18S, ubiquitin C) were tested for housekeeping purposes (data not shown). Analysis with the 18S ribosomal RNA revealed constant results. Thus, normalization to 18S was used to calculate the relative abundance of sample mRNA.

2.2.7 Microarray

2.2.7.1 Sample preparation and labeling

An expression BeadChip Kit was performed to obtain detailed knowledge about PPARγ ligand-related gene expression during adipogenesis. Therefore, 3T3-L1 cells were differentiated with newly designed PPARγ agonists, pioglitazone and telmisartan as described above. Due to the results of the PPARγ-transactivation assay, a ligand concentration of 10µM was chosen for the experiment. At day 6 of differentiation, RNA of three technical replicas were extracted as explained under 2.2.6.

The integrity and quantity of total RNA was analyzed using the Agilent RNA 6000 Nano Kit and measured with the Agilent Bioanalyzer as indicated in the instructions of the manufacturer. Electropherograms from the ladder and one sample, representative for all measured RNA samples, are shown in figure 12.

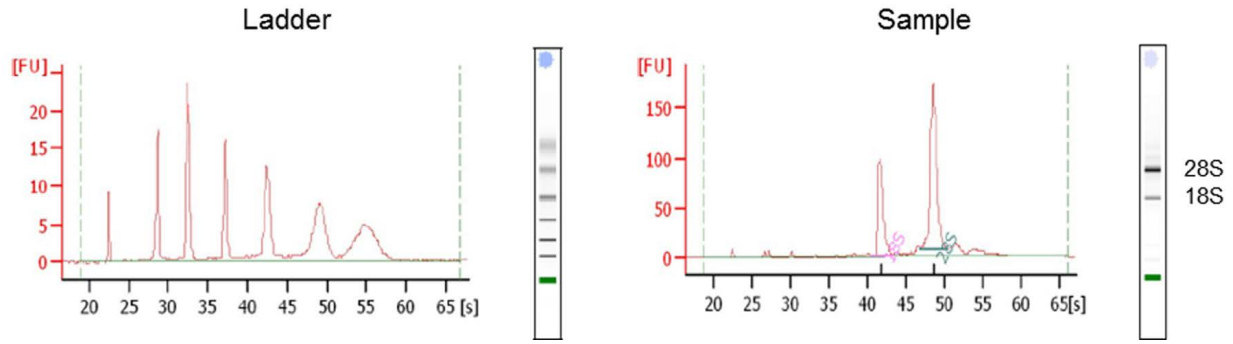

Figure 12: Electropherogram of total RNA quality. RNA integrity and concentration was measured with a Bioanalyzer. Suitable quality of the sample is characterized by well-defined peaks of the 18S and 28S ribosomal subunits. FU=Fluorescence Unit

To validate the treatment response, RNA was reverse transcribed into cDNA with M-MLV Reverse Transcriptase kit and expression of 18S, adiponectin, ap2, resistin and CD36 was measured by quantitative real-time PCR as indicated under 2.2.6.

An amount of 400ng/11µl total RNA was biotinylated and amplified with the Illumina® TotalPrep™ RNA Amplification Kit according the manufacturer's instructions. The basic principle of this assay is shown in figure 13. Concentration of labeled cRNA was measured with a spectrophotometer and adjusted for hybridization to 10µg/11µl.

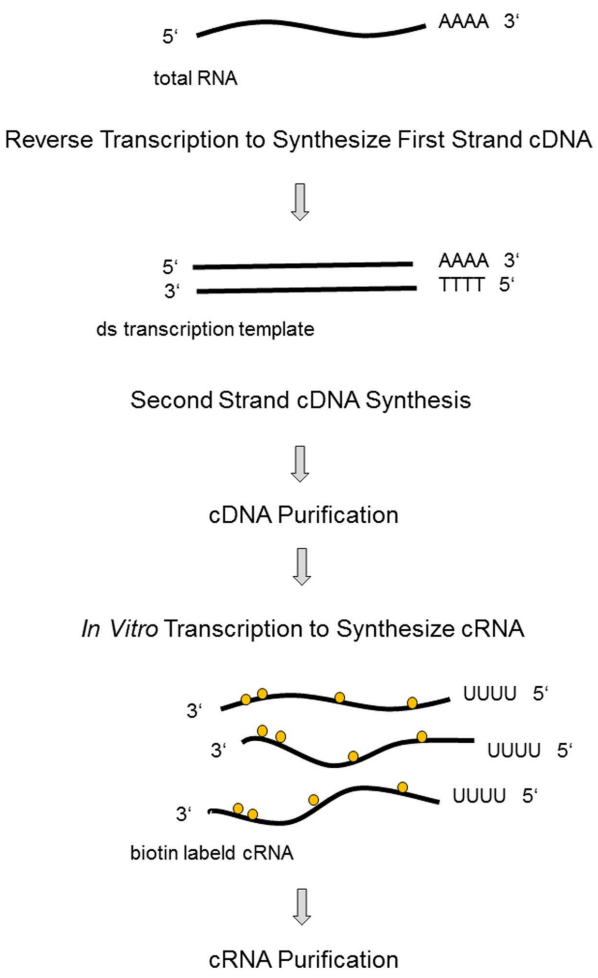

Figure 13: Overview of Illumina's TotalPrep RNA amplification. Tthe first strand of cDNA was synthesized by reverse transcription. Afterwards, single-stranded cDNA was converted to a double-strand template and purified. Next, multiple copies of cRNA containing biotinylated nucleotides were synthesized and in a final step purified for direct use in hybridization arrays. Picture was modified from Illumina's TotalPrep RNA amplification manual.

2.2.7.2 Hybridization

Biotinylated samples were transferred to the Max Delbrück Center, Berlin-Buch/ Germany and hybridization was performed by G. Born at the microarray facility of Prof. Hübner with Illumina's Whole Genome MouseWG-6 v2.0 Expression BeadChip Kit according the manufacturer's instructions. More than 45 200 transcripts, derived from the National Center for Biotechnology Information Reference Sequence (NCBI RefSeq)

database (Build 36, Release 22), the Mouse Exonic Evidence Based Oligonucliotide (MEEBO) set and protein-coding sequences described in the RIKEN FANTOM2 database, were included.

The BeadChips contained oligonucleotides which were immobilized to beads and held in microwells on the surface of an array substrate. The design of a bead-probe bound to cRNA is shown in figure 14, and the application of samples on a BeadChip is demonstrated in figure 15. During hybridization BeadChips and cRNA was incubated for 15h at 58°C. Afterwards, chips were washed and incubated with Cy3-Streptavidin which binds to biotinylated cRNA, hybridized to the BeadChip. To detect signals, chips were excited during a scanning process and light emissions were recorded. (figure 15). Data were obtained with Illumina's Bead Array Reader/ GenomeStudio using the decode files of the chips to reveal the name and position of each transcript.

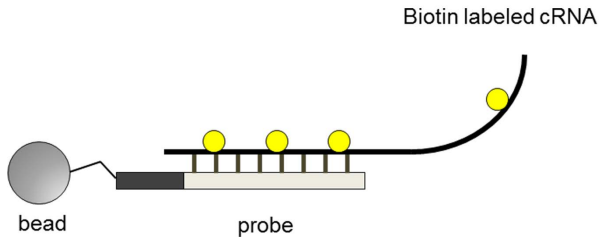

Figure 14: Bead-probe design for direct hybridization [138 modified]. Each bead is linked to 29-mer address sequences and a 50-mer transcript sequence, which can be recognized by biotin-labeled cRNA samples.

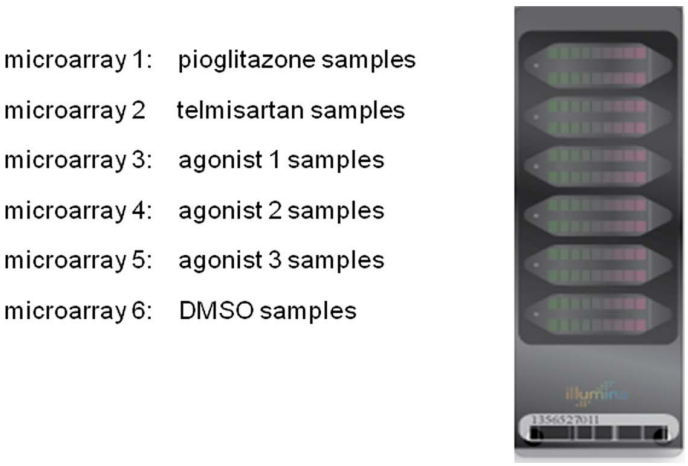

Figure 15: Sample application on Illumina's MouseWG-6 v2.0 Expression BeadChip.

2.2.7.3 Data analysis

Microarray raw data were further processed with the program R using the packages lumi and limma. Lumi package was used for log_2 transformation, quantile normalization and background subtraction. Fold-changes were calculated by probe wise division of the expression values from the experimental condition by the expression values from the control condition. Experimental conditions were samples derived from cells treated with pioglitazone, telmisartan, agonist 1, agonist 2 and agonist3, whereas control conditions represented the DMSO control. Group comparism was implemented with limma package. Finally, a logarithmic transformation was performed for each data point according to the formula: fold change = log_2 (signal experimental condition/ signal control condition). The Benjamini-Hochberg procedure was consulted for false discovery rate (FDR) multiple testing corrections [139]. All genes possessing an mRNA level with a log_2 fold-change smaller -1 and higher than 1, and a p-value of < 0.01 were considered to be statistically significant.

The intersection of different microarray data sets were presented in venn diagrams using limma package. And principle component analysis (PCA) was determined using the Partek Genomic Suite program.

The cluster analysis was done for data sets of intersected genes with the Cluster Eisen software and the TreeView program according to Eisen et al. [140]. The results were calculated as the mean of triplicate fold-change values, and displayed in a hierarchical cluster for genes with in increased or decreased mRNA level. To elucidate selective gene expression, results were displayed in a mean hierarchical cluster profile.

Furthermore, selective groups of genes were uploaded to DAVID (**D**atabase for **A**nnotation, **V**isualization and **I**ntegrated **D**iscovery; *www.david.niaid.nih.gov*) and further analyzed for gene onthology and pathway enrichment. The biological function of differentially expressed genes was determined with *www.ncbi.nlm.nih.gov/pubmed* and *www.ncbi.nlm.nih.gov/omim*.

2.2.8 Glucose uptake

3T3-L1 cells were cultured as triplicates in 12-well plates and differentiated as described under 2.2.1.1. Mature adipocytes were treated with 10µM synthesized compounds, pioglitazone and telmisartan. For glucose up-take measurement, adipocytes were washed twice with warm 1x PBS and starved for 2h with medium without FBS. Afterwards, cells were washed with Krebs-Ringer Buffer (pH 7.4, 25mM HEPES, 130mM NaCl, 5mM KCl, 2.5mM $CaCl_2$, 2.5mM NaH_2PO_3, 1.2mM $MgCl_2$) and incubated in Krebs-Ringer Buffer containing 0.1mM deoxyglucose with and without 100nM insulin for 30min. For the last 6min of incubation, a mixture of 0.1mM deoxyglucose and 0.5µCi ^{3}H-labeld deoxyglucose was added. To stop glucose up-take, cell culture plates were put on ice pads and cells were washed twice with ice-cold 1x PBS. Cells were lysed in 300µl 1N NaOH immediately. To determine up-take of radioactively labeled glucose, 100µl of the lysate were mixed with 5ml of scintillation solution and counts were measured for one minute per sample with a ß-counter. Scintillation solution with 100µl labeled glucose mixture was used to control ^{3}H-labeld deoxyglucose activity. Scintillation solution without lysate served as negative control and values were subtracted from the measured sample values.

2.2.9 Statistical analysis

Unless differently indicated experiments were done in triplicates and repeated at least three times. All data represent means ± SD and were considered to be statistically significant at $p<0.05$. Glucose uptake and qPCR results were statistically analyzed by parametric student's t-test or ANOVA with post hoc test (Bonferroni) where appropriate. As mentioned above microarray data were statistically analyzed according the Benjamini-Hochberg procedure. TR-FRET and transactivation data represent the mean of three independent experiments measured in triplicates. TR-FRET data were normalized to 1 and transactivation data were normalized to 100% for the maximum PPARγ activation by pioglitazone. EC_{50}-values and area under the curve (AUC) was calculated with GraphPad Prism 5.01.

2.2.10 Lipophilicity

Based on the chemical structure, lipophilicity of pioglitazone, telmisartan and the synthesized compounds was calculated for ph7.4 with MarvinSketch 5.4.0.0. The chemical structures were drawn with ACD/ ChemSketch.

3 Results

3.1 Morphological changes during 3T3-L1 differentiation

3T3-L1 cells are mouse embryonic fibroblasts, which represent a well-established *in vitro* model for studies on adipose tissue and screening of potential adipogenic agents [141, 142]. During differentiation 3T3-L1 cells underwent a distinct morphological change from preadipocyte-like fibroblasts to a mature adipocyte-like phenotype. Pictures of the different stages during 3T3-L1 differentiation are shown in figure 16.

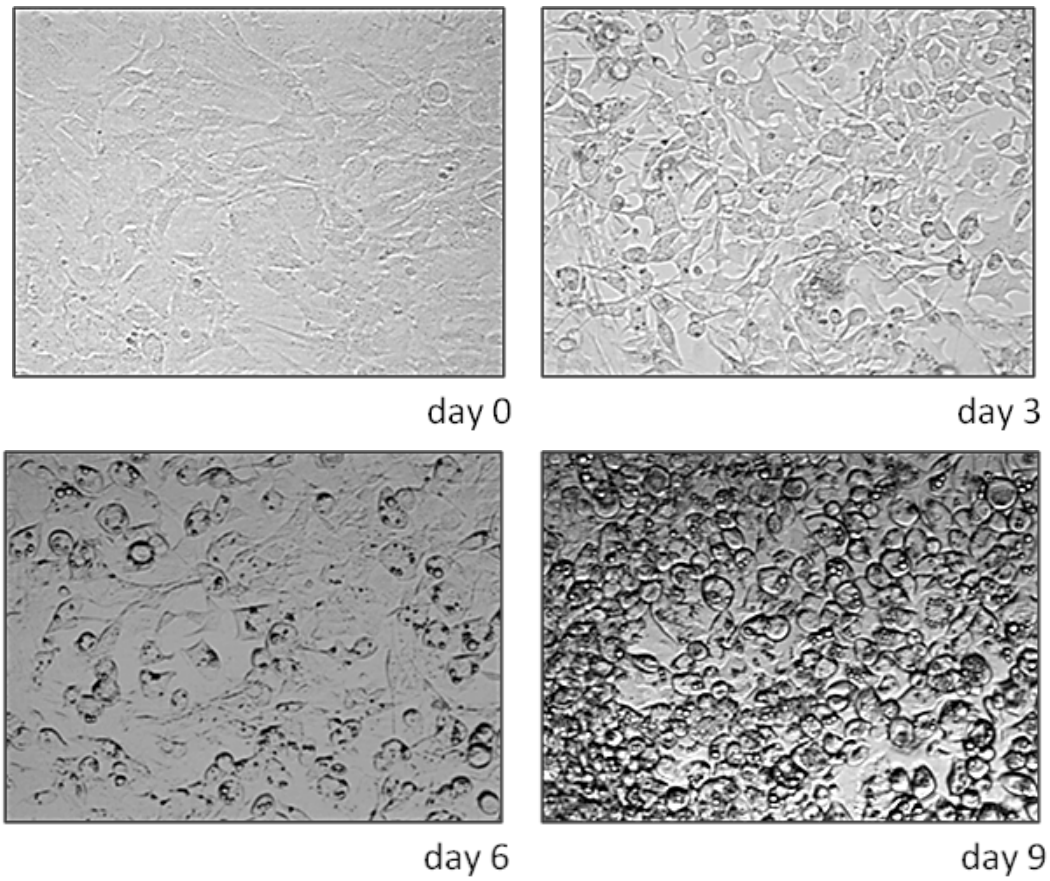

Figure 16: Morphological changes of 3T3-L1 cells during differentiation into adipocytes. 3T3-L1 preadipocytes were grown to confluence and differentiated into mature adipocytes with a medium containing dexamethasone, insulin and pioglitazone. Phase-contrast-microscopic pictures were taken at day 0, day 3, day 6 and day 9 (200x magnification).

At day 3 during differentiation, cells started to pull together and easily detached from the surface of the flask. At day 9 of differentiation, the cells appeared fully rounded and possessed numerous large lipid spheres. At this stage, 3T3-L1 cells were considered to be mature adipocytes.

3.2 Triglyceride accumulation in 3T3-L1 adipocytes

Intracellular lipid spheres within adipocytes differentiated from 3T3-L1 cells were visualized with Oil-Red O staining (figure 17). Oil-Red O is a lysochrome diazo dye to specifically stain neutral triglycerides and cholesterol lipids. The degree of the staining is acknowledged to be directly proportional with the degree of differentiation [57]. Triglyceride accumulation was exclusive in 3T3-L1 adipocytes, and absent in 3T3-L1 preadipocytes.

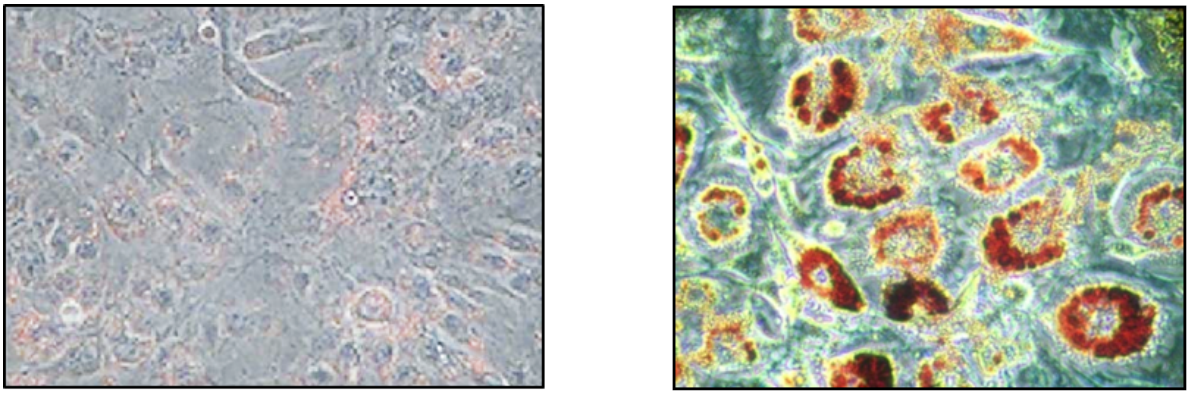

Figure 17: Oil-Red O staining in 3T3-L1 preadipocytes and adipocytes. Cells were differentiated into adipocytes for 9 days as previously described. Intracellular triglycerides were stained with Oil-Red O. Phase-contrast-microscopic pictures (400x magnification) were representative for at least three independent experiments and were taken at day 0 (preadipocytes) and day 9 (adipocytes).

3.3 Expression of PPARγ2 mRNA in 3T3-L1 preadipocytes and adipocytes

Adipogenesis is a complex cellular process regulated by PPARγ [143]. PPARγ2 mRNA became highly expressed in 3T3-L1 adipocytes compared to preadipocytes, as shown in figure 18. Therefore, the expression level of PPARγ could be directly correlated with the degree of differentiation and the degree of triglyceride accumulation.

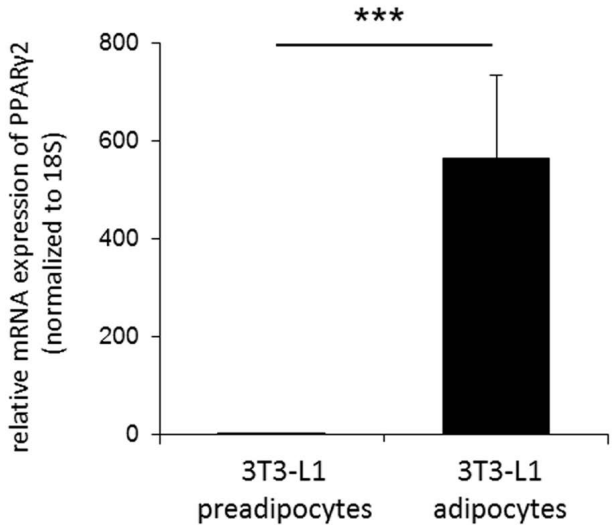

Figure 18: Expression of PPARγ2 mRNA in 3T3-L1 preadipocytes and adipocytes. 3T3-L1 preadipocytes were differentiated into adipocytes for 9 days as previously described. Total RNA of preadipocytes and adipocytes was extracted and analysed by qRT-PCR for murine PPARγ2. Data were normalized against 18S expression. Error bars represent the mean (± SD) of three independent experiments performed in triplicates. *** $p < 0,001$

3.4 PPARγ activation by partial and full agonists

3.4.1 PPARγ transactivation by partial and full agonists

For *in vitro* analysis, three compounds based on the structure of telmisartan were chosen to investigate the consequences of partial (telmisartan-like agonist) and full (pioglitazone-like agonist) PPARγ activation, and activation of PPARγ with a more potent agonist than pioglitazone.

From the first project period preliminary results were obtained about the influence of certain modifications on PPARγ activity. Using this knowledge, compounds with known or anticipated agonistic action were selected and compared with pioglitazone and telmisartan, respectively. To confirm the correct selection of compounds the degree of PPARγ activation was measured with a luciferase transactivation assay using Cos-7 cells transiently transfected with pGal4-hPPARγDEF and pGal5-Tk-pGL3. The basis of this system was the interaction of the Gal4 transcription factor fused with the hPPARγ-LBD and the Gal4 DBD. Dose-response curves are shown in figure 19A and structures of the selected compounds are shown in figure 19B. Pioglitazone was used as positive control and maximum activation was set to 100%. The basic scaffold of the telmisartan structure was chosen to represent the partial (telmisartan-like) agonist, here referred to as agonist 1. It achieved the same efficacy like telmisartan, but with less potency. Replacing the benzimidazole scaffold of agonist 1 with an 1H-naphto[2,3-d]imidazole in agonist 2 dramatically increased potency and efficacy compared to telmisartan, and turned it into a pioglitazone-like agonist for PPARγ. Potency of agonist 2 was very similar to the potency of pioglitazone. However, efficacy was lower (75% maximum activation; table 1). Based on the structure of agonist 2, but with an elongated alkyl chain, agonist 3 further increased potency and efficacy. Hence, agonist 3 became a full agonist, and more potent than pioglitazone. EC_{50}- and maximum activation values are demonstrated in table 2.

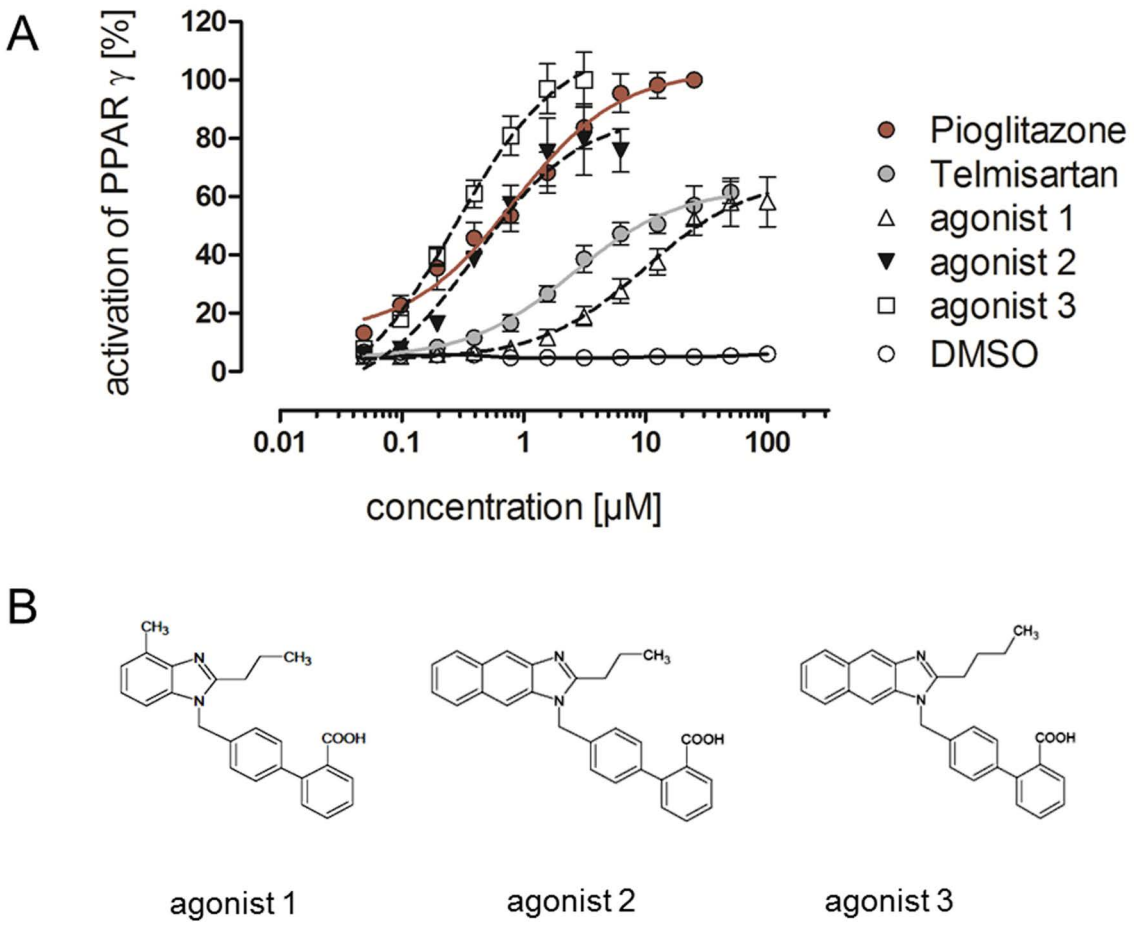

Figure 19: PPARγ-activation induced by agonists 1, 2 and 3 measured with transactivation assay. (A) COS-7 cells transiently transfected with pGal4-hPPARγDEF and pGal5-Tk-pGL3 were stimulated with the synthesized compounds 1, 2 and 3, and the reference substances pioglitazone (maximum activation was set to 100%) and telmisartan in a dose-dependent manner. Firefly luciferase activity was measured after 36h and normalized with activity of co-transfected pCMV-Renilla. Data points represent the mean (±SD) of three independent experiments. (B) Chemical structures of compounds 1, 2 and 3.

Dose-response curves of agonist 1 (published as compound 5) and agonist 2 (published as compound 9) confirmed results from Goebel et al. [133, 134].

Table 2: Overview of EC_{50}-values and efficacy after transactivation of the hPPARγ-LBD with agonist 1, 2 and 3, and control PPARγ agonists. Data represent the mean of three independent experiments calculated with GraphPad Prism 5.01 by the use of the dose-response curves (figures 19A). The maximal activation shows the highest relative PPARγ-activation triggered by the compounds in comparison to pioglitazone (=100%).

Compound	EC_{50} [µM]	efficacy [%]
Pioglitazone	0.83	100
Telmisartan	2.53	62
agonist 1	9.90	58
agonist 2	0.40	75
agonist 3	0.27	100

3.4.2 Differentiation of 3T3-L1 cells by partial and full agonists

Oil-red O staining demonstrates another technique for the assessment of cellular PPARγ activation. Overall, dose-dependent differentiation of 3T3-L1 cells (figure 20) confirmed the results from the transactivation assay. Pioglitazone and telmisartan were confirmed to be full and partial agonists for PPARγ, respectively. Absence of triglyceride accumulation in 3T3-L1 cells after treatment with DMSO proved that the activation of PPARγ was triggered by pioglitazone, telmisartan or the analyzed agonists. The differentiation pattern of agonist 2 and agonist 3 was similar to the degree of differentiation obtained with pioglitazone at 1µM and 10µM, but slightly weaker at 0.1µM treatment. And agonist 1 was confirmed to be a partial agonist like telmisartan with a lower differentiation pattern at 1µM, indicating a lower potency.

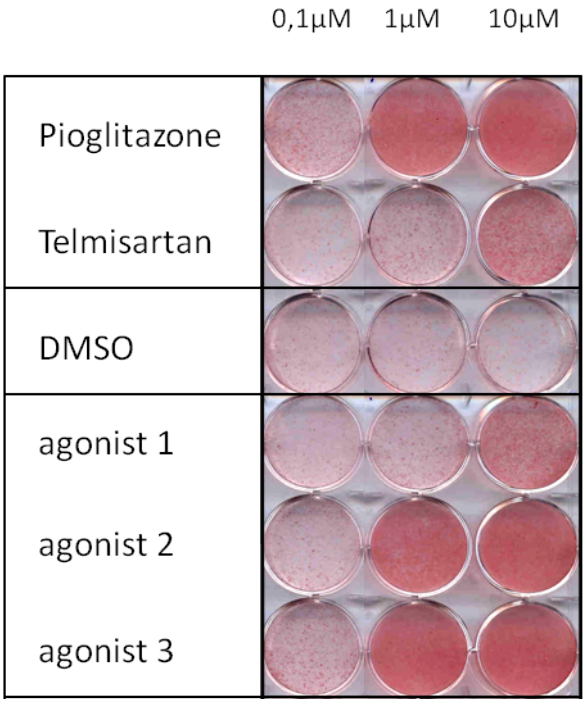

Figure 20: Differential PPARγ-ligand dependent adipocyte differentiation with partial and full agonists. 3T3-L1 cells were differentiated with pioglitazone, telmisartan and the agonists 1, 2 and 3 in three different concentrations (0.1µM; 1µM; 10µM). After 9 days Oil-Red O staining was performed. Picture is representative for three independent experiments.

3.4.3 Lipophilicity of specific partial and full agonists

Lipophilicity is one of the predominant factors influencing the pharmacokinetic behavior of a drug. It strongly affects absorption, distribution, metabolism and excretion of the pharmacological agent. Compounds with high lipophilicity are preferentially distributed to hydrophobic compartments. They passively and non-selectively diffuse the cell membrane to reach their intended target, but are often intensively metabolized. Compounds with low lipophilicity largely depend on active transport into the cell, however are more tissue selective with less adverse effects. Thus, an intermediate distribution coefficient (clogD-value) would be beneficial for optimal absorption, distribution, metabolism and excretion of a drug [144, 145].

Lipophilicity values of pioglitazone, telmisartan and the three agonists are shown in table 3. Modifications of the selected telmisartan-based compounds lowered clogD-values compared to telmisartan, and even to pioglitazone: telmisartan > pioglitazone > agonist 3 > agonist 2 > agonist 1.

Table 3: Lipophilicity of three selected synthesized compounds, pioglitazone and telmisartan. Lipophilicity is represented by clogD-values and was determined with MarvinSketch 5.4.0.0.

Compound	clogD (pH 7.4)
Pioglitazone	1.97
Telmisartan	2.34
agonist 1	1.64
agonist 2	1.80
agonist 3	1.95

3.4.4 Cofactor interaction of partial and full agonists

As described in detail above, transcriptional regulation of PPARγ target genes is highly dependent on the interaction of cofactors with the PPARγ-LBD. In this study, we were interested in differences of ligand-dependent corepressor release/ coactivator recruitment induced by graded PPARγ activators. Therefore, nuclear cofactor PPARγ-LBD binding studies using TR-FRET were performed. The dose-dependent release pattern of corepressor NCoR1 after binding to PPARγ is shown in figure 21.

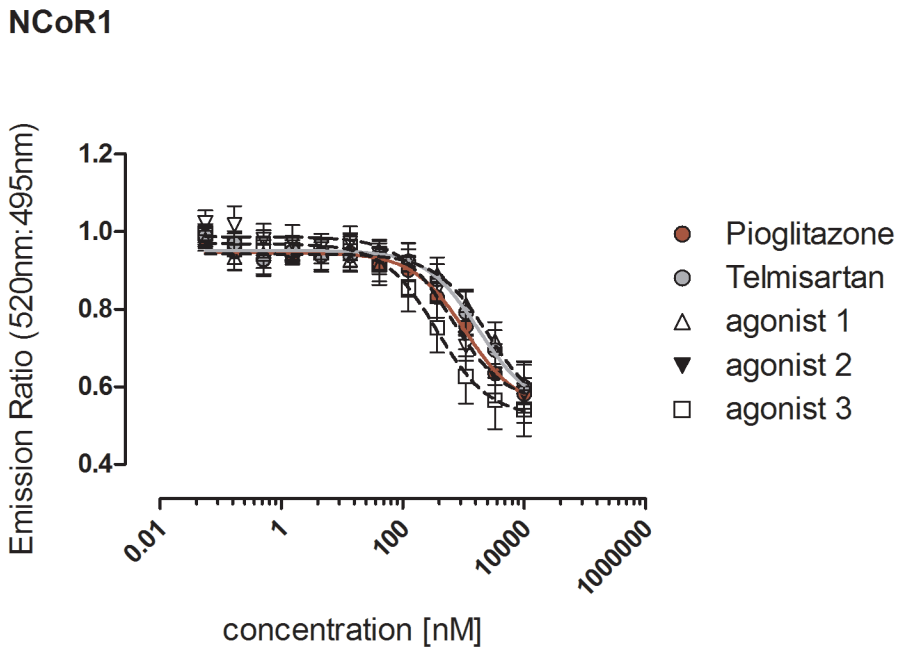

Figure 21: Release of cofactor NCoR1 by TR-FRET with partial and full agonists. Fluorescein-labeled corepressor NCoR1 was incubated with PPARγ ligand-binding domain protein labeled with terbium in the presence of increasing concentrations of the agonists 1, 2, 3, pioglitazone or telmisartan. FRET-signal was calculated as a ratio of 520nm (fluorescein) to 495nm (terbium) and was decreased upon ligand activated co-repressor displacement. Data were normalized to 1 and represent the mean (±SD) of three independent experiments.

Telmisartan and agonist 1 (telmisartan-like agonist) exhibited the same dose-dependent release of NCoR1, as well as pioglitazone and agonist 2 (pioglitazone-like agonist).

Binding of agonist 3 mediated a slightly more pronounced release of NCoR1 than pioglitazone, also demonstrated by a smaller area under the curve (AUC) compared to the other ligands (table 4).

Table 4: AUC for cofactor NCoR1 dissociation with partial and full agonists determined by TR-FRET assay. Data represent the mean of three independent experiments calculated by the use of TR-FRET dose-response curves of figure 21. Values were analyzed with GraphPad Prism 5.01 using the bottom baseline of each curve.

Compound	AUC
Pioglitazone	1.815
Telmisartan	1.878
agonist 1	1.916
agonist 2	1.916
agonist 3	1.697

A higher baseline of agonist 2 compensated the stronger release of corepressor NCoR1 and created the same AUC-value like agonist 1. Furthermore, coactivator peptides for SRC1 (steroid receptor coactivator 1), PGC-1α (PPARγ coactivator 1 α) and TRAP220 (thyroid hormone receptor-associated protein 220) were used for FRET assay. They represent members of the most important coactivator families which were shown to interact with PPARγ. SRC1 stimulates transactivation by histone acetyltransferase activity [146], PGC-1α induces a conformational change of the receptor permitting the binding of SRC1 and CBP/p300 [147], and TRAP220 is required for stable association of PPARγ with the mediator complex which facilitates recruitment of polymerase II [148]. Results of ligand-induced interaction of these coactivators with the PPARγ-LBD are shown in figures 22-24.

Strongest recruitment of SRC1 was induced by pioglitazone (figure 22). Agonist 2 and agonist 3 reached the same saturated level of SRC1 at 10µM, which was slightly lower compared to pioglitazone. However, agonist 3 presented a more pronounced effect than pioglitazone at intermediate concentrations. Telmisartan was hardly able to recruit SRC1, and the telmisartan-like agonist (agonist 1) didn't recruit SRC1.

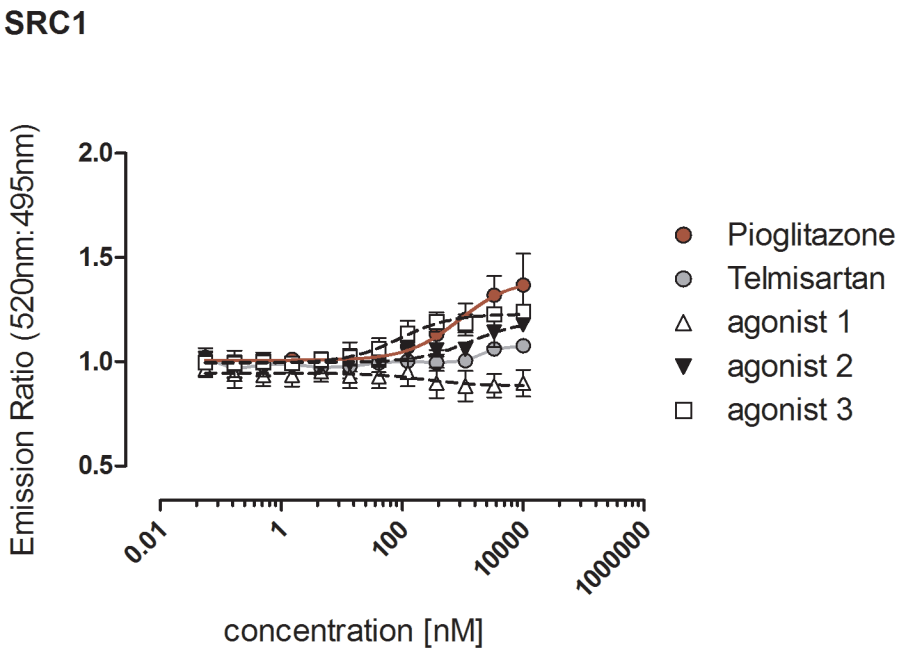

Figure 22: Recruitment of cofactor SRC1 by TR-FRET with partial and full agonists. Fluorescein-labeled coactivator SRC1 was incubated with PPARγ ligand-binding domain protein labeled with terbium in the presence of increasing concentrations of the synthesized compounds 1, 2, 3, pioglitazone or telmisartan. FRET-signal increased when terbium and fluorescein are in close proximity. Recruitment of SRC1 was calculated as a ratio of 520nm (fluorescein) to 495nm (terbium). Data were normalized to 1 and represent the mean (±SD) of three independent experiments.

The highest dose-response curve for PGC-1α recruitment was detected with agonist 3 (figure 23). Lower recruitment levels were obtained with pioglitazone and pioglitazone-like agonist (agonist 2), whereas their dose-response curves were almost identical. Recruitment of PGC-1α by telmisartan was very weak, and only detectable at high ligand concentrations. Agonist 1 was not able to recruit PGC-1α.

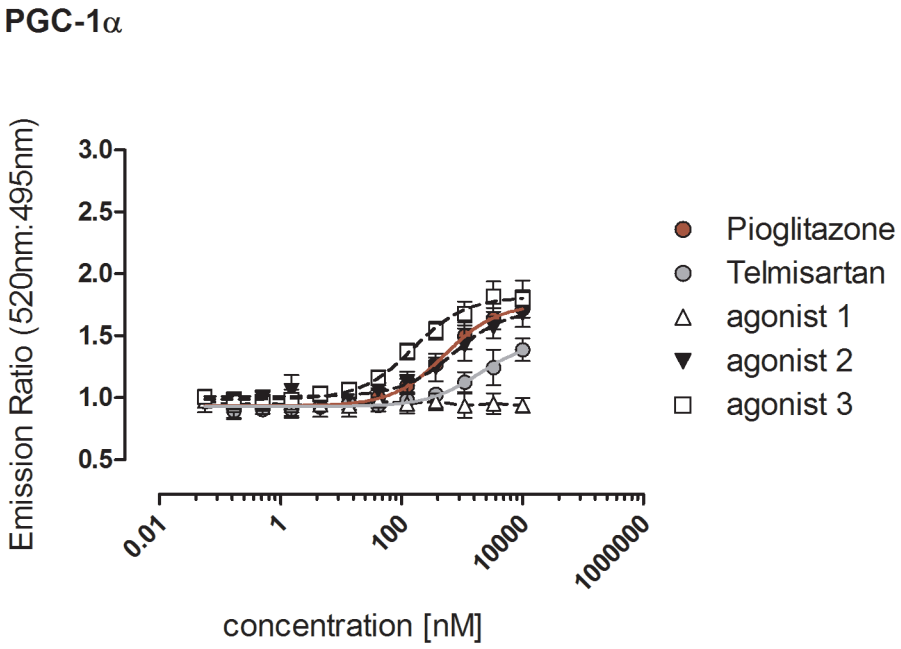

Figure 23: Recruitment of cofactor PGC-1α by TR-FRET with partial and full agonists. Fluorescein-labeled coactivator PGC-1α was incubated with PPARγ ligand-binding domain protein labeled with terbium in the presence of increasing concentrations of the synthesized compounds 1, 2, 3, pioglitazone or telmisartan. FRET-signal increased when terbium and fluorescein are in close proximity. Recruitment of PGC-1α was calculated as a ratio of 520nm (fluorescein) to 495nm (terbium). Data were normalized to 1 and represent the mean (±SD) of three independent experiments.

The coactivator TRAP220 was strongly recruited by pioglitazone (figure 24). Only half of this level was achieved with agonist 2 and agonist 3 in saturated conditions. However, the recruitment of TRAP220 with agonist 3 was higher with agonist 2, and similar to pioglitazone at intermediate concentrations. Telmisartan was hardly able to recruit TRAP220, and agonist 1 didn't show any interaction with the coactivator TRAP220.

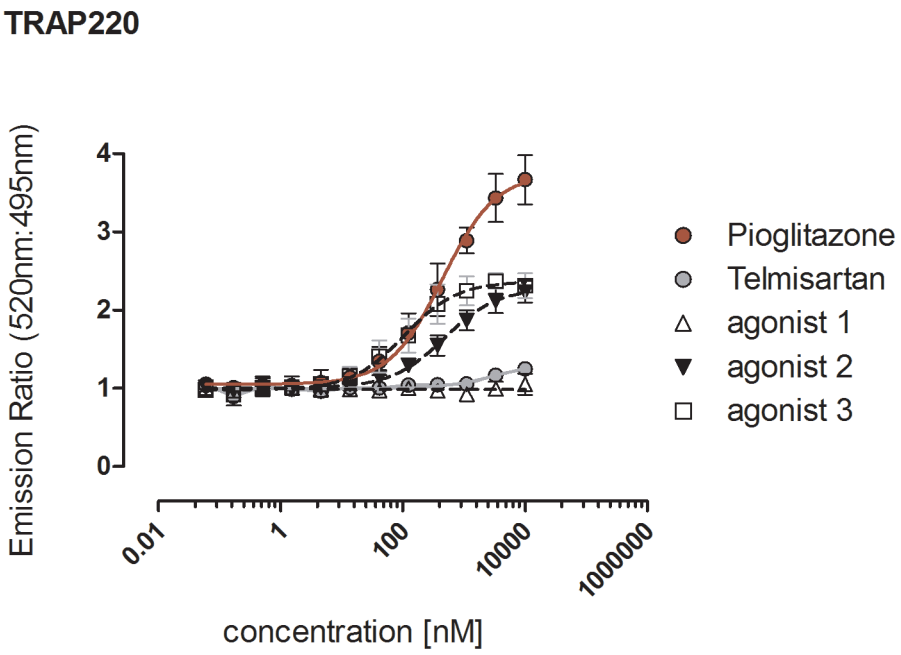

Figure 24: Recruitment of cofactor TRAP220 by TR-FRET with partial and full agonists. Fluorescein-labeled coactivator TRAP220 was incubated with PPARγ ligand-binding domain protein labeled with terbium in the presence of increasing concentrations of the synthesized compounds 1, 2, 3 pioglitazone or telmisartan. FRET-signal increased when terbium and fluorescein are in close proximity. Recruitment of TRAP220 was calculated as a ratio of 520nm (fluorescein) to 495nm (terbium). Data were normalized to 1 and represent the mean (±SD) of three independent experiments.

An overview of the results from the FRET assay is shown in table 5. The highest AUC-value represented the strongest coactivator recruitment.

Table 5: AUC-values for recruitment of the coactivators SRC1, PGC-1α and TRAP220 with partial and full agonists determined by TR-FRET assay. Data represent the mean of three independent experiments calculated from TR-FRET dose response curves shown in figure 22-24. Values were analyzed with GraphPad Prism 5.01 using the bottom baseline of each curve. n.r.: no recruitment

	AUC		
Compound	SRC1	PGC-1α	TRAP220
Pioglitazone	0.463	1.114	3.494
Telmisartan	0.098	0.515	0.206
agonist 1	n.r.	n.r.	n.r.
agonist 2	0.252	1.206	1.884
agonist 3	0.525	1.758	2.841

Agonist 1 was not able to recruit any of the three coactivators. However, pioglitazone, agonist 2 (pioglitazone-like PPARγ agonist) and agonist 3 (PPARγ agonist more potent than pioglitazone) revealed a preference for TRAP220 > PGC-1α > SRC1. Telmisartan instead, preferred PGC-1α > TRAP220 > SRC1, but all three of them in a weak manner.

3.4.5 Gene expression during adipogenesis induced by partial and full agonists

3.4.5.1 Expression of PPARγ target genes at day 6 during 3T3-L1 differentiation

Further interest concerned differences in gene expression of partial and full PPARγ activators. Therefore, known PPARγ target genes which were involved in energy metabolism were selected for pilot experiments. 3T3-L1 cells were differentiated with the indicated compounds (pioglitazone, telmisartan, agonist 1, agonist 2, agonist 3 at

10µM). Day 6 during differentiation was chosen for measurement of mRNA expression. At that time point, 3T3-L1 cells were not completely differentiated by full PPARγ agonists, but were already dedicated to a committed cell-fate. Furthermore, PPARγ mRNA expression is still increasing at day 6 [149]. In mature adipocytes, PPARγ agonists were shown to auto-regulate receptor expression, probably to protect the cell from hyperactivity [150]. Strongest down-regulation of PPARγ expression was observed with full PPARγ agonists [151].

Depending on different PPARγ activation potential of the indicated compounds, cells resided in a diverse differentiation status. These status can be monitored in the gene expression of ap2 (figure 25B). The ap2 protein is a carrier for FAs, responsible for their transfer between extra- and intracellular membranes, and expression of ap2 gradually increases during adipogenesis [152]. Data from qRT-PCR confirmed transactivation results. Highest mRNA expression of ap2 was measured after treatment with agonist 3. Expression level of ap2 was slightly lower with pioglitazone and agonist 2 treatments, and telmisartan and agonist 1 showed only half of the ap2 expression level or lower, compared to pioglitazone.

Adiponectin is exclusively secreted from adipose tissue into the bloodstream and regulates energy homeostasis, glucose and lipid metabolism [153]. High adiponectin expression was shown to be beneficial against insulin resistance and type 2 diabetes mellitus [154]. Adiponectin mRNA expression was up-regulated by pioglitazone, telmisartan, agonist 2 and agonist 3 (figure 25A). Agonist 1 treated cells showed only low adiponectin mRNA expression at day 6 during differentiation.

Resistin is a cytocine secreted by adipose tissue in rodents [155]. Evidence of *in vivo* experiments connected elevated resistin levels with the development of insulin resistance [86]. Expression of resistin mRNA with agonist 2 and agonist 3 was higher during differentiation of 3T3-L1 cells at day 6, than with pioglitazone and telmisartan treatment. Resistin expression with agonist 1 was considerably lower than with telmisartan, and even more pronounced than with pioglitazone (figure 25C).

Another gene selected for pilot studies was CD36. CD36 is an integral membrane glycoprotein which is involved in FA and glucose metabolism. Mice deficient for CD36 exhibit a defect in FA uptake by several tissues and develop insulin resistance [156, 157]. During differentiation of 3T3-L1 cells, CD36 mRNA expression was directly correlated to the activation status of PPARγ (figure 25D).

To resume, expression of mRNA for all four genes was dependent on the level of differentiation.

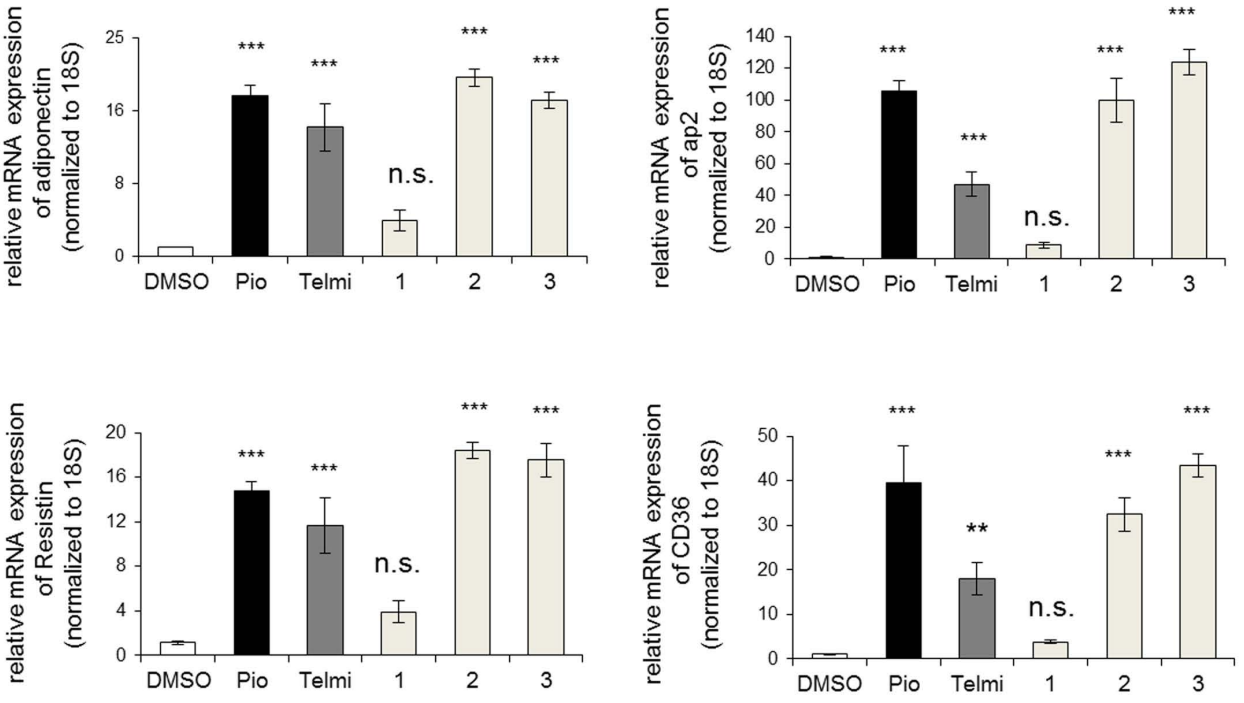

Figure 25: mRNA expression of PPARγ target genes at day 6 of 3T3-L1 differentiation. 3T3-L1 preadipocytes were differentiated with agonists 1, 2, 3, pioglitazone or telmisartan as previously described. Total RNA was extracted at day 6 during differentiation and relative mRNA expression of murine (A) adiponectin, (B) ap2, (C) resistin and (D) CD36 was analyzed by quantitative real-time PCR. Data were normalized against 18S expression. Error bars represent the mean (± SD) of three independent experiments performed in triplicates. ** $p < 0.01$ vs. DMSO; *** $p < 0.001$ vs. DMSO; n.s. not significant

3.4.5.2 Transcriptome analysis at day 6 during 3T3-L1 differentiation

Global transcriptional microarray analyses using Illumina's MouseWG-6 v2.0 Expression BeadChip Kit were performed to detect differentially expressed genes independent of the differentiation status of the cells. Six microarrays were performed in triplicates and fold-changes were calculated versus the DMSO control chip (table 17). Additionally, table 17 containes the number of genes with a signicicantly changed mRNA level and a cut off $\log_2$ fold-change < -1 or > 1 and a p-value < 0.01.

Table 6: Overview about the data set of microarray analyses. 3T3-L1 cells were differentiated with medium containing dexamethasone (1 µM), insulin (0.17 µM), and pioglitazone (10µM), telmisartan (10µM), agonist 1 (10µM), agonist 2 (10µM) or agonist 3 (10µM), respectively. At day 6 during differentiation mRNA was extracted and pepared for hybridization on Illumina's MouseWG-6 v2.0 Expression BeadChip. Resulting data were related to DMSO and analyzed using the program R. Calculated fold-changes with a $\log_2$ cut off value < -1 or > 1 and p-value < 0.01 were considered as significant. The number of genes with an altered mRNA level for each data set is shown in the last column.

Data set	Combination	Number of differentially expressed genes
1	Pioglitazone vs. DMSO	1348
2	Telmisartan vs. DMSO	669
3	agonist 1 vs. DMSO	589
4	agonist 2 vs. DMSO	1169
5	agonist 3 vs. DMSO	1185

The microarray expression data were characterized by using principal component (PC) analysis. PC mapping reduces dimensionality of transformed data to reveal its variance in the most informative point of view. PC 1 predominantly discriminated DMSO from the other samples, since cells treated with DMSO didn't undergo adipogenesis. Furthermore, both PCs discriminated telmisartan and agonist 1 samples from

pioglitazone, agonist 2 and agonist 3 samples. Hence, telmisartan and agonist 1 (group 1), as well as pioglitazone, agonist 2 and agonist 3 (group 2) demonstrated a similar gene expression profile (figure 26).

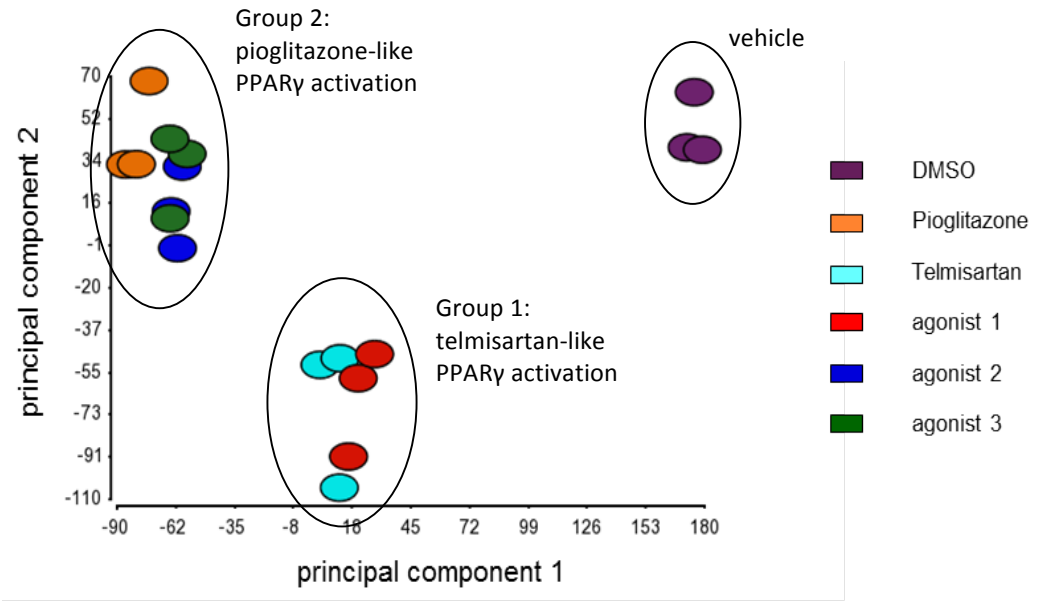

Figure 26: Principal component analysis of microarray analyses. PCA shows the internal structure of the gene expression dataset for 3T3-L1 cells treated with pioglitazone, telmisartan, agonists 1, 2, 3 or DMSO for 6 days. PC 1 represented the greatest dataset variance with 37.2%. PC 2 shows with 13.2% the second greatest data set variance. PCA was performed using Partek Genomic Suite.

The further aim was to find differentially expressed genes between all performed and analyzed microarrays. Therefore, an intersection between all data sets was generated. In total 463 genes were detected, as shown in a venn diagram demonstrated in figure 27. From 463 genes, 69 genes were hypothetically and functionally uncharacterized, and for that reason excluded from further analyses. The intersected genes were further investigated regarding differential gene expression independent of differentiation. Genes which didn't pursue the following differentiation pattern of strongest activation by agonist 3 and pioglitazone > agonist 2 > telmisartan > agonist 1 were selected.

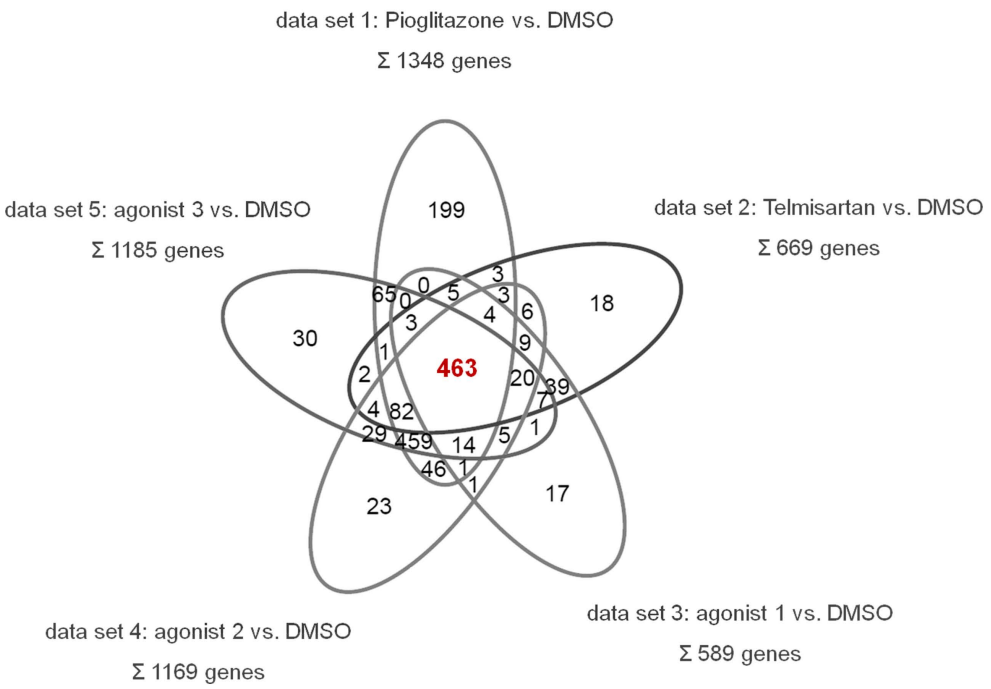

Figure 27: Venn diagram showing the intersection of differentially expressed genes. 3T3-L1 cells were differentiated with pioglitazone (10µM), telmisartan (10µM), agonist 1 (10µM), agonist 2 (10µM) or agonist 3 (10µM), respectively. At day 6 during differentiation mRNA was extracted and pepared for hybridization on Illumina's MouseWG-6 v2.0 Expression BeadChip. Numbers were calculated using the program R.

Due to morphological and functional changes during adipogenesis most of the 394 genes were either implicated in metabolic (163 genes, p-value 1.2E-6) or in cellular processes (198 genes, p-value 4.2E-6). Several pathways, including the citrate cycle, pyruvate metabolism, PPAR signaling, FA metabolism and arachidonic acid metabolism were involved and hierarchically clustered. The expression level of these genes is demonstrated in a heat map shown in figure 28.

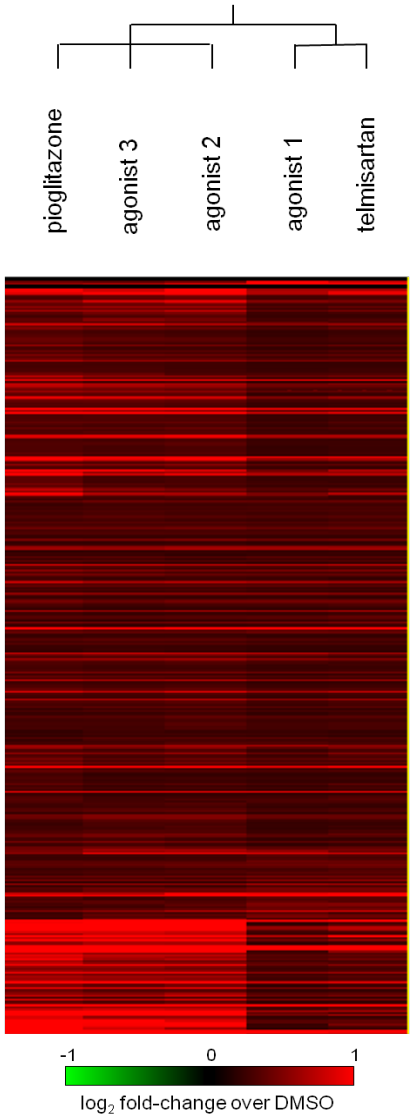

Figure 28: Heat map representing the gene expression level of 3T3-L1 cells after treatment with partial and full PPARγ agonists at day 6 during differentiation. Microarray data sets were generated using R programming. The 394 genes were clustered with Cluster-TreeView. Data represent the mean of three technical replicas. (p-value < 0.01 and log_2-fold chance < -1 or > 1)

All 394 genes exhibited an increased mRNA level compared to DMSO. However, different shades of red in the heat map indicate different expression levels. For easier detection and a more clear representation of selective gene expression, mean hierarchical clustering was applied. Results are shown in figure 29. For mean clustering, the mean expression level of all treatment groups was calculated for each gene.

Expression lower and expression higher than the mean were displayed in different colors. Furthermore, the hierarchy showed a strong relationship between the regulated genes of data set 2 and 3, and a strong relationship between data set 1, data set 4 and data set 5.

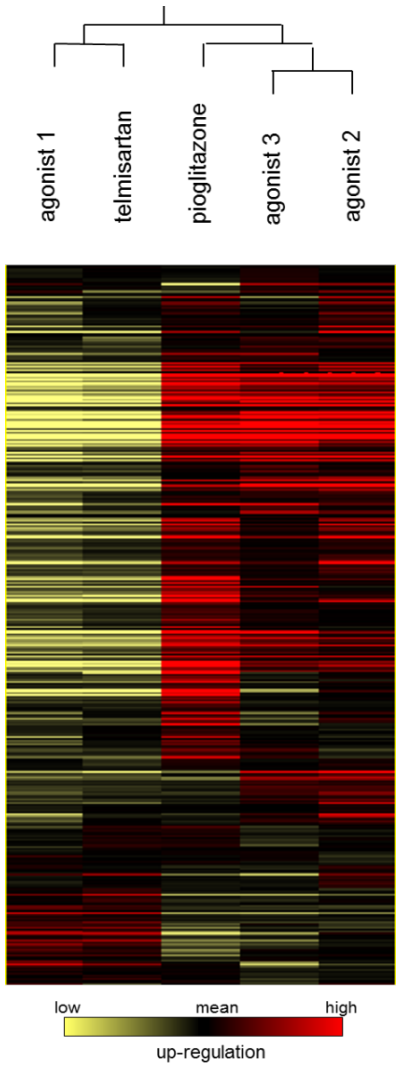

Figure 29: Heat map representing mean hierarchical clustering. 3T3-L1 cells were treated with different PPARγ agonists, and mRNA was extracted at day 6 during differentiation. The microarray data-set was generated using R (p-value < 0.01 and $\log_2$-fold chance < -1 or > 1). Differentially regulated genes of the intersection of all five treatment groups were hierarchically mean-clustered with Cluster-TreeView, applying the mean gene expression of all treatment groups for each gene. Data represent the mean of three technical replicas.

Genes which play a role in energy metabolism and which were found to an increased mRNA level by the different PPARγ agonists were chosen, and are shown in figure 30. Corresponding fold-changes were summarized in table 7.

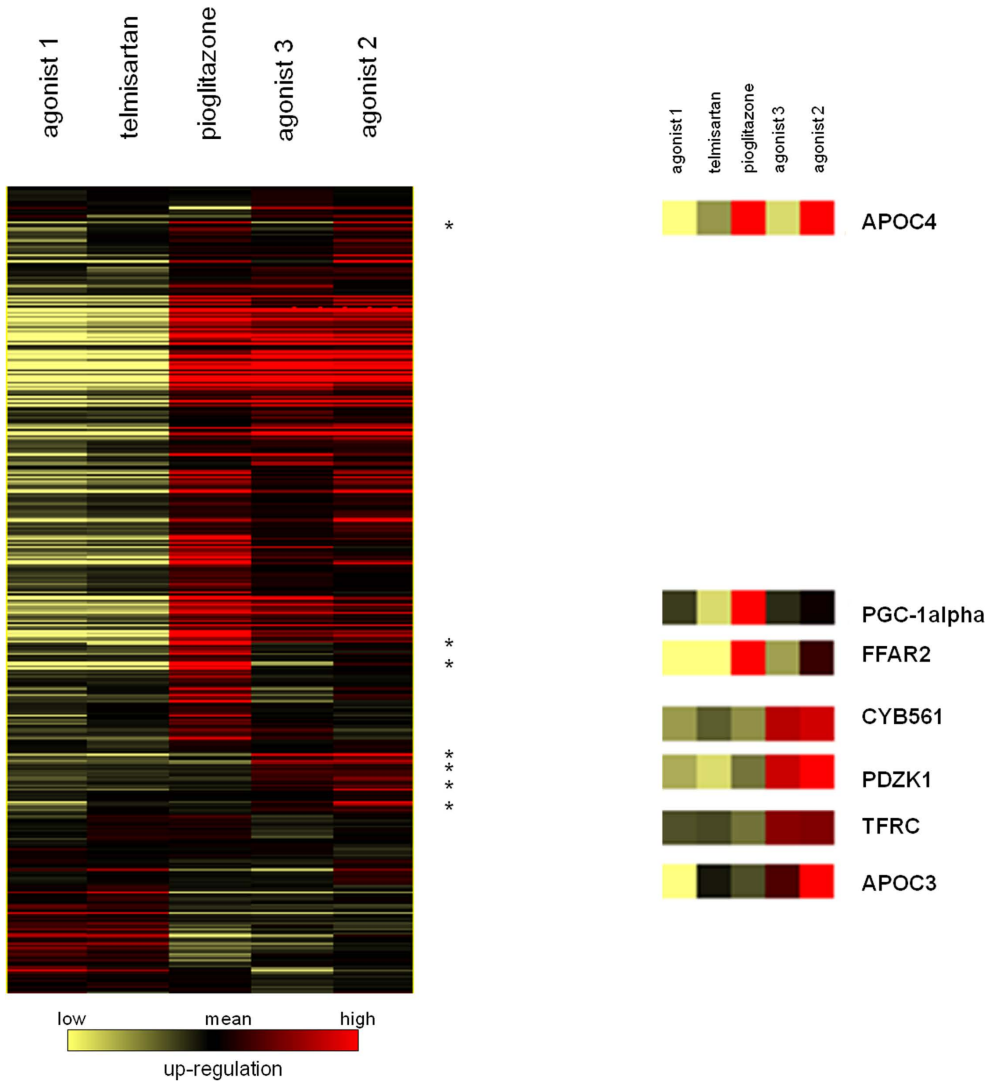

Figure 30: Mean hierarchical cluster and selective gene expression. 3T3-L1 cells were treated with different PPARγ agonists, and mRNA was extracted during day 6 of differentiation. Microarray data was processed using R programming (p-value < 0.01 and log_2-fold chance < -1 or > 1), and mean hierarchically clustered. Emphasized genes are selectively expressed and involved in metabolic processes.

Table 7: Fold-change of differentially expressed genes.

RefSeq	Symbol	Name	log_2 fold-change over DMSO				
			agonist 1	telmisartan	pioglitazone	agonist 3	agonist 2
NM_007805	CYB561	cytochrome b-561	2,41	2,89	2,49	5,06	5,26
NM_011638	TFRC	transferrin receptor	4,71	4,77	4,44	6,42	6,36
NM_001146001	PDZK1	PDZ domain containing 1	5,15	4,77	5,58	8,10	8,91
NM_008904	PGC-1α	PPAR gamma coactivator 1 alpha	4,62	3,37	7,54	4,74	5,19
NM_023114	APOC3	apolipoprotein C-III	6,86	9,14	8,71	9,93	11,98
NM_007385	APOC4	apolipoprotein C-IV	7,14	9,20	13,01	8,66	13,93
NM_001168512	FFAR2	free fatty acid receptor 2	13,47	10,90	42,37	20,72	22,42

Genes differentially regulated within group 1 (telmisartan-like activation) or group 2 (pioglitazone-like activation) were considered to be differentially expressed. Most of the genes listed on table 11 play a role in lipid metabolism. The biological function of these genes will be described in the discussion (4.1). Expression of cofactor PGC-1α measured by qPCR confirmed microarray expression data (figure 31). High PGC-1α expression was determined after pioglitazone treatment, but not in cells after treatment with the agonists 2 and 3. Although these three compounds are full activators of PPARγ, they differentially induced PGC-1α mRNA expression level.

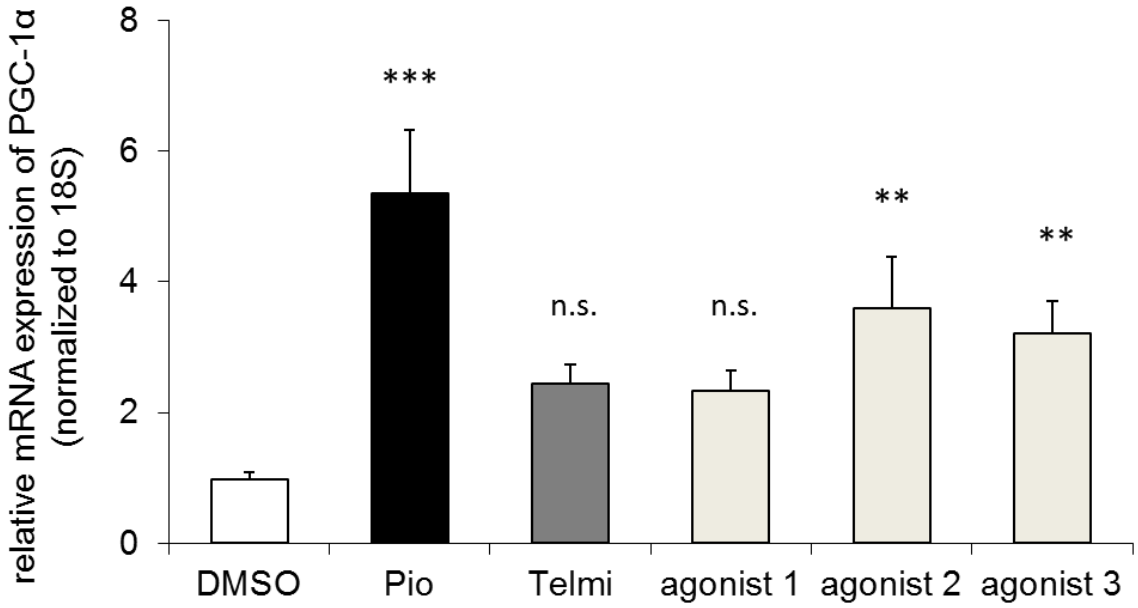

Figure 31: mRNA expression of PGC-1α at day 6 during differentiation with different PPARγ agonists. Data was analyzed by qPCR and normalized against 18S expression. Error bars represent the mean (± SD) of three independent experiments performed in triplicates. *** $p < 0.001$ vs. DMSO; ** $p < 0.01$ vs. DMSO; n.s. not significant

3.4.6 Glucose uptake with partial and full agonists

Besides the skeletal muscle, adipose tissue is the primary target of insulin-mediated glucose uptake. Basal glucose transport is very low, however, after an insulin stimulus glucose transporters are translocated from the cytoplasm to the plasma membrane, effecting glucose transport into the cell. The concentration gradient is the major determinant of glucose flux. In adipose tissue, GLUT4 is the predominant contributor of insulin-induced glucose transport. Yet, GLUT1 is expressed to a lower extent. In insulin resistant cells glucose transport is strongly attenuated and recruitment of glucose transporters to the plasma membrane is decreased in presence of insulin [158, 159]. To compare insulin sensitivity after treatment with different PPARγ agonists, mature adipocytes differentiated from 3T3-L1 cells were stimulated with the indicated compounds for 72h. Results are shown in figure 32. In the basal state glucose uptake was increased with pioglitazone and pioglitazone-like PPARγ activators (pioglitazone,

agonist 2, agonist 3), but not with telmisartan and the telmisartan-like PPARγ activator (agonist 1). Uptake of glucose into adipocytes with insulin stimulation was increased in all treatment groups, but represented highest significant results with pioglitazone incubation.

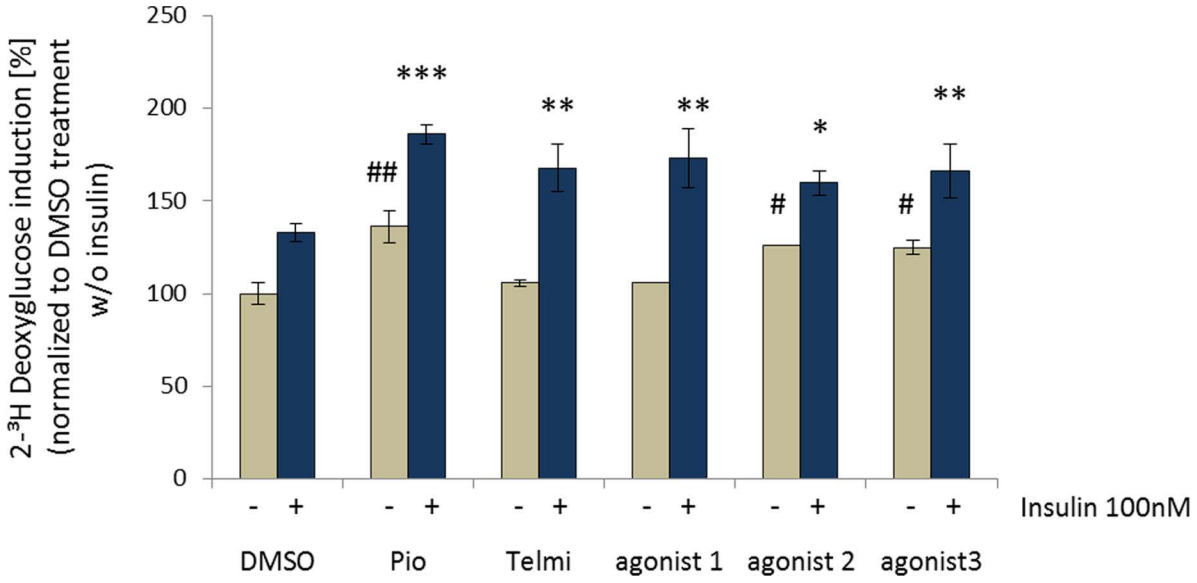

Figure 32: Deoxyglucose uptake in mature 3T3-L1 adipocytes after incubation with PPARγ agonists for 72h. Cells were differentiated into mature adipocytes with medium containing dexamethasone, insulin and IBMX for 9 days and incubated with pioglitazone or telmisartan, agonist 1, 2, 3, DMSO (at 10µM respectively) for 72h. To determine glucose uptake, cells were stimulated with and without insulin and incubated with ^{3}H-labeled deoxy-D-glucose. Radioactivity was measured with a β-counter. Data was normalized to DMSO treatment without insulin stimulation. Results are representative for 3 independent experiments performed in duplicates. Treatment without insulin stimulation: # $p < 0.05$ vs. DMSO; ## $p < 0.01$ vs DMSO; Treatment with insulin stimulation: * $p < 0.05$ vs. DMSO; ** $p < 0.01$ vs. DMSO; *** $p < 0.001$ vs. DMSO.

3.5 PPARγ activation – importance of position 5 and 6 of the telmisartan scaffold

3.5.1 Relevance of position 5 and 6 of the telmisartan scaffold for PPARγ transactivation

In previous work of our group, a selection of telmisartan-derived compounds with different lipophilic moieties at position 5 or 6 of the telmisartan scaffold was demonstrated to influence PPARγ activity [135]. To get closer insight into the relevance of these positions, six compounds with benzimidazole (agonists 4), benzofurane (agonists 5) or benzothiophene (agonists 6) moieties either at position 5 or position 6 of the telmisartan scaffold were used for the investigation. The first number in the nomenclature stands for the compound number, and the second number represents the position of the moiety. Dose-response curves for PPARγ activation by agonists 4-5 and 4-6 with a benzimidazole moiety are shown in figure 33. Transactivation assays were performed as described above. Since agonist 4-6 possesses almost the same structure like telmisartan, their dose-response curves for PPARγ transactivation were identical. The shift of the benzimidazole moiety from position 6 to position 5 implemented an identical dose-response curve to telmisartan and agonist 4-6 in low concentrations, but a decreased efficacy.

The replacement of the benzimidazole moiety with a benzofuran moiety at position 6 increased efficacy and potency compared to telmisartan (figure 34). Potency was even more pronounced compared to pioglitazone, but efficacy remained lower than efficacy of pioglitazone. The shift of the benzofuran moiety to position 5 strongly decreased potency and efficacy, although potency was still higher compared to telmisartan.

The presence of a benzothiophene moiety at position 6 also increased efficacy and potency compared to telmisartan (figure 35). The dose-response curve was very similar to the curve of pioglitazone, but with a slightly lower efficacy. The shift to position 5 decreased efficacy and potency similar to agonist 5-5.

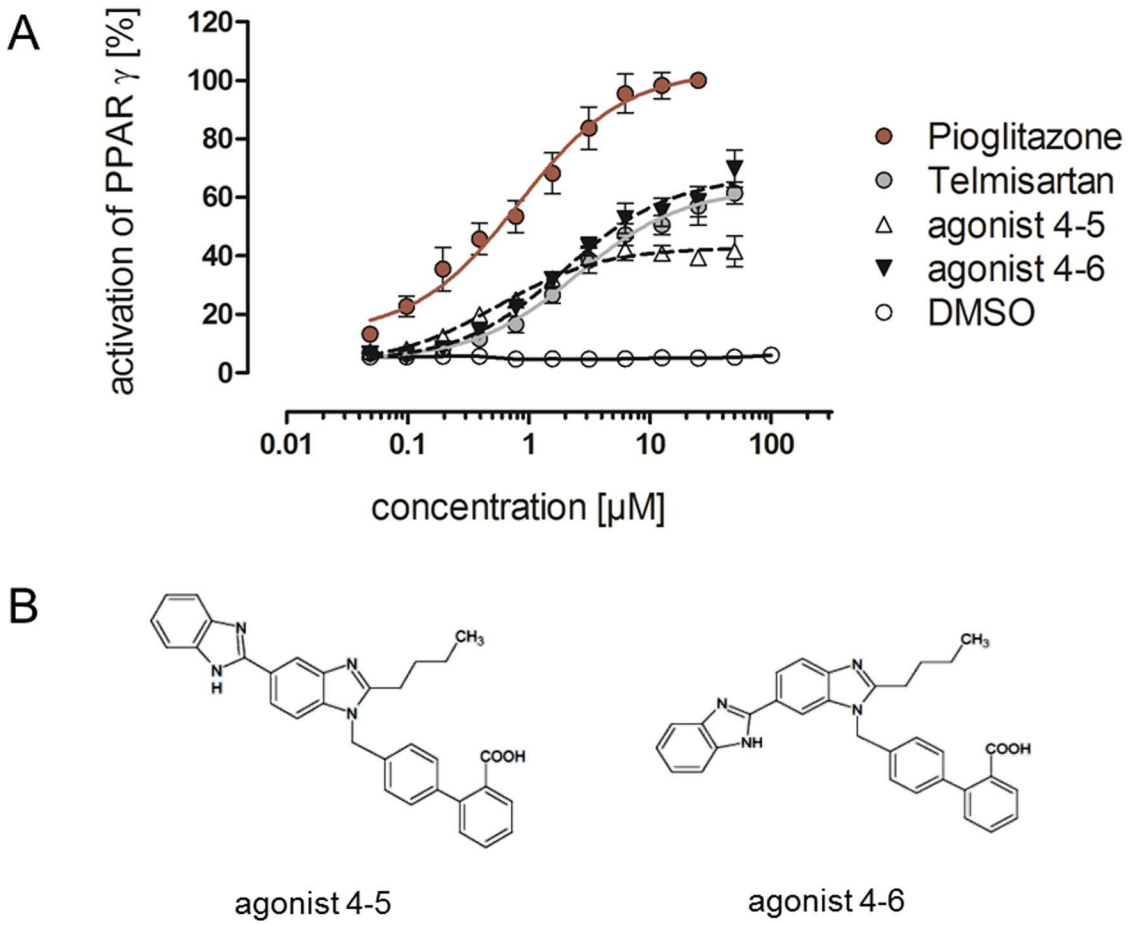

Figure 33: PPARγ-activation induced by agonists 4-5 and 4-6 measured with transactivation assay. (A) Cos-7 cells transiently transfected with pGal4-hPPARγDEF and pGal5-Tk-pGL3 were stimulated with the synthesized compounds 4-5 and 4-6, and the reference substances pioglitazone (maximum activation was set to 100%) and telmisartan in a dose-dependent manner. Firefly luciferase activity was measured after 36h and normalized with activity of cotransfected pCMV-Renilla. Data points represent the mean (±SD) of three independent experiments. (B) Structure of agonists 4-5 and 4-6 with benzimidazole moiety.

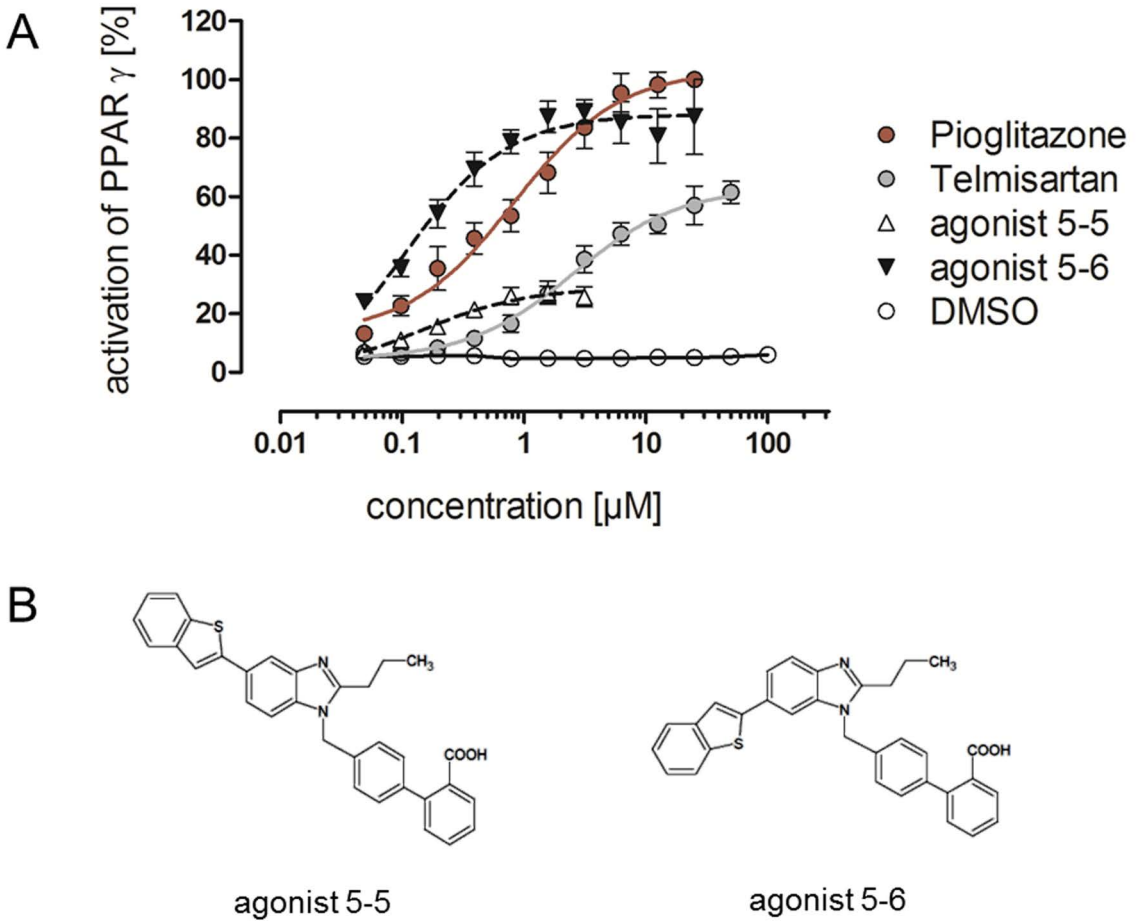

Figure 34: PPARγ-activation induced by agonists 5-5 and 5-6 measured with transactivation assay. (A) Cos-7 cells transiently transfected with pGal4-hPPARγDEF and pGal5-Tk-pGL3 were stimulated with the synthesized compounds 5-5 and 5-6, and the reference substances pioglitazone (maximum activation was set to 100%) and telmisartan in a dose-dependent manner. Firefly luciferase activity was measured after 36h and normalized with activity of co-transfected pCMV-Renilla. Data points represent the mean (±SD) of three independent experiments. (B) Structure of agonists 5-5 and 5-6 with benzofuran moiety.

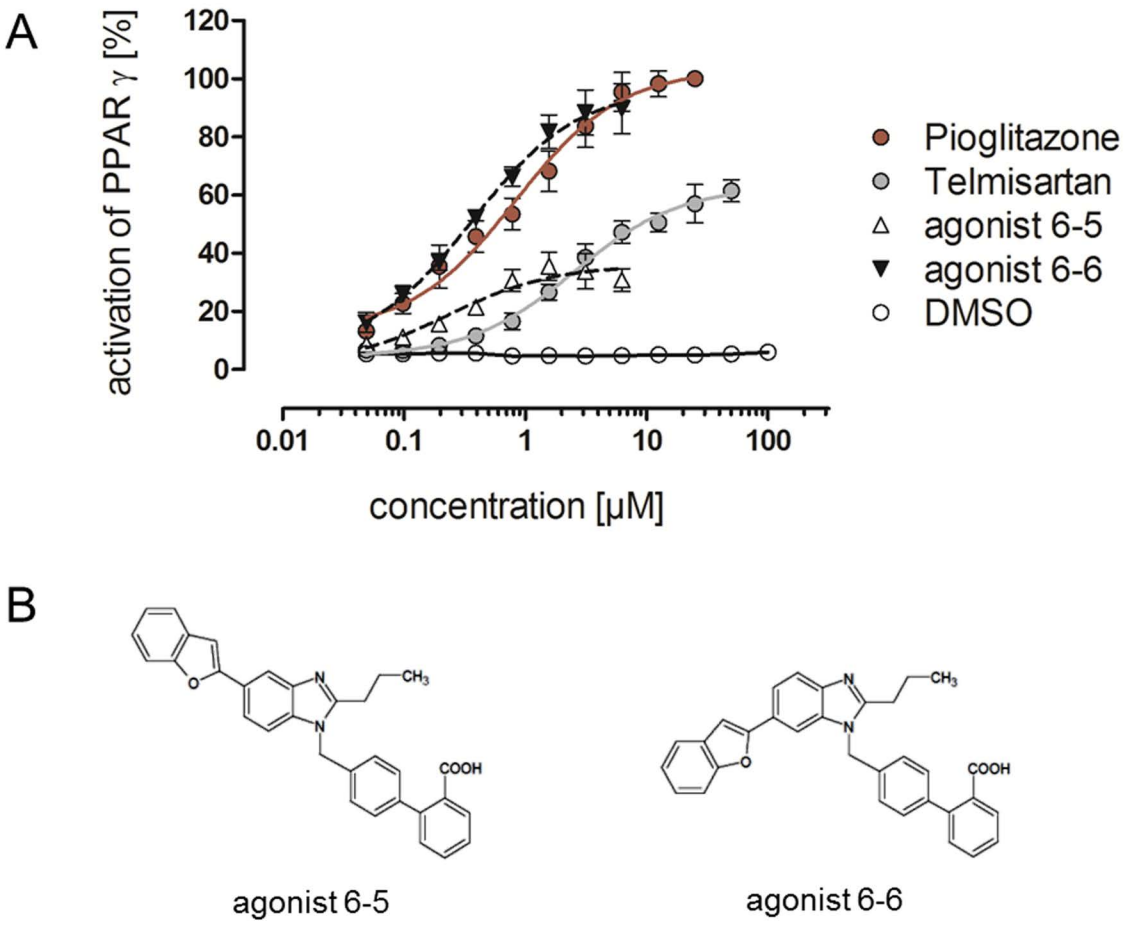

Figure 35: PPARγ-activation induced by agonists 6-5 and 6-6 measured with transactivation assay. (A) Cos-7 cells transiently transfected with pGal4-hPPARγDEF and pGal5-Tk-pGL3 were stimulated with the synthesized compounds 6-5 and 6-6, and the reference substances pioglitazone (maximum activation was set to 100%) and telmisartan in a dose-dependent manner. Firefly luciferase activity was measured after 36h and normalized with activity of co-transfected pCMV-Renilla. Data points represent the mean (±SD) of three independent experiments. (B) Structure of agonists 6-5 and 6-6 with benzothiophene moiety.

A summary of EC_{50}-values and efficacy for all newly designed compounds, pioglitazone and telmisartan is demonstrated in table 8. All telmisartan-derived compounds showed lower EC_{50}-values compared to the telmisartan EC_{50}-value. Except from agonist 4-6 the EC_{50}-values were even lower compared to the EC_{50}-value of pioglitazone. Best results were obtained with agonists 5-5 and 5-6 containing a benzofuran moiety. The EC_{50}-value of agonist 5-6 was almost 10-times lower than the pioglitazone EC_{50}-value.

Table 8: Overview of EC_{50}-values and efficacy after transactivation of the hPPARγ-LBD with newly synthesized and control PPARγ agonists. Data represent the mean of three independent experiments calculated with GraphPad Prism 5.01 by the use of the dose response curves (figures 33-35). The maximal activation shows the highest relative PPARγ-activation triggered by the compounds in comparison to pioglitazone (=100%).

Compound	EC_{50} [µM]	efficacy [%]
Pioglitazone	0.83	100
Telmisartan	2.53	62
agonist 4-5	0.55	41
agonist 4-6	1.99	69
agonist 5-5	0.14	26
agonist 5-6	0.09	87
agonist 6-5	0.23	34
agonist 6-6	0.37	90

3.5.2 Relevance of position 5 and 6 of the telmisartan scaffold for the differentiation of 3T3-L1 cells

Oil-Red O staining (figure 36) confirmed the results from the transactivation assay. Experiments were performed as described before.

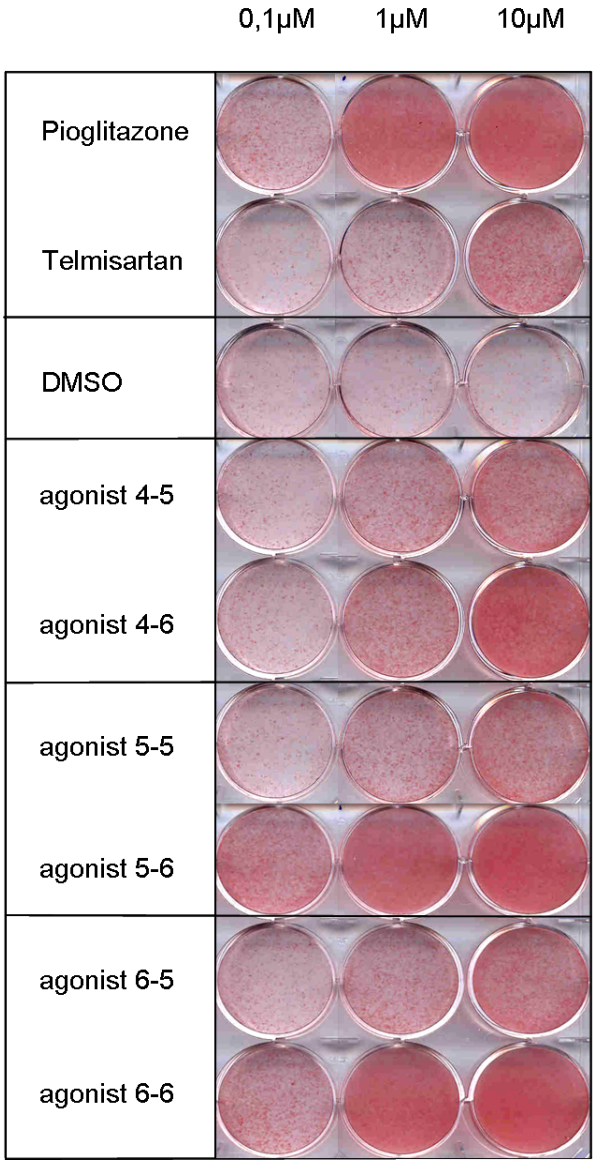

Figure 36: Differential PPARγ-ligand dependent adipocyte differentiation with compounds 4-5/6, 5-5/6 and 6-5/6. 3T3-L1 cells were differentiated with pioglitazone, telmisartan and the agonists 4-5/6 to 6-5/6 in three different concentrations (0.1µM; 1µM; 10µM). After 9 days Oil-Red O staining was performed. Picture is representative for three independent experiments.

Pioglitazone and telmisartan served as control and confirmed the differentiation pattern of a full and a partial agonist. Vehicle treatment didn't induce differentiation.

In accordance with results from the PPARγ-transactivation assay, cells treated with compound 5-6 and 6-6 exhibited the highest degree of adipocyte differentiation, and therefore the highest degree of PPARγ activation. All other partial agonist showed a similar differentiation pattern like telmisartan. At 10μM, agonist 4-6 was more efficicous than agonist 4-5.

3.5.3 Lipophilicity of agonists with different moieties at position 5 and 6

Lipophilicity increased considerably with the new compounds compared to telmisartan (table 9). Highest clogD-values were obtained with the agonists 5-5 and 5-6.

Table 9: Lipophilicity of newly synthesized compounds, pioglitazone and telmisartan. Lipophilicity is represented by clogD-values, determined with MarvinSketch 5.4.0.0.

Compound	clogD (pH 7.4)
Pioglitazone	1.97
Telmisartan	2.34
agonist 4-5	4.51
agonist 4-6	4.51
agonist 5-5	5.39
agonist 5-6	5.39
agonist 6-5	4.46
agonist 6-6	4.46

3.5.4 Relevance of position 5 and 6 for cofactor interaction

Cofactor interaction with the PPARγ-LBD after binding of the newly designed ligands was studied using FRET assay as described before. At first, release of corepressor NCoR1 was elucidated and dose-response curves were demonstrated in figure 37. Compounds with strong PPARγ activation properties like 5-6 and 6-6 showed a strong dose-dependent release of NCoR1.

An overview of calculated AUC-values for corepressor release is listed in table 10. Strongest release was represented by the lowest AUC, and could be sorted from strong to weak release: agonist 5-6 > agonist 6-6 > agonist 5-5 > agonist 6-5 > pioglitazone > agonist 4-5 > telmisartan > agonist 4-6.

Table 10: AUC-values for release of corepressor NCoR1 with newly synthesized compounds determined by TR-FRET assay. Data represent the mean of three independent experiments calculated by the use of TR-FRET dose response curves in figure 37. Values were analyzed with GraphPad Prism 5.01 using the bottom baseline of each curve.

Compound	AUC
Pioglitazone	1.815
Telmisartan	1.878
agonist 4-5	1.858
agonist 4-6	2.031
agonist 5-5	1.654
agonist 5-6	1.305
agonist 6-5	1.823
agonist 6-6	1.652

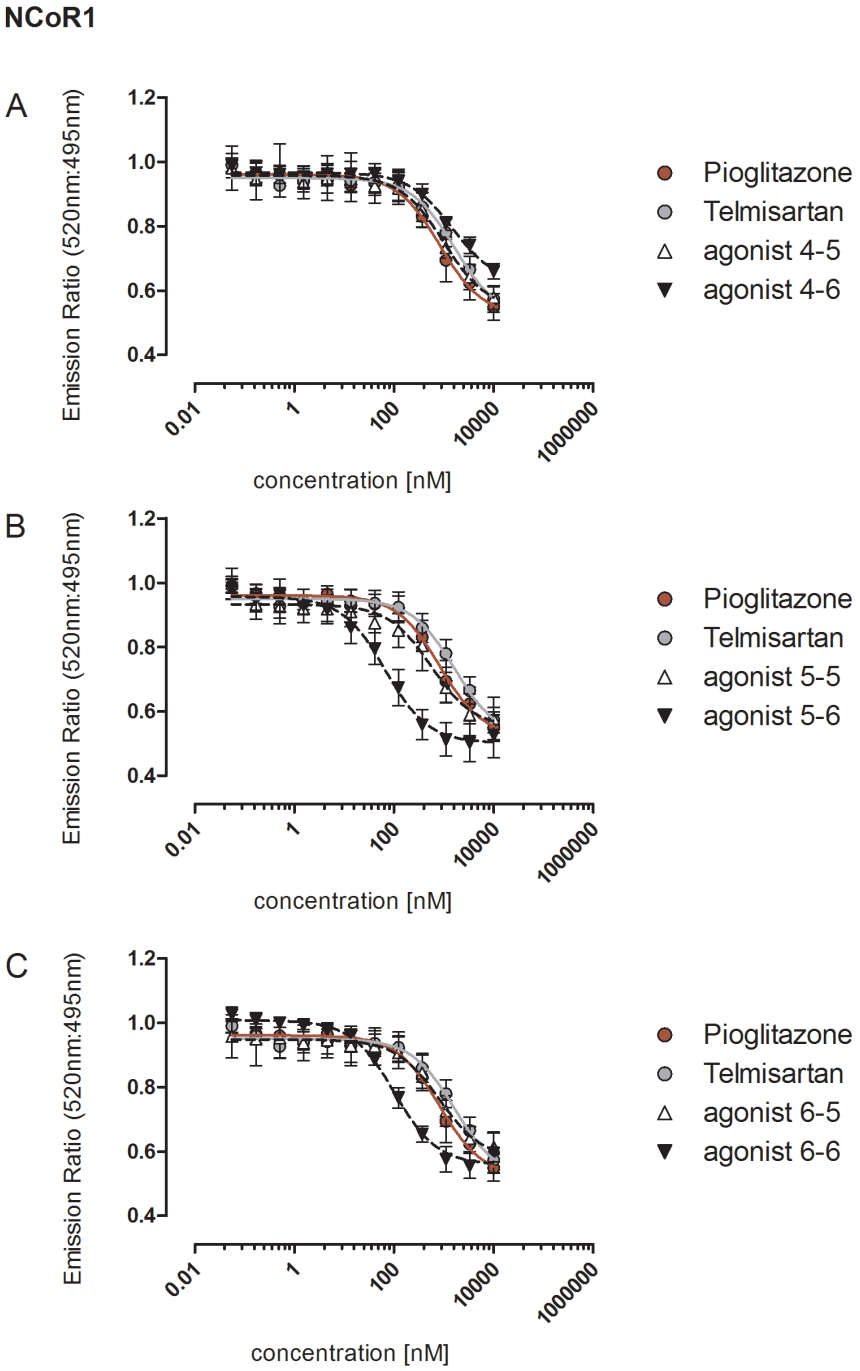

Figure 37: Release of cofactor NCoR1 with agonists 4-5/6, 5-5/6 and 6-5/6 by TR-FRET. Fluorescein-labeled corepressor NCoR1 was incubated with PPARγ ligand-binding domain protein labeled with terbium in the presence of increasing concentrations of pioglitazone, telmisartan and the synthesized compounds (A) agonists 4-5/6; (B) agonists 5-5/6 and (C) agonist 6-5/6. Data were normalized to 1 and represent the mean (±SD) of three independent experiments.

Consistent with observations from FRET experiments of the first part of this thesis, PPARγ activity seemed to be directly correlated with the degree of corepressor release and coactivator recruitment. Dose-response curves after treatment of PPARγ agonists with modifications of the telmisartan scaffold at position 5 and 6 are presented in figure 38 for SRC1 recruitment, figure 39 for PGC-1α recruitment, and figure 40 for TRAP220 recruitment.

SRC1 was not recruited by the agonists 4-5 and 4-6, agonist 5-5 and agonist 6-5. Furtheremore, there was only weak recruitment with these agonists for TRAP220 and PGC-1α in high concentrations. On the other side, strong PPARγ agonists like agonist 5-6 and 6-6 strongly recruited SRC1, PGC-1α and TRAP220. However, in high concentrations recruitment of TRAP220 was stronger with pioglitazone than with agonist 5-6 and 6-6.

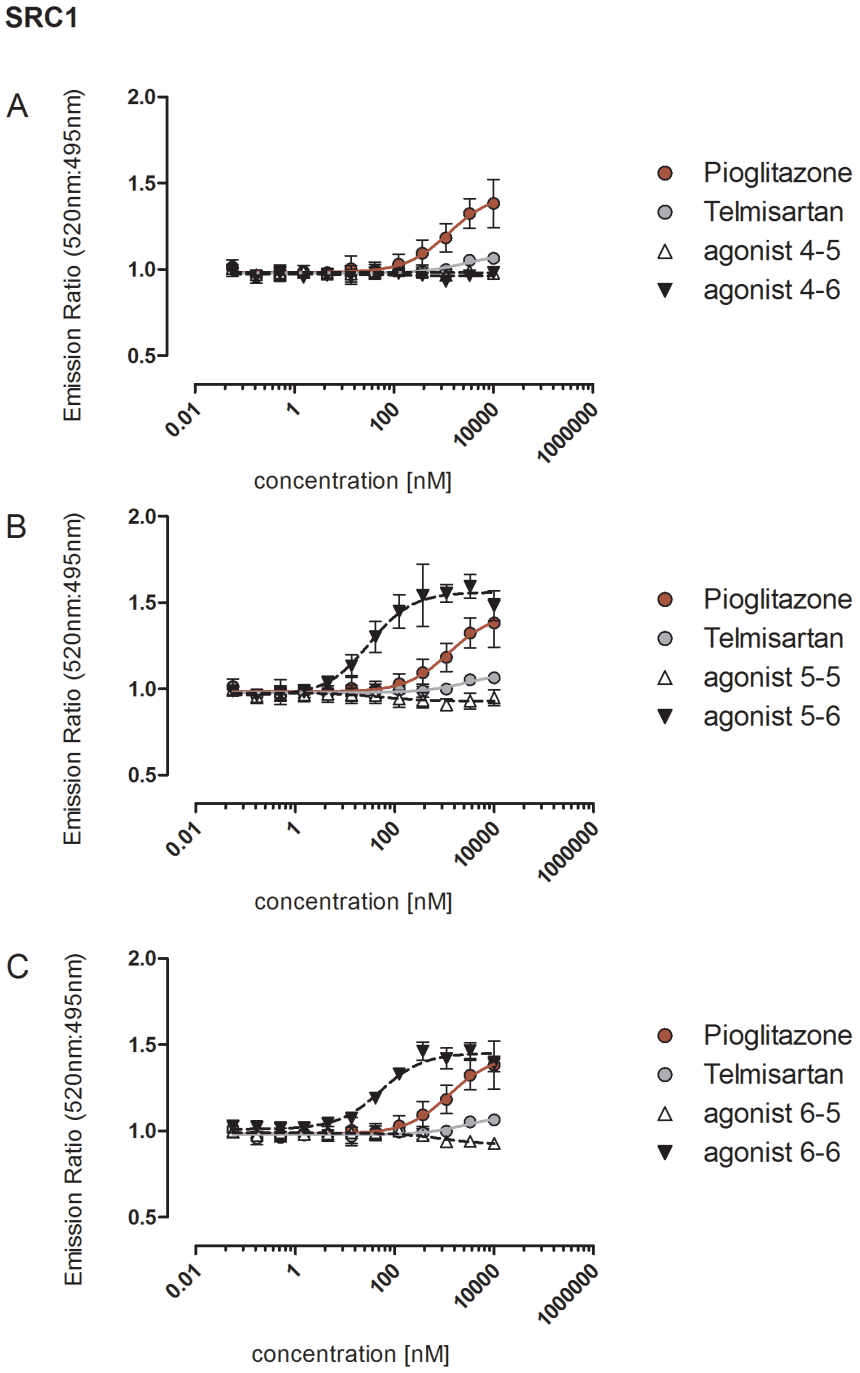

Figure 38: Recruitment of cofactor SRC1 with agonists 4-5/6, 5-5/6 and 6-5/6 by TR-FRET. Fluorescein-labeled coactivator SRC1 was incubated with PPARγ ligand-binding domain protein labeled with terbium in the presence of increasing concentrations of the synthesized compounds (A) agonists 4-5/6, (B) 5-5/6 and (C) 6-5/6, pioglitazone or telmisartan. FRET-signal increases when terbium and fluorescein are in close proximity. Recruitment of SRC1 was calculated as a ratio of 520nm (fluorescein) to 495nm (terbium). Data were normalized to 1 and represent the mean (±SD) of three independent experiments.

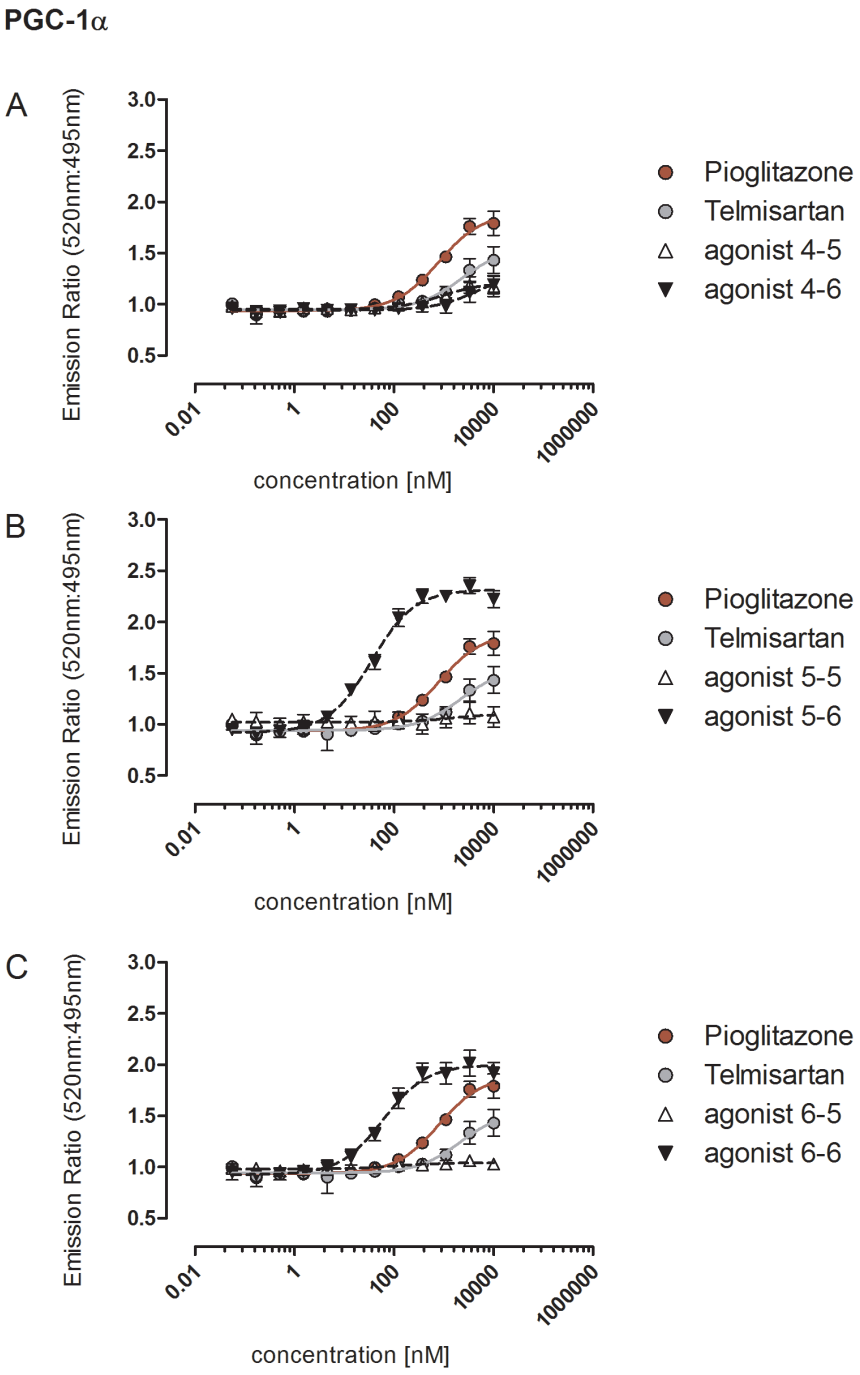

Figure 39: Recruitment of cofactor PGC-1α with agonists 4-5/6, 5-5/6 and 6-5/6 by TR-FRET. Fluorescein-labeled coactivator SRC1 was incubated with PPARγ ligand-binding domain protein labeled with terbium in the presence of increasing concentrations of the synthesized compounds (A) agonists 4-5/6, (B) 5-5/6 and (C) 6-5/6, pioglitazone or telmisartan. FRET-signal increases when terbium and fluorescein are in close proximity. Recruitment of SRC1 was calculated as a ratio of 520nm (fluorescein) to 495nm (terbium). Data were normalized to 1 and represent the mean (±SD) of three independent experiments.

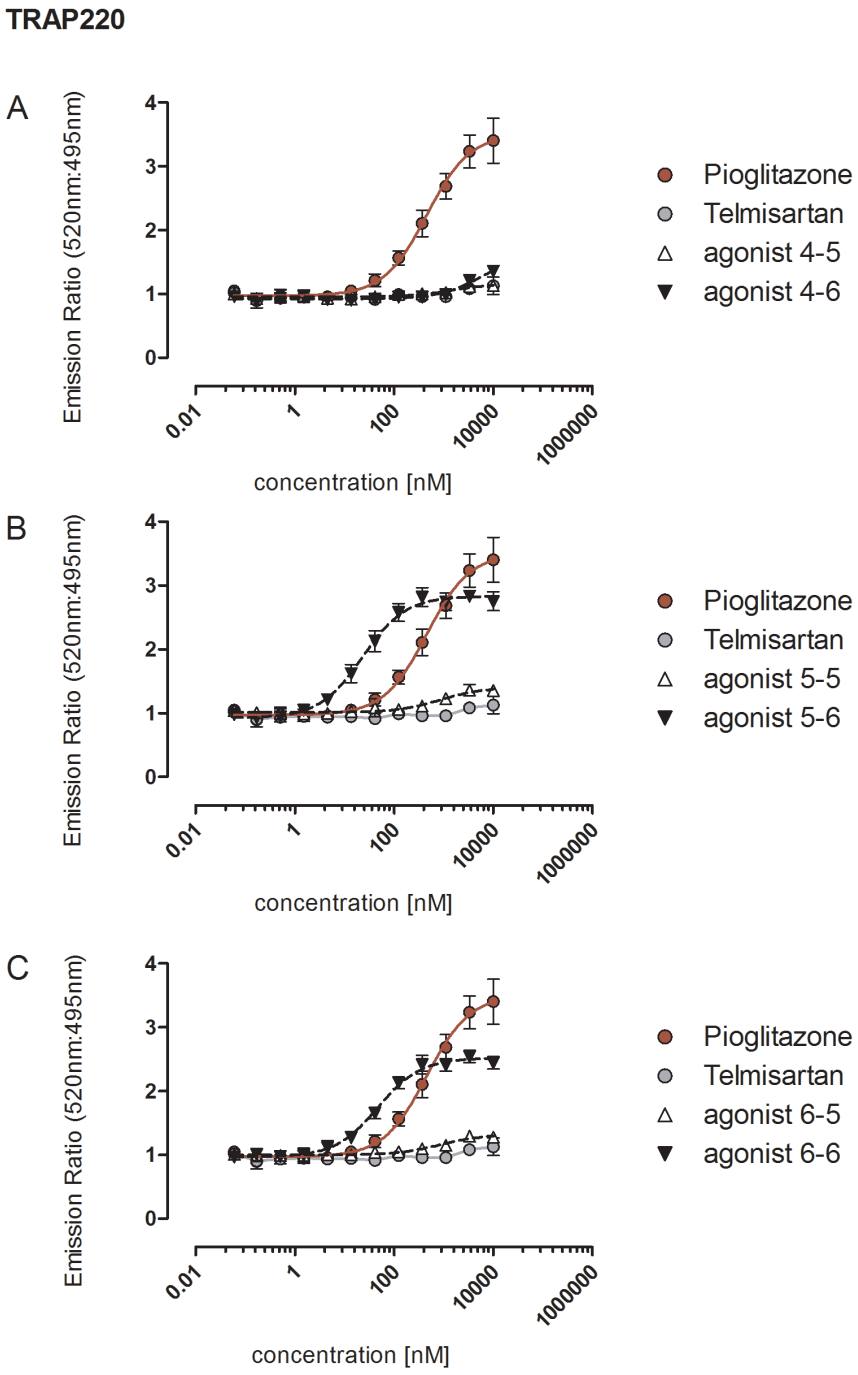

Figure 40: Recruitment of cofactor TRAP220 with agonists 4-5/6, 5-5/6 and 6-5/6 by TR-FRET. Fluorescein-labeled co-activator SRC1 was incubated with PPARγ ligand-binding domain protein labeled with terbium in the presence of increasing concentrations of the synthesized compounds (A) agonists 4-5/6, (B) 5-5/6 and (C) 6-5/6, pioglitazone or telmisartan. FRET-signal increases when terbium and fluorescein are in close proximity. Recruitment of SRC1 was calculated as a ratio of 520nm (fluorescein) to 495nm (terbium). Data were normalized to 1 and represent the mean (±SD) of three independent experiments.

Table 11 shows an overview of TR-FRET results for coactivator recruitment. The agonists 5-6 and 6-6 present the same recruitment preference for TRAP220 > PGC-1α > SRC1 like pioglitazone. Agonists 5-5 and 6-5 weakly recruited TRAP220, but not PGC-1α or SRC1, and the agonists 4-5 and 4-6 weakly recruited PGC-1α and TRAP220, but not SRC1.

Table 11: AUC-values for recruitment of the coactivators SRC1, PGC-1α and TRAP220 with newly synthesized agonists determined by TR-FRET assay. Data represent the mean of three independent experiments calculated by the use of TR-FRET dose response curves shown in figure 38-40. Values were analyzed with GraphPad Prism 5.01 using the bottom baseline of each curve. n.r.: no recruitment

	AUC		
Compound	SRC1	PGC-1α	TRAP220
Pioglitazone	0.463	1.114	3.494
Telmisartan	0.098	0.515	0.206
agonist 4-5	n.r.	0.365	0.207
agonist 4-6	n.r.	0.236	0.285
agonist 5-5	n.r.	n.r.	0.334
agonist 5-6	1.432	3.367	4.842
agonist 6-5	n.r.	n.r.	0.315
agonist 6-6	1.159	2.338	3.602

4 Discussion

4.1 Telmisartan-derived structures are selective PPARγ modulators

Telmisartan is a well-tolerated drug which blocks the AT_1-receptor [160], but also acts as a partial agonist for PPARγ [130]. Modifications on the telmisartan core structure were performed to improve its effectiveness on PPARγ regarding potency and selective receptor activation. Goebel et al. (2009, 2010) analyzed the influence of different moieties at position 2, 4, 5 and 6 on PPARγ activity [133–135]. With continuative studies presented in this thesis, cofactor interactions, mRNA expression and glucose uptake of partial and full telmisartan-derived PPARγ activators were compared. First of all, potency and efficiency of these compounds activating the PPARγ-LBD were verified by the PPARγ transactivation assay and confirmed with the 3T3-L1 differentiation assay. The compounds activated PPARγ in the following order: agonist 1 < telmisartan < agonist 2 < pioglitazone < agonist 3. Results of both techniques correlated, and provided the foundation for further studies. Differential receptor modulation was characterized by selective cofactor recruitment or release and selective gene expression. The large PPARγ-binding pocket was demonstrated to offer several binding possibilities and enough space for cofactor interaction [161]. Using TR-FRET assay, a strong PPARγ activation was found to be correlated with a strong cofactor interaction after incubation with full PPARγ agonists. While agonist 1 as a weak agonist for PPARγ hardly recruited any of the investigated coactivators, agonist 3 which represented a very potent and efficacious activator strongly recruited the coactivators SRC1, PGC-1α and TRAP220. Furthermore, the release of corepressor NCoR1 was stronger with full agonists, than with weak agonists. Although agonist 3 is a more potent full PPARγ agonist than pioglitazone, its coactivator recruitment was slightly stronger for PGC-1α recruitment, similar for SRC1 and lower for TRAP220 compared to pioglitazone. Thus, the degree of cofactor recruitment does not directly correlate with the degree of PPARγ activity. The binding mode of compounds to the PPARγ-LBD is the crucial factor influencing cofactor interaction and receptor activation. Bruning et al. (2007) demonstrated that partial agonists bind via independent mechanisms of helix 12 [162]. In contrast, stabilizing helix 12 is required for full agonist activity [163]. Recently, Hughes et al. (2012) published results related to the dynamics of ligand binding [164].

They performed NMR studies and proposed that a conformational disorientation, due to the ability of ligands to sample different binding modes, contributes to reduced receptor activation [164] and therefore lead to an unfavorable conformation for cofactor binding. These findings were supported by Amano et al. (2012), who investigated the binding mode of telmisartan and PPARγ [165]. Crystallization showed that telmisartan formed only one intermolecular hydrogen bond (Tyr473) with the LBD, suggesting a weaker binding. Furthermore, the propyl group changed the position of His323, which impaired the recruitment of coactivator peptides [165]. In 3D pharmacophore-driven docking studies performed by Goebel et al. (2010), demonstrated that agonist 3 has a very high binding stability [135], which reflected its full receptor activation property and its strong ability to interact with cofactors.

In a next step, microarray and qPCR was used to investigate the gene expression level in 3T3-L1 cells after stimulation with telmisartan-derived partial and full PPARγ agonists. To elucidate the detailed effect of the compounds on adipogenesis a time point during differentiation was chosen to extract RNA. The dissimilar differentiation status of the cells, dependent on the degree of PPARγ activation, represented the major challenge for data analysis to determine selective gene expression. PCA mapping demonstrated the differentiation status in the following order: agonist 1, telmisartan < agonist 2, agonist 3, pioglitazone. These results reflected the degree of oil-red O staining from the differentiation assay and clearly distinguished between partial and full PPARγ activation. Expression levels of genes which didn't fit into this pattern were considered to be selectively expressed. To compare expression levels between the partial and full telmisartan-derived PPARγ agonists at day 6 during differentiation, 394 annotated genes (p-value < 0.01 and $\log_2$-fold chance < -1 or > 1) which were commonly regulated by all of the compounds were in the focus of the investigation. Due to tremendous morphological changes during differentiation, it was not surprising that all of these genes were up-regulated. Moreover, seven genes involved in glucose and FA metabolism were chosen and shown to be selectively expressed. The APOC3 and APOC4 genes encode for lipid binding proteins which belong to the apolipoprotein gene family [166, 167]. APOC3 is able to inhibit the lipoprotein lipase, and therefore inhibits hepatic uptake of TG-rich particles [168]. Null-mutations of APOC3 in human resulted in

lower fasting and postprandial serum triglycerides, higher levels of HDL-cholesterol and lower levels of LDL-cholesterol [169]. The results from the microarray performed for this thesis demonstrated an increased mRNA level of APOC3 after treatment with agonist 2 and 3 compared to pioglitazone, suggesting a contribution of agonist 2 and agonist 3 to the manifestation of hypertriglyceridemia. TFRC protein is involved in iron uptake, and therefore important for erythrocyte and neuronal development [170], and fundamental for osteoclast activation [171]. FFAR2 regulates lipid plasma levels via binding of short-chain FAs [172], PGC-1α regulates glucose and lipid homeostasis [173]. And PDZK1 plays a critical role in cholesterol metabolism by regulating the HDL receptor [174]. Regarding CYB561 biological function, CYB561 KO-mice were found to have a decreased circulating glucose level [175]. The mRNA levels of CYB561, TFRC and PDZK1 were increased with agonists 2 and 3 compared to pioglitazone treatment, and decreased for FFAR2 with agonists 2 and 3 compared to pioglitazone mRNA levels. However, the mechanisms involved in insulin resistance are complex, and require the interaction of several genes and signaling pathways (section 1.3.2). Whether differential expression of the indicated genes contributes to improved or impaired insulin sensitizing effects compared to TZDs needs to be elucidated in an *in vivo* model.

Basal glucose uptake in adipocytes derived from 3T3-L1 cells was significantly increased after stimulation with pioglitazone, agonist 2 and agonist 3. In presence of insulin intracellular glucose levels increased in all treatment groups compared to basal levels due to translocation of GLUT4 to the cell membrane. The effect was stronger with PPARγ agonists, compared to DMSO treatment. However, the increase was not very pronounced and only significant for pioglitazone treated cells. One possibility for the lack of higher glucose levels might be a saturated level of intracellular glucose and an elevated excretion of glucose via GLUT1 [176].

In a second project part, the effects of sterioisomers with different moieties at position 5 or position 6 of the telmisartan scaffold on PPARγ activity and cofactor interaction were investigated. With a benzofuran or a benzothiophene moiety, position 6 has a huge impact on both potency and efficacy of PPARγ activity, but also on corepressor release and coactivator recruitment. This effect was not observed with the benzimidazole moiety

at position 6, suggesting that agonist 4-6 might have a completely different binding mode than agonists 5-6 and 6-6. The dose-responses for PPARγ activation with agonist 6-6 were almost identical to the dose-responses with pioglitazone. However, their interactions with cofactors were different. Agonist 6-6 strongly released corepressor NCoR1 and highly efficaciously recruited the coactivators SRC1, PGC-1α and TRAP220 compared to pioglitazone. Similar results for cofactor interaction were obtained with agonist 5-6. The related compounds with a benzofuran or a benzothiophene moiety at position 5 of the telmisartan scaffold were partial agonists for PPARγ. They didn't recruit any of the tested coactivators.

Conclusively, structure modifications around the telmisartan scaffold which were analyzed in this thesis created compounds with different PPARγ activation potential with SPPARγM characteristics *in vitro*.

4.2 Side effects of PPARγ activation

As already mentioned in the introduction, the central problem in treating insulin resistance with TZDs is the frequent occurrence of side effects [177, 178]. In clinical studies, full activation of PPARγ by TZDs was highly associated with weight gain [179, 180]. However, the mechanisms underlying TZD-induced weight gain are not completely understood. It is still in debate, if the activation of the PPARγ receptor or rather the distinct binding and conformational change of PPARγ after TZD treatment is responsible for the observed increase in weight. The concept of selective receptor modulation by different compound structures pointes towards the latter. In fact, the dogma in nuclear receptor modulation of the last decade assumed that different cofactor recruitment causes different or less side effects. Therefore, the strategy of the research field in the last years was to enforce the development of partial modulators. Furthermore, Rosen and Spiegelman (2006) pointed out that 'having more fat cells does not make an animal fatter', but 'in the absence of altered energy balance, an increase in adipogenesis will result in smaller fat cells with no change in total adiposity' [181]. Since PPARγ activation and adipocyte differentiation are directly correlated, full agonists (agonists 2, 3, 5-6 and 6-6) derived from the telmisartan core-structure induced strong

differentiation of 3T3-L1 cells similar to pioglitazone. However, weight gain is a complex mechanism and an increase in adipogenesis may only be a small part of it. Moreover, it was shown that mice treated with TZDs increase weight via fluid retention resulting in edema formation [182]. These processes are at least partially explained by activation of PPARγ in the collecting duct of the kidney, followed by up-regulation of the Na transporter ENaC or water channels (aquaporins) and subsequent fluid retention [183].

In addition, PPARγ is also expressed in regions of the hypothalamus where it contributes to the central regulation of energy balance [184, 185]. Neuron-specific PPARγ-KO mice challenged with a HFD exhibited a reduced food intake and increased energy expenditure, resulting in reduced weight gain compared to floxed mice. Treatment of neuron-specific PPARγ-KO mice with rosiglitazone didn't increase weight either, but also didn't increase hepatic insulin sensitivity [186]. In 2011, Ryan et al. represented an important correlation between PPARγ in the central nervous system (CNS) and diet-induced obesity [187]. They specifically activated PPARγ with TZDs or a viral-regulated PPARγ fusion gene in the hypothalamus of rats, and found a higher chow intake and a higher body weight after treatment with rosiglitazone for 4h, and also twice as much body fat 4 weeks after virus infusion [187]. Following on these findings a PPARγ agonist should only moderately activate PPARγ in the brain to prevent massive weight gain due to an enhanced hunger feeling, but should keep a certain activation level to maintain its anti-diabetic effects.

As already mentioned before, other side effects reported to be caused by PPARγ activation via TZDs is loss of bone mineral density, and therefore a higher risk for fractures [108], and an increased risk for cardiovascular events [107]. Whether or not the newly synthesized compounds contribute to the risk of these conditions remains unclear. However, their influence on hypertension which is the mayor contributor to cardiovascular diseases is discussed in the next chapter.

A new strategy for the development of anti-diabetic drugs was established by the group of B. Spiegelman and published by Choi et al. (2010) [188]. They detected an obesity-related activation of Cdk5, which resulted in phosphorylation of PPARγ at serine 273. Phosphorylation of PPARγ at this specific position was associated with a decrease in

anti-diabetic gene expression (e.g. down-regulation of insulin-sensitizing adiponectin levels). Furthermore, they demonstrated *in vitro* and *in vivo* that Cdk5-mediated phosphorylation of PPARγ was blocked by the PPARγ ligands rosiglitazone and MRL24, and that this effect was completely independent of PPARγ agonism [188]. In 2011, Choi et al. described novel synthetic compounds, which completely lack PPARγ agonism, but still block the Cdk5-mediated phosphorylation of PPARγ [189]. These compounds (SR1664, SR1824) were derived from telmisartan-related compounds published by Lamotte et al. (2010) [189, 190]. Compound SR1664 was shown to possess anti-diabetic activity without causing fluid retention and weight gain in insulin resistant mice. Hence, the occurrence of many of the known side effects is a consequence of classical PPARγ agonism. Specifically blocking Cdk5-mediated phosphorylation of PPARγ might be the explanation for the success of PPARγ modulators in the treatment of insulin resistance [189]. Consequently, preventing phosphorylation of PPARγ at position serine 273, and low PPARγ activity is favorable for the development of anti-diabetic drugs. Whether the blockage of phosphorylation of PPARγ by new compounds holds any therapeutic value has to be seen in the future.

4.3 Dual pharmacology of telmisartan-derived structures

Telmisartan as an AT_1-receptor blocker and partial agonist for PPARγ bares a simultaneous opportunity for prevention and treatment of diabetes and cardiovascular risk factors in patients with the metabolic syndrome. However, concentrations necessary for PPARγ activation are in the µM-range (maximum efficacy at 10-20µM) [130], while AT_1-receptor blockage is achieved in the nM-range [191]. Under normal circumstances typical telmisartan plasma concentrations (at around 0.54µM) are about 10-fold lower than the PPARγ EC_{50} [128]. Small clinical trials have demonstrated that telmisartan was able to decrease free plasma glucose and insulin levels in patients with metabolic syndrome after 3 months 80mg daily-dose [192]. In another clinical trial, patients with metabolic syndrome were treated for 14 weeks with a high-dose of telmisartan. PPARγ target gene expression was induced in monocytes, but pro-inflammatory serum cytokine levels (IL-6) were not reduced [193]. In both clinical trials,

improvements in the metabolic syndrome were reasonably attributed due to the weak activity of telmisartan at PPARγ. Thus, telmisartan does only have minor effects via PPARγ signaling in humans.

Therefore, we and others modified the telmisartan structure to obtain lower EC_{50}-values. Except from agonist 1, all telmisartan-derived compounds from this thesis exhibited lower EC_{50}-values compared to telmisartan, and except from agonist 4-6 they were even lower than with pioglitazone. Strongest potency was measured with the agonists 5-5 (0.14µM EC_{50}-value, 26% maximum activation) and 5-6 (0.09µM EC_{50}-value, 87% maximum activity). Unfortunately, agonist 5-6 lost the partial agonism. In 2010, Lamotte et al. published very potent (<0.001µM) telmisartan-derived partial PPARγ agonists by replacing the central benzimidazole ring with an indole [190]. The AT_1 antagonism was completely abolished. *In vivo*, their most potent compound showed a similar decrease of plasma glucose and triglyceride levels compared to the full PPARγ agonist, but with less pronounced weight gain [190]. Furthermore, Casimiro-Garcia et al. (2011) presented telmisartan analogous with a central imidazol ring [194]. Their compound 2l was identified as potent dual agonist for both receptors (AT_1 IC_{50}=1.6nM, PPARγ EC_{50}=0.212µM, 31% maximum PPARγ activity). However, AT_1 IC_{50} of compound 2l was 3-fold higher compared to telmisartan (AT_1 IC_{50}=0.49nM) [194].

In fact, several studies observed a down-regulation of AT_1-receptor expression and ACE activity after PPARγ activation [195–197]. Previous studies done by M. Goebel, showed a negative correlation between PPARγ activation and AT_1-receptor blockage of selective telmisartan-derived compounds (unpublished data). The same correlation is present with most of the compounds published in Casimiro-Garcia et al. (2011) [194]. Consistent with these observations, agonists 5-5 (26% maximum PPARγ activity) and 6-5 (34% maximum PPARγ activation) might still be able to block the AT_1-receptor.

4.4 Further application options

PPARγ ligands have a potential benefit value beyond the treatment of insulin resistance. As already mentioned PPARγ is not only expressed in adipocytes, but can

also be found in many other tissues like small and large intestine, macrophages, kidney, liver, spleen and muscle [92].

Several publications reported about the anti-inflammatory function of PPARγ [198, 199]. PPARγ ligands were shown to inhibit macrophage inflammatory genes, such as TNFα, MMP-9 and IL-1ß, and therefore seem to be of therapeutic value for atherosclerosis or rheumatoid arthritis [200]. Moreover, TZDs were capable of reducing lipopolysaccharide-induced neuroinflammation and neuronal death *in vitro* by a PPARγ dependent mechanism [201]. Hence, treatment with PPARγ agonists might influence the progression of neurodegenerative diseases (e.g. multiple sklerosis, parkinson's and alzheimer's diseases) in a positive manner.

Furthermore, PPARγ is expressed in many different cancers, including colon, breast and prostate cancer with almost equivalent levels to normal adipose tissue [82]. In metastatic breast adenocarcinomas, activation of PPARγ with TZDs caused differentiation of preadipocytes and induced changes in breast epithelial gene expression associated with a more differentiated, less malignant state and a reduction in growth rate [202]. Treatment of prostatic adenocarcinomas with troglitazone as well inhibited cell growth [203]. Indeed it was recently published that the interaction of PPAR-γ agonist troglitazone and recombinant IFN-ß antagonizes survival pathways induced by STAT-3-dependent escape pathways in pancreatic cancer cell lines. The effect was associated with cell cycle arrest in G0/G1 phase and an increase in autophagic cell death [204].

Hence, activation of PPARγ with synthetic ligands possesses further possibilities for disease intervention. So far, neither compounds reported in this thesis, nor previously reported telmisartan-derived compounds from our group were tested in other disease models, but due to their excellent EC_{50}-values might as well be promising compounds in other diseases.

4.5 Conclusion and outlook

SAR studies confirmed partial and full PPARγ activation potential for agonist 1, agonist 2 and agonist 3 respectively. TR-FRET assays and gene expression analyses revealed differential cofactor interactions and differential mRNA expression levels for these compounds, characterizing them as SPPARγMs. Additionally, the importance of position 5 of the telmisartan scaffold for partial PPARγ activation was discovered. Further modifications should be performed on position 5 to further increase potency, but with similar efficacy as compound 5-5 and 6-5. Apart from that, the newly designed compounds with modifications at position 5 or 6 of the telmisartan scaffold provided beneficial EC_{50}- and lipophilicity values that make them highly competitive to PPARγ agonists from the literature. Conclusively, results from this thesis provide essential and promising information for the investigation of the side effect profile *in vivo*.

References

[1] S. I. Fox, *Human Physiology*, 9th ed. McGraw-Hill Science/Engineering/Math, 2006.

[2] N. V. Bhagavan, *Medical Biochemistry, Fourth Edition*, 4th ed. Academic Press, 2001.

[3] A. R. Saltiel and C. R. Kahn, “Insulin signalling and the regulation of glucose and lipid metabolism,” *Nature*, vol. 414, no. 6865, pp. 799–806, Dec. 2001.

[4] H. J. Harwood Jr, “The adipocyte as an endocrine organ in the regulation of metabolic homeostasis,” *Neuropharmacology*, Dec. 2011.

[5] L. Weiss, *Cell and Tissue Biology: A Textbook of Histology*, 6th Revised ed. Urban & Schwarzenberg, 1988.

[6] F. M. Gregoire, “Adipocyte differentiation: from fibroblast to endocrine cell,” *Exp. Biol. Med. (Maywood)*, vol. 226, no. 11, pp. 997–1002, Dec. 2001.

[7] R. M. Cowherd, R. E. Lyle, and R. E. McGehee, “Molecular regulation of adipocyte differentiation,” *Semin. Cell Dev. Biol*, vol. 10, no. 1, pp. 3–10, Feb. 1999.

[8] G. H. Goossens and F. Karpe, “Human adipose tissue blood flow and micromanipulation of human subcutaneous blood flow,” *Methods Mol. Biol*, vol. 456, pp. 97–107, 2008.

[9] P. Trayhurn and J. H. Beattie, “Physiological role of adipose tissue: white adipose tissue as an endocrine and secretory organ,” *Proc Nutr Soc*, vol. 60, no. 3, pp. 329–339, Aug. 2001.

[10] E. E. Kershaw and J. S. Flier, “Adipose tissue as an endocrine organ,” *J. Clin. Endocrinol. Metab*, vol. 89, no. 6, pp. 2548–2556, Jun. 2004.

[11] A. R. Saltiel, “You are what you secrete,” *Nat. Med*, vol. 7, no. 8, pp. 887–888, Aug. 2001.

[12] A. H. Berg, T. P. Combs, and P. E. Scherer, “ACRP30/adiponectin: an adipokine regulating glucose and lipid metabolism,” *Trends Endocrinol. Metab*, vol. 13, no. 2, pp. 84–89, Mar. 2002.

[13] P. G. McTernan, F. M. Fisher, G. Valsamakis, R. Chetty, A. Harte, C. L. McTernan, P. M. S. Clark, S. A. Smith, A. H. Barnett, and S. Kumar, “Resistin and type 2 diabetes: regulation of resistin expression by insulin and rosiglitazone and the effects of recombinant resistin on lipid and glucose metabolism in human differentiated adipocytes,” *J. Clin. Endocrinol. Metab*, vol. 88, no. 12, pp. 6098–6106, Dec. 2003.

[14] F. M. Gregoire, C. M. Smas, and H. S. Sul, “Understanding adipocyte differentiation,” *Physiol. Rev*, vol. 78, no. 3, pp. 783–809, Jul. 1998.

[15] J. R. Speakman, “Obesity: the integrated roles of environment and genetics,” *J. Nutr*, vol. 134, no. 8 Suppl, p. 2090S–2105S, Aug. 2004.

[16] “WHO TRS 916 - Diet, nutrition and the prevention of chronic disease.” Geneva/Rome: WHO 2003.

[17] K. M. Flegal, M. D. Carroll, C. L. Ogden, and L. R. Curtin, “Prevalence and Trends in Obesity Among US Adults, 1999-2008,” *JAMA: The Journal of the American Medical Association*, vol. 303, no. 3, pp. 235 –241, Jan. 2010.

[18] “Obesity and Overweight for Professionals: Data and Statistics: U.S. Obesity Trends | DNPAO | CDC.” [Online]. Available: http://www.cdc.gov/obesity/data/trends.html#County. [Accessed: 28-Jan-2012].

[19] J. C. Seidell, “Obesity in Europe: scaling an epidemic,” *Int. J. Obes. Relat. Metab. Disord*, vol. 19 Suppl 3, pp. S1–4, Sep. 1995.

[20] P. T. James, N. Rigby, and R. Leach, “The obesity epidemic, metabolic syndrome and future prevention strategies,” *Eur J Cardiovasc Prev Rehabil*, vol. 11, no. 1, pp. 3–8, Feb. 2004.

[21] C. L. Ogden, M. D. Carroll, B. K. Kit, and K. M. Flegal, “Prevalence of Obesity and Trends in Body Mass Index Among US Children and Adolescents, 1999-2010,” *JAMA: The Journal of the American Medical Association*, Jan. 2012.

[22] M. Nestle and M. F. Jacobson, “Halting the obesity epidemic: a public health policy approach,” *Public Health Rep*, vol. 115, no. 1, pp. 12–24, Feb. 2000.

[23] M. Jernås, J. Palming, K. Sjöholm, E. Jennische, P.-A. Svensson, B. G. Gabrielsson, M. Levin, A. Sjögren, M. Rudemo, T. C. Lystig, B. Carlsson, L. M. S. Carlsson, and M. Lönn, “Separation of human adipocytes by size: hypertrophic fat cells display distinct gene expression,” *FASEB J*, vol. 20, no. 9, pp. 1540–1542, Jul. 2006.

[24] “Plan and operation of the Third National Health and Nutrition Examination Survey, 1988-94. Series 1: programs and collection procedures,” *Vital Health Stat 1*, no. 32, pp. 1–407, Jul. 1994.

[25] M. Zeyda and T. M. Stulnig, “Obesity, inflammation, and insulin resistance--a mini-review,” *Gerontology*, vol. 55, no. 4, pp. 379–386, 2009.

[26] P.-L. Liew, W.-J. Lee, W. Wang, Y.-C. Lee, W.-Y. Chen, C.-L. Fang, and M.-T. Huang, “Fatty liver disease: predictors of nonalcoholic steatohepatitis and gallbladder disease in morbid obesity,” *Obes Surg*, vol. 18, no. 7, pp. 847–853, Jul. 2008.

[27] R. Pais, H. Silaghi, A.-C. Silaghi, M.-L. Rusu, and D.-L. Dumitrascu, “Metabolic syndrome and risk of subsequent colorectal cancer,” *World J. Gastroenterol*, vol. 15, no. 41, pp. 5141–5148, Nov. 2009.

[28] R. H. Eckel, K. G. M. M. Alberti, S. M. Grundy, and P. Z. Zimmet, “The metabolic syndrome,” *Lancet*, vol. 375, no. 9710, pp. 181–183, Jan. 2010.

[29] J. P. Sutherland, B. McKinley, and R. H. Eckel, “The metabolic syndrome and inflammation,” *Metab Syndr Relat Disord*, vol. 2, no. 2, pp. 82–104, Jun. 2004.

[30] S. Efrat, “Beta-cell expansion for therapeutic compensation of insulin resistance in type 2 diabetes,” *Int J Exp Diabesity Res*, vol. 4, no. 1, pp. 1–5, Mar. 2003.

[31] B. B. Kahn, “Type 2 diabetes: when insulin secretion fails to compensate for insulin resistance,” *Cell*, vol. 92, no. 5, pp. 593–596, Mar. 1998.

[32] S. Schenk, M. Saberi, and J. M. Olefsky, “Insulin sensitivity: modulation by nutrients and inflammation,” *J. Clin. Invest*, vol. 118, no. 9, pp. 2992–3002, Sep. 2008.

[33] “Executive Summary of The Third Report of The National Cholesterol Education Program (NCEP) Expert Panel on Detection, Evaluation, And Treatment of High Blood Cholesterol In Adults (Adult Treatment Panel III),” *JAMA*, vol. 285, no. 19, pp. 2486–2497, May 2001.

[34] S. S. Daskalopoulou, V. G. Athyros, G. D. Kolovou, K. K. Anagnostopoulou, and D. P. Mikhailidis, “Definitions of metabolic syndrome: Where are we now?,” *Curr Vasc Pharmacol*, vol. 4, no. 3, pp. 185–197, Jul. 2006.

[35] R. Ratner, R. Goldberg, S. Haffner, S. Marcovina, T. Orchard, S. Fowler, and M. Temprosa, “Impact of intensive lifestyle and metformin therapy on cardiovascular disease risk factors in the diabetes prevention program,” *Diabetes Care*, vol. 28, no. 4, pp. 888–894, Apr. 2005.

[36] J. Tuomilehto, J. Lindström, J. G. Eriksson, T. T. Valle, H. Hämäläinen, P. Ilanne-Parikka, S. Keinänen-Kiukaanniemi, M. Laakso, A. Louheranta, M. Rastas, V. Salminen, and M. Uusitupa, “Prevention of type 2 diabetes mellitus by changes in lifestyle among subjects with impaired glucose tolerance,” *N. Engl. J. Med.*, vol. 344, no. 18, pp. 1343–1350, May 2001.

[37] S. Haffner and H. Taegtmeyer, “Epidemic obesity and the metabolic syndrome,” *Circulation*, vol. 108, no. 13, pp. 1541–1545, Sep. 2003.

[38] T. D. Filippatos and D. P. Mikhailidis, “Lipid-lowering drugs acting at the level of the gastrointestinal tract,” *Curr. Pharm. Des.*, vol. 15, no. 5, pp. 490–516, 2009.

[39] S. J. Lewis, “Lipid-lowering therapy: who can benefit?,” *Vasc Health Risk Manag*, vol. 7, pp. 525–534, 2011.

[40] D. W. Laight, “Therapeutic inhibition of the renin angiotensin aldosterone system,” *Expert Opin Ther Pat*, vol. 19, no. 6, pp. 753–759, Jun. 2009.

[41] S. Koshy and G. L. Bakris, “Therapeutic approaches to achieve desired blood pressure goals: focus on calcium channel blockers,” *Cardiovasc Drugs Ther*, vol. 14, no. 3, pp. 295–301, Jun. 2000.

[42] B. Viollet, B. Guigas, N. Sanz Garcia, J. Leclerc, M. Foretz, and F. Andreelli, “Cellular and molecular mechanisms of metformin: an overview,” *Clin. Sci.*, vol. 122, no. 6, pp. 253–270, Mar. 2012.

[43] M. Stumvoll and H.-U. Häring, “Glitazones: clinical effects and molecular mechanisms,” *Ann. Med.*, vol. 34, no. 3, pp. 217–224, 2002.

[44] H. S. Weintraub, “Treatment of multiple-risk patients: using combination therapy to treat beyond LDL lowering,” *Curr. Hypertens. Rep.*, vol. 7, no. 4, pp. 265–270, Aug. 2005.

[45] M. Robinson-Rechavi, H. E. Garcia, and V. Laudet, “The nuclear receptor superfamily,” *Journal of Cell Science*, vol. 116, no. 4, pp. 585 –586, Feb. 2003.

[46] I. Issemann and S. Green, “Activation of a member of the steroid hormone receptor superfamily by peroxisome proliferators,” *Nature*, vol. 347, no. 6294, pp. 645–650, Oct. 1990.

[47] S. S. Lee, T. Pineau, J. Drago, E. J. Lee, J. W. Owens, D. L. Kroetz, P. M. Fernandez-Salguero, H. Westphal, and F. J. Gonzalez, “Targeted disruption of the alpha isoform of the peroxisome proliferator-activated receptor gene in mice results in abolishment of the pleiotropic effects of peroxisome proliferators,” *Mol. Cell. Biol.*, vol. 15, no. 6, pp. 3012–3022, Jun. 1995.

[48] “A unified nomenclature system for the nuclear receptor superfamily,” *Cell*, vol. 97, no. 2, pp. 161–163, Apr. 1999.

[49] M. A. Carson-Jurica, W. T. Schrader, and B. W. O’Malley, “Steroid receptor family: structure and functions,” *Endocr. Rev.*, vol. 11, no. 2, pp. 201–220, May 1990.

[50] V. Chandra, P. Huang, Y. Hamuro, S. Raghuram, Y. Wang, T. P. Burris, and F. Rastinejad, “Structure of the intact PPAR-gamma-RXR-alpha nuclear receptor complex on DNA,” *Nature*, pp. 350–356, Oct. 2008.

[51] H. Gronemeyer, J.-A. Gustafsson, and V. Laudet, “Principles for modulation of the nuclear receptor superfamily,” *Nat Rev Drug Discov*, vol. 3, no. 11, pp. 950–964, Nov. 2004.

[52] B. Desvergne and W. Wahli, “Peroxisome Proliferator-Activated Receptors: Nuclear Control of Metabolism,” *Endocrine Reviews*, vol. 20, no. 5, pp. 649 –688, Oktober 1999.

[53] S. A. Kliewer, B. M. Forman, B. Blumberg, E. S. Ong, U. Borgmeyer, D. J. Mangelsdorf, K. Umesono, and R. M. Evans, “Differential expression and activation of a family of murine peroxisome proliferator-activated receptors,” *Proc. Natl. Acad. Sci. U.S.A.*, vol. 91, no. 15, pp. 7355–7359, Jul. 1994.

[54] P. Tontonoz, E. Hu, R. A. Graves, A. I. Budavari, and B. M. Spiegelman, “mPPAR gamma 2: tissue-specific regulator of an adipocyte enhancer,” *Genes Dev.*, vol. 8, no. 10, pp. 1224–1234, May 1994.

[55] L. Fajas, J. C. Fruchart, and J. Auwerx, “PPARgamma3 mRNA: a distinct PPARgamma mRNA subtype transcribed from an independent promoter,” *FEBS Lett.*, vol. 438, no. 1–2, pp. 55–60, Oct. 1998.

[56] R. Nielsen, T. A. Pedersen, D. Hagenbeek, P. Moulos, R. Siersbaek, E. Megens, S. Denissov, M. Børgesen, K.-J. Francoijs, S. Mandrup, and H. G. Stunnenberg, “Genome-wide profiling of PPARgamma:RXR and RNA polymerase II occupancy reveals temporal activation of distinct metabolic pathways and changes in RXR dimer composition during adipogenesis,” *Genes Dev.*, vol. 22, no. 21, pp. 2953–2967, Nov. 2008.

[57] S. Green and W. Wahli, “Peroxisome proliferator-activated receptors: finding the orphan a home,” *Mol. Cell. Endocrinol.*, vol. 100, no. 1–2, pp. 149–153, Apr. 1994.

[58] A. IJpenberg, E. Jeannin, W. Wahli, and B. Desvergne, “Polarity and specific sequence requirements of peroxisome proliferator-activated receptor (PPAR)/retinoid X receptor heterodimer binding to DNA. A functional analysis of the malic enzyme gene PPAR response element,” *J. Biol. Chem.*, vol. 272, no. 32, pp. 20108–20117, Aug. 1997.

[59] M. Schupp and M. A. Lazar, “Endogenous ligands for nuclear receptors: digging deeper,” *J. Biol. Chem.*, vol. 285, no. 52, pp. 40409–40415, Dec. 2010.

[60] S. A. Kliewer, K. Umesono, D. J. Noonan, R. A. Heyman, and R. M. Evans, “Convergence of 9-cis retinoic acid and peroxisome proliferator signalling pathways through heterodimer formation of their receptors,” *Nature*, vol. 358, no. 6389, pp. 771–774, Aug. 1992.

[61] X. Hu and M. A. Lazar, “The CoRNR motif controls the recruitment of corepressors by nuclear hormone receptors,” *Nature*, vol. 402, no. 6757, pp. 93–96, Nov. 1999.

[62] D. M. Heery, E. Kalkhoven, S. Hoare, and M. G. Parker, “A signature motif in transcriptional co-activators mediates binding to nuclear receptors,” *Nature*, vol. 387, no. 6634, pp. 733–736, Jun. 1997.

[63] H.-P. Guan, T. Ishizuka, P. C. Chui, M. Lehrke, and M. A. Lazar, “Corepressors selectively control the transcriptional activity of PPARgamma in adipocytes,” *Genes Dev.*, vol. 19, no. 4, pp. 453–461, Feb. 2005.

[64] V. Perissi, A. Aggarwal, C. K. Glass, D. W. Rose, and M. G. Rosenfeld, “A corepressor/coactivator exchange complex required for transcriptional activation by nuclear receptors and other regulated transcription factors,” *Cell*, vol. 116, no. 4, pp. 511–526, Feb. 2004.

[65] A. Bugge and S. Mandrup, “Molecular Mechanisms and Genome-Wide Aspects of PPAR Subtype Specific Transactivation,” *PPAR Res*, vol. 2010, 2010.

[66] L. la C. Poulsen, M. Siersbæk, and S. Mandrup, “PPARs: Fatty acid sensors controlling metabolism,” *Seminars in Cell & Developmental Biology*, Jan. 2012.

[67] S. Yu and J. K. Reddy, “Transcription coactivators for peroxisome proliferator-activated receptors,” *Biochim. Biophys. Acta*, vol. 1771, no. 8, pp. 936–951, Aug. 2007.

[68] O. van Beekum, V. Fleskens, and E. Kalkhoven, “Posttranslational modifications of PPAR-gamma: fine-tuning the metabolic master regulator,” *Obesity (Silver Spring)*, vol. 17, no. 2, pp. 213–219, Feb. 2009.

[69] J. Berger and D. E. Moller, “The mechanisms of action of PPARs,” *Annu. Rev. Med.*, vol. 53, pp. 409–435, 2002.

[70] R. M. Evans, G. D. Barish, and Y.-X. Wang, “PPARs and the complex journey to obesity,” *Nat. Med.*, vol. 10, no. 4, pp. 355–361, Apr. 2004.

[71] O. Braissant, F. Foufelle, C. Scotto, M. Dauça, and W. Wahli, “Differential expression of peroxisome proliferator-activated receptors (PPARs): tissue distribution of PPAR-alpha, -beta, and -gamma in the adult rat,” *Endocrinology*, vol. 137, no. 1, pp. 354–366, Jan. 1996.

[72] S. Kersten, J. Seydoux, J. M. Peters, F. J. Gonzalez, B. Desvergne, and W. Wahli, “Peroxisome proliferator-activated receptor alpha mediates the adaptive response to fasting,” *J. Clin. Invest.*, vol. 103, no. 11, pp. 1489–1498, Jun. 1999.

[73] M. Guerre-Millo, P. Gervois, E. Raspé, L. Madsen, P. Poulain, B. Derudas, J. M. Herbert, D. A. Winegar, T. M. Willson, J. C. Fruchart, R. K. Berge, and B. Staels, “Peroxisome proliferator-activated receptor alpha activators improve insulin sensitivity and reduce adiposity,” *J. Biol. Chem.*, vol. 275, no. 22, pp. 16638–16642, Jun. 2000.

[74] T. Lemberger, R. Saladin, M. Vázquez, F. Assimacopoulos, B. Staels, B. Desvergne, W. Wahli, and J. Auwerx, “Expression of the peroxisome proliferator-activated receptor alpha gene is stimulated by stress and follows a diurnal rhythm,” *J. Biol. Chem.*, vol. 271, no. 3, pp. 1764–1769, Jan. 1996.

[75] L. Canaple, J. Rambaud, O. Dkhissi-Benyahya, B. Rayet, N. S. Tan, L. Michalik, F. Delaunay, W. Wahli, and V. Laudet, “Reciprocal regulation of brain and muscle Arnt-like protein 1 and peroxisome proliferator-activated receptor alpha defines a novel positive feedback loop in the rodent liver circadian clock,” *Mol. Endocrinol.*, vol. 20, no. 8, pp. 1715–1727, Aug. 2006.

[76] Y. Barak, D. Liao, W. He, E. S. Ong, M. C. Nelson, J. M. Olefsky, R. Boland, and R. M. Evans, “Effects of peroxisome proliferator-activated receptor delta on placentation, adiposity, and colorectal cancer,” *Proc. Natl. Acad. Sci. U.S.A.*, vol. 99, no. 1, pp. 303–308, Jan. 2002.

[77] J. M. Peters, S. S. Lee, W. Li, J. M. Ward, O. Gavrilova, C. Everett, M. L. Reitman, L. D. Hudson, and F. J. Gonzalez, “Growth, adipose, brain, and skin alterations resulting from targeted disruption of the mouse peroxisome proliferator-activated receptor beta(delta),” *Mol. Cell. Biol.*, vol. 20, no. 14, pp. 5119–5128, Jul. 2000.

[78] C.-H. Lee, A. Chawla, N. Urbiztondo, D. Liao, W. A. Boisvert, R. M. Evans, and L. K. Curtiss, “Transcriptional repression of atherogenic inflammation: modulation by PPARdelta,” *Science*, vol. 302, no. 5644, pp. 453–457, Oct. 2003.

[79] Y.-X. Wang, C.-L. Zhang, R. T. Yu, H. K. Cho, M. C. Nelson, C. R. Bayuga-Ocampo, J. Ham, H. Kang, and R. M. Evans, “Regulation of muscle fiber type and running endurance by PPARdelta,” *PLoS Biol.*, vol. 2, no. 10, p. e294, Oct. 2004.

[80] H. C. Chong, M. J. Tan, V. Philippe, S. H. Tan, C. K. Tan, C. W. Ku, Y. Y. Goh, W. Wahli, L. Michalik, and N. S. Tan, “Regulation of epithelial-mesenchymal IL-1 signaling by PPARbeta/delta is essential for skin homeostasis and wound healing,” *J. Cell Biol.*, vol. 184, no. 6, pp. 817–831, Mar. 2009.

[81] P. Tontonoz, E. Hu, and B. M. Spiegelman, “Stimulation of adipogenesis in fibroblasts by PPAR gamma 2, a lipid-activated transcription factor,” *Cell*, vol. 79, no. 7, pp. 1147–1156, Dec. 1994.

[82] P. Tontonoz and B. M. Spiegelman, “Fat and beyond: the diverse biology of PPARgamma,” *Annu. Rev. Biochem.*, vol. 77, pp. 289–312, 2008.

[83] E. D. Rosen, C.-H. Hsu, X. Wang, S. Sakai, M. W. Freeman, F. J. Gonzalez, and B. M. Spiegelman, “C/EBPalpha induces adipogenesis through PPARgamma: a unified pathway,” *Genes Dev.*, vol. 16, no. 1, pp. 22–26, Jan. 2002.

[84] J. K. Hamm, B. H. Park, and S. R. Farmer, “A role for C/EBPbeta in regulating peroxisome proliferator-activated receptor gamma activity during adipogenesis in 3T3-L1 preadipocytes,” *J. Biol. Chem.*, vol. 276, no. 21, pp. 18464–18471, May 2001.

[85] K. T. Uysal, S. M. Wiesbrock, M. W. Marino, and G. S. Hotamisligil, “Protection from obesity-induced insulin resistance in mice lacking TNF-alpha function,” *Nature*, vol. 389, no. 6651, pp. 610–614, Oct. 1997.

[86] C. M. Steppan, S. T. Bailey, S. Bhat, E. J. Brown, R. R. Banerjee, C. M. Wright, H. R. Patel, R. S. Ahima, and M. A. Lazar, “The hormone resistin links obesity to diabetes,” *Nature*, vol. 409, no. 6818, pp. 307–312, Jan. 2001.

[87] E. Hu, P. Liang, and B. M. Spiegelman, “AdipoQ is a novel adipose-specific gene dysregulated in obesity,” *J. Biol. Chem.*, vol. 271, no. 18, pp. 10697–10703, May 1996.

[88] Y. Barak, M. C. Nelson, E. S. Ong, Y. Z. Jones, P. Ruiz-Lozano, K. R. Chien, A. Koder, and R. M. Evans, “PPAR gamma is required for placental, cardiac, and adipose tissue development,” *Mol. Cell*, vol. 4, no. 4, pp. 585–595, Oct. 1999.

[89] A. L. Hevener, W. He, Y. Barak, J. Le, G. Bandyopadhyay, P. Olson, J. Wilkes, R. M. Evans, and J. Olefsky, “Muscle-specific Pparg deletion causes insulin resistance,” *Nat. Med.*, vol. 9, no. 12, pp. 1491–1497, Dec. 2003.

[90] N. Kubota, Y. Terauchi, H. Miki, H. Tamemoto, T. Yamauchi, K. Komeda, S. Satoh, R. Nakano, C. Ishii, T. Sugiyama, K. Eto, Y. Tsubamoto, A. Okuno, K. Murakami, H. Sekihara, G. Hasegawa, M. Naito, Y. Toyoshima, S. Tanaka, K. Shiota, T. Kitamura, T. Fujita, O. Ezaki, S. Aizawa, and T. Kadowaki, “PPAR gamma mediates high-fat diet-induced adipocyte hypertrophy and insulin resistance,” *Mol. Cell*, vol. 4, no. 4, pp. 597–609, Oct. 1999.

[91] I. Barroso, M. Gurnell, V. E. Crowley, M. Agostini, J. W. Schwabe, M. A. Soos, G. L. Maslen, T. D. Williams, H. Lewis, A. J. Schafer, V. K. Chatterjee, and S. O'Rahilly, "Dominant negative mutations in human PPARgamma associated with severe insulin resistance, diabetes mellitus and hypertension," *Nature*, vol. 402, no. 6764, pp. 880–883, Dec. 1999.

[92] L. Fajas, D. Auboeuf, E. Raspé, K. Schoonjans, A. M. Lefebvre, R. Saladin, J. Najib, M. Laville, J. C. Fruchart, S. Deeb, A. Vidal-Puig, J. Flier, M. R. Briggs, B. Staels, H. Vidal, and J. Auwerx, "The organization, promoter analysis, and expression of the human PPARgamma gene," *J. Biol. Chem.*, vol. 272, no. 30, pp. 18779–18789, Jul. 1997.

[93] J. I. Odegaard, R. R. Ricardo-Gonzalez, M. H. Goforth, C. R. Morel, V. Subramanian, L. Mukundan, A. Red Eagle, D. Vats, F. Brombacher, A. W. Ferrante, and A. Chawla, "Macrophage-specific PPARgamma controls alternative activation and improves insulin resistance," *Nature*, vol. 447, no. 7148, pp. 1116–1120, Jun. 2007.

[94] M. Ricote, A. C. Li, T. M. Willson, C. J. Kelly, and C. K. Glass, "The peroxisome proliferator-activated receptor-gamma is a negative regulator of macrophage activation," *Nature*, vol. 391, no. 6662, pp. 79–82, Jan. 1998.

[95] W. Wahli, P. R. Devchand, A. lJpenberg, and B. Desvergne, "Fatty acids, eicosanoids, and hypolipidemic agents regulate gene expression through direct binding to peroxisome proliferator-activated receptors," *Adv. Exp. Med. Biol.*, vol. 447, pp. 199–209, 1999.

[96] L. C. Bell-Parikh, T. Ide, J. A. Lawson, P. McNamara, M. Reilly, and G. A. FitzGerald, "Biosynthesis of 15-deoxy-delta12,14-PGJ2 and the ligation of PPARgamma," *J. Clin. Invest.*, vol. 112, no. 6, pp. 945–955, Sep. 2003.

[97] S. S. Davies, A. V. Pontsler, G. K. Marathe, K. A. Harrison, R. C. Murphy, J. C. Hinshaw, G. D. Prestwich, A. S. Hilaire, S. M. Prescott, G. A. Zimmerman, and T. M. McIntyre, "Oxidized alkyl phospholipids are specific, high affinity peroxisome proliferator-activated receptor gamma ligands and agonists," *J. Biol. Chem.*, vol. 276, no. 19, pp. 16015–16023, May 2001.

[98] T. Waku, T. Shiraki, T. Oyama, K. Maebara, R. Nakamori, and K. Morikawa, “The nuclear receptor PPARγ individually responds to serotonin- and fatty acid-metabolites,” *EMBO J.*, vol. 29, no. 19, pp. 3395–3407, Oct. 2010.

[99] I. Tzameli, H. Fang, M. Ollero, H. Shi, J. K. Hamm, P. Kievit, A. N. Hollenberg, and J. S. Flier, “Regulated production of a peroxisome proliferator-activated receptor-gamma ligand during an early phase of adipocyte differentiation in 3T3-L1 adipocytes,” *J. Biol. Chem.*, vol. 279, no. 34, pp. 36093–36102, Aug. 2004.

[100] K. J. Cheung, I. Tzameli, P. Pissios, I. Rovira, O. Gavrilova, T. Ohtsubo, Z. Chen, T. Finkel, J. S. Flier, and J. M. Friedman, “Xanthine oxidoreductase is a regulator of adipogenesis and PPARgamma activity,” *Cell Metab.*, vol. 5, no. 2, pp. 115–128, Feb. 2007.

[101] M. Schupp, M. I. Lefterova, J. Janke, K. Leitner, A. G. Cristancho, S. E. Mullican, M. Qatanani, N. Szwergold, D. J. Steger, J. C. Curtin, R. J. Kim, M.-J. Suh, M. Suh, M. R. Albert, S. Engeli, L. J. Gudas, and M. A. Lazar, “Retinol saturase promotes adipogenesis and is downregulated in obesity,” *Proc. Natl. Acad. Sci. U.S.A.*, vol. 106, no. 4, pp. 1105–1110, Jan. 2009.

[102] J. J. Nolan, B. Ludvik, P. Beerdsen, M. Joyce, and J. Olefsky, “Improvement in glucose tolerance and insulin resistance in obese subjects treated with troglitazone,” *N. Engl. J. Med.*, vol. 331, no. 18, pp. 1188–1193, Nov. 1994.

[103] J. Berger, P. Bailey, C. Biswas, C. A. Cullinan, T. W. Doebber, N. S. Hayes, R. Saperstein, R. G. Smith, and M. D. Leibowitz, “Thiazolidinediones produce a conformational change in peroxisomal proliferator-activated receptor-gamma: binding and activation correlate with antidiabetic actions in db/db mice,” *Endocrinology*, vol. 137, no. 10, pp. 4189–4195, Oct. 1996.

[104] E. J. Murphy, T. J. Davern, A. O. Shakil, L. Shick, U. Masharani, H. Chow, C. Freise, W. M. Lee, and N. M. Bass, “Troglitazone-induced fulminant hepatic failure. Acute Liver Failure Study Group,” *Dig. Dis. Sci.*, vol. 45, no. 3, pp. 549–553, Mar. 2000.

[105] R. S. Savkur and A. R. Miller, “Investigational PPAR-gamma agonists for the treatment of Type 2 diabetes,” *Expert Opin Investig Drugs*, vol. 15, no. 7, pp. 763–778, Jul. 2006.

[106] Y. Guan, C. Hao, D. R. Cha, R. Rao, W. Lu, D. E. Kohan, M. A. Magnuson, R. Redha, Y. Zhang, and M. D. Breyer, “Thiazolidinediones expand body fluid volume through PPARgamma stimulation of ENaC-mediated renal salt absorption,” *Nat. Med.*, vol. 11, no. 8, pp. 861–866, Aug. 2005.

[107] S. E. Nissen and K. Wolski, “Effect of rosiglitazone on the risk of myocardial infarction and death from cardiovascular causes,” *N. Engl. J. Med.*, vol. 356, no. 24, pp. 2457–2471, Jun. 2007.

[108] L. Pei and P. Tontonoz, “Fat’s loss is bone’s gain,” *J. Clin. Invest.*, vol. 113, no. 6, pp. 805–806, Mar. 2004.

[109] J. D. Lewis, A. Ferrara, T. Peng, M. Hedderson, W. B. Bilker, C. P. Quesenberry Jr, D. J. Vaughn, L. Nessel, J. Selby, and B. L. Strom, “Risk of bladder cancer among diabetic patients treated with pioglitazone: interim report of a longitudinal cohort study,” *Diabetes Care*, vol. 34, no. 4, pp. 916–922, Apr. 2011.

[110] B. R. Henke, S. G. Blanchard, M. F. Brackeen, K. K. Brown, J. E. Cobb, J. L. Collins, W. W. Harrington Jr, M. A. Hashim, E. A. Hull-Ryde, I. Kaldor, S. A. Kliewer, D. H. Lake, L. M. Leesnitzer, J. M. Lehmann, J. M. Lenhard, L. A. Orband-Miller, J. F. Miller, R. A. Mook Jr, S. A. Noble, W. Oliver Jr, D. J. Parks, K. D. Plunket, J. R. Szewczyk, and T. M. Willson, “N-(2-Benzoylphenyl)-L-tyrosine PPARgamma agonists. 1. Discovery of a novel series of potent antihyperglycemic and antihyperlipidemic agents,” *J. Med. Chem.*, vol. 41, no. 25, pp. 5020–5036, Dec. 1998.

[111] S. Rocchi, F. Picard, J. Vamecq, L. Gelman, N. Potier, D. Zeyer, L. Dubuquoy, P. Bac, M. F. Champy, K. D. Plunket, L. M. Leesnitzer, S. G. Blanchard, P. Desreumaux, D. Moras, J. P. Renaud, and J. Auwerx, “A unique PPARgamma ligand with potent insulin-sensitizing yet weak adipogenic activity,” *Mol. Cell*, vol. 8, no. 4, pp. 737–747, Oct. 2001.

[112] J. M. Lehmann, J. M. Lenhard, B. B. Oliver, G. M. Ringold, and S. A. Kliewer, “Peroxisome proliferator-activated receptors alpha and gamma are activated by indomethacin and other non-steroidal anti-inflammatory drugs,” *J. Biol. Chem.*, vol. 272, no. 6, pp. 3406–3410, Feb. 1997.

[113] C. Knouff and J. Auwerx, “Peroxisome proliferator-activated receptor-gamma calls for activation in moderation: lessons from genetics and pharmacology,” *Endocr. Rev.*, vol. 25, no. 6, pp. 899–918, Dec. 2004.
[114] P. D. Miles, Y. Barak, W. He, R. M. Evans, and J. M. Olefsky, “Improved insulin-sensitivity in mice heterozygous for PPAR-gamma deficiency,” *J. Clin. Invest.*, vol. 105, no. 3, pp. 287–292, Feb. 2000.
[115] L. S. Higgins and A. M. Depaoli, “Selective peroxisome proliferator-activated receptor gamma (PPARgamma) modulation as a strategy for safer therapeutic PPARgamma activation,” *Am. J. Clin. Nutr.*, vol. 91, no. 1, p. 267S–272S, Jan. 2010.
[116] J. S. Lewis and V. C. Jordan, “Selective estrogen receptor modulators (SERMs): mechanisms of anticarcinogenesis and drug resistance,” *Mutat. Res.*, vol. 591, no. 1–2, pp. 247–263, Dec. 2005.
[117] H. Gronemeyer, J.-A. Gustafsson, and V. Laudet, “Principles for modulation of the nuclear receptor superfamily,” *Nat Rev Drug Discov*, vol. 3, no. 11, pp. 950–964, Nov. 2004.
[118] C. L. Smith and B. W. O’Malley, “Coregulator function: a key to understanding tissue specificity of selective receptor modulators,” *Endocr. Rev.*, vol. 25, no. 1, pp. 45–71, Feb. 2004.
[119] L. S. Higgins and C. S. Mantzoros, “The Development of INT131 as a Selective PPARgamma Modulator: Approach to a Safer Insulin Sensitizer,” *PPAR Res*, vol. 2008, p. 936906, 2008.
[120] T. Allen, F. Zhang, S. A. Moodie, L. E. Clemens, A. Smith, F. Gregoire, A. Bell, G. E. O. Muscat, and T. A. Gustafson, “Halofenate is a selective peroxisome proliferator-activated receptor gamma modulator with antidiabetic activity,” *Diabetes*, vol. 55, no. 9, pp. 2523–2533, Sep. 2006.
[121] L. H. Krut, H. C. Seftel, and B. I. Joffe, “Comparison of clofibrate with halofenate in diabetics with hyperlipidaemia,” *S. Afr. Med. J.*, vol. 51, no. 11, pp. 348–352, Mar. 1977.
[122] D. J. Kudzma and S. J. Friedberg, “Potentiation of hypoglycemic effect of chlorpropamide and phenfromin by halofenate,” *Diabetes*, vol. 26, no. 4, pp. 291–295, Apr. 1977.

[123] F. M. Gregoire, F. Zhang, H. J. Clarke, T. A. Gustafson, D. D. Sears, S. Favelyukis, J. Lenhard, D. Rentzeperis, L. E. Clemens, Y. Mu, and B. E. Lavan, “MBX-102/JNJ39659100, a novel peroxisome proliferator-activated receptor-ligand with weak transactivation activity retains antidiabetic properties in the absence of weight gain and edema,” *Mol. Endocrinol.*, vol. 23, no. 7, pp. 975–988, Jul. 2009.

[124] T. Fujimura, H. Sakuma, S. Konishi, T. Oe, N. Hosogai, C. Kimura, I. Aramori, and S. Mutoh, “FK614, a novel peroxisome proliferator-activated receptor gamma modulator, induces differential transactivation through a unique ligand-specific interaction with transcriptional coactivators,” *J. Pharmacol. Sci.*, vol. 99, no. 4, pp. 342–352, Dec. 2005.

[125] T. Fujimura, H. Sakuma, A. Ohkubo-Suzuki, I. Aramori, and S. Mutoh, “Unique properties of coactivator recruitment caused by differential binding of FK614, an anti-diabetic agent, to peroxisome proliferator-activated receptor gamma,” *Biol. Pharm. Bull.*, vol. 29, no. 3, pp. 423–429, Mar. 2006.

[126] H. Minoura, S. Takeshita, C. Kimura, J. Hirosumi, S. Takakura, I. Kawamura, J. Seki, T. Manda, and S. Mutoh, “Mechanism by which a novel non-thiazolidinedione peroxisome proliferator-activated receptor gamma agonist, FK614, ameliorates insulin resistance in Zucker fatty rats,” *Diabetes Obes Metab*, vol. 9, no. 3, pp. 369–378, May 2007.

[127] F. Zhang, B. E. Lavan, and F. M. Gregoire, “Selective Modulators of PPAR-gamma Activity: Molecular Aspects Related to Obesity and Side-Effects,” *PPAR Res*, vol. 2007, p. 32696, 2007.

[128] S. C. Benson, H. A. Pershadsingh, C. I. Ho, A. Chittiboyina, P. Desai, M. Pravenec, N. Qi, J. Wang, M. A. Avery, and T. W. Kurtz, “Identification of telmisartan as a unique angiotensin II receptor antagonist with selective PPARgamma-modulating activity,” *Hypertension*, vol. 43, no. 5, pp. 993–1002, May 2004.

[129] K. J. McClellan and A. Markham, “Telmisartan,” *Drugs*, vol. 56, no. 6, pp. 1039–1044; discussion 1045–1046, Dec. 1998.

[130] M. Schupp, J. Janke, R. Clasen, T. Unger, and U. Kintscher, “Angiotensin type 1 receptor blockers induce peroxisome proliferator-activated receptor-gamma activity,” *Circulation*, vol. 109, no. 17, pp. 2054–2057, May 2004.

[131] M. C. Michel, H. Bohner, J. Köster, R. Schäfers, and U. Heemann, “Safety of telmisartan in patients with arterial hypertension : an open-label observational study,” *Drug Saf*, vol. 27, no. 5, pp. 335–344, 2004.
[132] C. Vitale, G. Mercuro, C. Castiglioni, A. Cornoldi, A. Tulli, M. Fini, M. Volterrani, and G. M. C. Rosano, “Metabolic effect of telmisartan and losartan in hypertensive patients with metabolic syndrome,” *Cardiovasc Diabetol*, vol. 4, p. 6, May 2005.
[133] M. Goebel, M. Clemenz, B. Staels, T. Unger, U. Kintscher, and R. Gust, “Characterization of new PPARgamma agonists: analysis of telmisartan’s structural components,” *ChemMedChem*, vol. 4, no. 3, pp. 445–456, Mar. 2009.
[134] M. Goebel, B. Staels, T. Unger, U. Kintscher, and R. Gust, “Characterization of new PPARgamma agonists: benzimidazole derivatives - the importance of position 2,” *ChemMedChem*, vol. 4, no. 7, pp. 1136–1142, Jul. 2009.
[135] M. Goebel, G. Wolber, P. Markt, B. Staels, T. Unger, U. Kintscher, and R. Gust, “Characterization of new PPARgamma agonists: benzimidazole derivatives-importance of positions 5 and 6, and computational studies on the binding mode,” *Bioorg. Med. Chem.*, vol. 18, no. 16, pp. 5885–5895, Aug. 2010.
[136] “LanthaScreen_PPARGamma_coactivator_man.pdf.” .
[137] J.-H. Zhang, T. D. Y. Chung, and K. R. Oldenburg, “A Simple Statistical Parameter for Use in Evaluation and Validation of High Throughput Screening Assays,” *Journal of Biomolecular Screening*, vol. 4, no. 2, pp. 67 –73, Apr. 1999.
[138] “Direct Hybridization Assay – Multiple hybridization from a single reaction.” [Online]. Available: http://www.illumina.com/technology/direct_hybridization_assay.ilmn. [Accessed: 22-Jan-2012].
[139] Y. Hochberg and Y. Benjamini, “More powerful procedures for multiple significance testing,” *Stat Med*, vol. 9, no. 7, pp. 811–818, Jul. 1990.
[140] M. B. Eisen, P. T. Spellman, P. O. Brown, and D. Botstein, “Cluster analysis and display of genome-wide expression patterns,” *Proc. Natl. Acad. Sci. U.S.A.*, vol. 95, no. 25, pp. 14863–14868, Dec. 1998.
[141] H. Green and O. Kehinde, “An established preadipose cell line and its differentiation in culture. II. Factors affecting the adipose conversion,” *Cell*, vol. 5, no. 1, pp. 19–27, May 1975.

[142] J. L. Ramírez-Zacarías, F. Castro-Muñozledo, and W. Kuri-Harcuch, “Quantitation of adipose conversion and triglycerides by staining intracytoplasmic lipids with Oil red O,” *Histochemistry*, vol. 97, no. 6, pp. 493–497, Jul. 1992.

[143] B. M. Spiegelman, E. Hu, J. B. Kim, and R. Brun, “PPAR gamma and the control of adipogenesis,” *Biochimie*, vol. 79, no. 2–3, pp. 111–112, Mar. 1997.

[144] H. Kubinyi, “Lipophilicity and drug activity,” *Prog Drug Res*, vol. 23, pp. 97–198, 1979.

[145] M. P. Edwards and D. A. Price, “Chapter 23 - Role of Physicochemical Properties and Ligand Lipophilicity Efficiency in Addressing Drug Safety Risks,” in *Annual Reports in Medicinal Chemistry*, vol. Volume 45, Academic Press, 2010, pp. 380–391.

[146] S. A. Oñate, S. Y. Tsai, M. J. Tsai, and B. W. O’Malley, “Sequence and characterization of a coactivator for the steroid hormone receptor superfamily,” *Science*, vol. 270, no. 5240, pp. 1354–1357, Nov. 1995.

[147] P. Puigserver, G. Adelmant, Z. Wu, M. Fan, J. Xu, B. O’Malley, and B. M. Spiegelman, “Activation of PPARγ Coactivator-1 Through Transcription Factor Docking,” *Science*, vol. 286, no. 5443, pp. 1368–1371, Nov. 1999.

[148] S. Malik and R. G. Roeder, “Dynamic regulation of pol II transcription by the mammalian Mediator complex,” *Trends Biochem. Sci.*, vol. 30, no. 5, pp. 256–263, May 2005.

[149] A. Chawla, E. J. Schwarz, D. D. Dimaculangan, and M. A. Lazar, “Peroxisome proliferator-activated receptor (PPAR) gamma: adipose-predominant expression and induction early in adipocyte differentiation,” *Endocrinology*, vol. 135, no. 2, pp. 798–800, Aug. 1994.

[150] S. Hauser, G. Adelmant, P. Sarraf, H. M. Wright, E. Mueller, and B. M. Spiegelman, “Degradation of the peroxisome proliferator-activated receptor gamma is linked to ligand-dependent activation,” *J. Biol. Chem.*, vol. 275, no. 24, pp. 18527–18533, Jun. 2000.

[151] M. Schupp, M. Clemenz, R. Gineste, H. Witt, J. Janke, S. Helleboid, N. Hennuyer, P. Ruiz, T. Unger, B. Staels, and U. Kintscher, “Molecular characterization of new selective peroxisome proliferator-activated receptor gamma modulators with angiotensin receptor blocking activity,” *Diabetes*, vol. 54, no. 12, pp. 3442–3452, Dec. 2005.

[152] M. Furuhashi, G. Tuncman, C. Z. Görgün, L. Makowski, G. Atsumi, E. Vaillancourt, K. Kono, V. R. Babaev, S. Fazio, M. F. Linton, R. Sulsky, J. A. Robl, R. A. Parker, and G. S. Hotamisligil, “Treatment of diabetes and atherosclerosis by inhibiting fatty-acid-binding protein aP2,” *Nature*, vol. 447, no. 7147, pp. 959–965, Jun. 2007.

[153] J. J. Díez and P. Iglesias, “The role of the novel adipocyte-derived hormone adiponectin in human disease,” *Eur. J. Endocrinol*, vol. 148, no. 3, pp. 293–300, Mar. 2003.

[154] Y. Matsuzawa, T. Funahashi, S. Kihara, and I. Shimomura, “Adiponectin and metabolic syndrome,” *Arterioscler. Thromb. Vasc. Biol.*, vol. 24, no. 1, pp. 29–33, Jan. 2004.

[155] M. A. Lazar, “Resistin- and Obesity-associated metabolic diseases,” *Horm. Metab. Res.*, vol. 39, no. 10, pp. 710–716, Oct. 2007.

[156] T. Hajri, X. X. Han, A. Bonen, and N. A. Abumrad, “Defective fatty acid uptake modulates insulin responsiveness and metabolic responses to diet in CD36-null mice,” *J. Clin. Invest.*, vol. 109, no. 10, pp. 1381–1389, May 2002.

[157] M. Pravenec, V. Landa, V. Zídek, A. Musilová, L. Kazdová, N. Qi, J. Wang, E. St Lezin, and T. W. Kurtz, “Transgenic expression of CD36 in the spontaneously hypertensive rat is associated with amelioration of metabolic disturbances but has no effect on hypertension,” *Physiol Res*, vol. 52, no. 6, pp. 681–688, 2003.

[158] A. H. Khan and J. E. Pessin, “Insulin regulation of glucose uptake: a complex interplay of intracellular signalling pathways,” *Diabetologia*, vol. 45, no. 11, pp. 1475–1483, Nov. 2002.

[159] J. M. Muretta and C. C. Mastick, “How insulin regulates glucose transport in adipocytes,” *Vitam. Horm.*, vol. 80, pp. 245–286, 2009.

[160] S. Yusuf, K. K. Teo, J. Pogue, L. Dyal, I. Copland, H. Schumacher, G. Dagenais, P. Sleight, and C. Anderson, “Telmisartan, ramipril, or both in patients at high risk for vascular events,” *N. Engl. J. Med.*, vol. 358, no. 15, pp. 1547–1559, Apr. 2008.
[161] H. E. Xu, M. H. Lambert, V. G. Montana, D. J. Parks, S. G. Blanchard, P. J. Brown, D. D. Sternbach, J. M. Lehmann, G. B. Wisely, T. M. Willson, S. A. Kliewer, and M. V. Milburn, “Molecular recognition of fatty acids by peroxisome proliferator-activated receptors,” *Mol. Cell*, vol. 3, no. 3, pp. 397–403, Mar. 1999.
[162] J. B. Bruning, M. J. Chalmers, S. Prasad, S. A. Busby, T. M. Kamenecka, Y. He, K. W. Nettles, and P. R. Griffin, “Partial agonists activate PPARgamma using a helix 12 independent mechanism,” *Structure*, vol. 15, no. 10, pp. 1258–1271, Oct. 2007.
[163] R. T. Nolte, G. B. Wisely, S. Westin, J. E. Cobb, M. H. Lambert, R. Kurokawa, M. G. Rosenfeld, T. M. Willson, C. K. Glass, and M. V. Milburn, “Ligand binding and co-activator assembly of the peroxisome proliferator-activated receptor-gamma,” *Nature*, vol. 395, no. 6698, pp. 137–143, Sep. 1998.
[164] T. S. Hughes, M. J. Chalmers, S. Novick, D. S. Kuruvilla, M. R. Chang, T. M. Kamenecka, M. Rance, B. A. Johnson, T. P. Burris, P. R. Griffin, and D. J. Kojetin, “Ligand and receptor dynamics contribute to the mechanism of graded PPARγ agonism,” *Structure*, vol. 20, no. 1, pp. 139–150, Jan. 2012.
[165] Y. Amano, T. Yamaguchi, K. Ohno, T. Niimi, M. Orita, H. Sakashita, and M. Takeuchi, “Structural basis for telmisartan-mediated partial activation of PPAR gamma,” *Hypertension Research: Official Journal of the Japanese Society of Hypertension*, Feb. 2012.
[166] W. H. Li, M. Tanimura, C. C. Luo, S. Datta, and L. Chan, “The apolipoprotein multigene family: biosynthesis, structure, structure-function relationships, and evolution,” *J. Lipid Res.*, vol. 29, no. 3, pp. 245–271, Mar. 1988.
[167] C. M. Allan, D. Walker, J. P. Segrest, and J. M. Taylor, “Identification and characterization of a new human gene (APOC4) in the apolipoprotein E, C-I, and C-II gene locus,” *Genomics*, vol. 28, no. 2, pp. 291–300, Jul. 1995.

[168] C. O. Mendivil, C. Zheng, J. Furtado, J. Lel, and F. M. Sacks, “Metabolism of Very-Low-Density Lipoprotein and Low-Density Lipoprotein Containing Apolipoprotein C-III and Not Other Small Apolipoproteins,” *Arteriosclerosis, Thrombosis, and Vascular Biology*, vol. 30, no. 2, pp. 239–245, Feb. 2010.

[169] T. I. Pollin, C. M. Damcott, H. Shen, S. H. Ott, J. Shelton, R. B. Horenstein, W. Post, J. C. McLenithan, L. F. Bielak, P. A. Peyser, B. D. Mitchell, M. Miller, J. R. O’Connell, and A. R. Shuldiner, “A null mutation in human APOC3 confers a favorable plasma lipid profile and apparent cardioprotection,” *Science*, vol. 322, no. 5908, pp. 1702–1705, Dec. 2008.

[170] J. E. Levy, O. Jin, Y. Fujiwara, F. Kuo, and N. C. Andrews, “Transferrin receptor is necessary for development of erythrocytes and the nervous system,” *Nat. Genet.*, vol. 21, no. 4, pp. 396–399, Apr. 1999.

[171] K. Ishii, T. Fumoto, K. Iwai, S. Takeshita, M. Ito, N. Shimohata, H. Aburatani, S. Taketani, C. J. Lelliott, A. Vidal-Puig, and K. Ikeda, “Coordination of PGC-1beta and iron uptake in mitochondrial biogenesis and osteoclast activation,” *Nat. Med.*, vol. 15, no. 3, pp. 259–266, Mar. 2009.

[172] E. Le Poul, C. Loison, S. Struyf, J.-Y. Springael, V. Lannoy, M.-E. Decobecq, S. Brezillon, V. Dupriez, G. Vassart, J. Van Damme, M. Parmentier, and M. Detheux, “Functional characterization of human receptors for short chain fatty acids and their role in polymorphonuclear cell activation,” *J. Biol. Chem.*, vol. 278, no. 28, pp. 25481–25489, Jul. 2003.

[173] H. Liang and W. F. Ward, “PGC-1α: a key regulator of energy metabolism,” *Advances in Physiology Education*, vol. 30, no. 4, pp. 145–151, Dec. 2006.

[174] D. L. Silver, N. Wang, and S. Vogel, “Identification of small PDZK1-associated protein, DD96/MAP17, as a regulator of PDZK1 and plasma high density lipoprotein levels,” *J. Biol. Chem.*, vol. 278, no. 31, pp. 28528–28532, Aug. 2003.

[175] A. Gerdin, “The Sanger Mouse Genetics Programme: high throughput characterisation of knockout mice,” *Acta Ophthalmologica*, vol. 88, p. 0–0, Sep. 2010.

[176] A. Klip and M. R. Pâquet, “Glucose transport and glucose transporters in muscle and their metabolic regulation,” *Diabetes Care*, vol. 13, no. 3, pp. 228–243, Mar. 1990.

[177] J. P. Berger, T. E. Akiyama, and P. T. Meinke, “PPARs: therapeutic targets for metabolic disease,” *Trends Pharmacol. Sci.*, vol. 26, no. 5, pp. 244–251, May 2005.
[178] R. W. Nesto, D. Bell, R. O. Bonow, V. Fonseca, S. M. Grundy, E. S. Horton, M. Le Winter, D. Porte, C. F. Semenkovich, S. Smith, L. H. Young, and R. Kahn, “Thiazolidinedione use, fluid retention, and congestive heart failure: a consensus statement from the American Heart Association and American Diabetes Association,” *Diabetes Care*, vol. 27, no. 1, pp. 256–263, Jan. 2004.
[179] K. Henriksen, I. Byrjalsen, P. Qvist, H. Beck-Nielsen, G. Hansen, B. J. Riis, H. Perrild, O. L. Svendsen, J. Gram, M. A. Karsdal, and C. Christiansen, “Efficacy and safety of the PPARγ partial agonist balaglitazone compared with pioglitazone and placebo: a phase III, randomized, parallel-group study in patients with type 2 diabetes on stable insulin therapy,” *Diabetes Metab. Res. Rev.*, vol. 27, no. 4, pp. 392–401, May 2011.
[180] F. L. Dunn, L. S. Higgins, J. Fredrickson, and A. M. DePaoli, “Selective modulation of PPARγ activity can lower plasma glucose without typical thiazolidinedione side-effects in patients with Type 2 diabetes,” *J. Diabetes Complicat.*, vol. 25, no. 3, pp. 151–158, Jun. 2011.
[181] E. D. Rosen and B. M. Spiegelman, “Adipocytes as regulators of energy balance and glucose homeostasis,” *Nature*, vol. 444, no. 7121, pp. 847–853, Dec. 2006.
[182] Y. Guan, C. Hao, D. R. Cha, R. Rao, W. Lu, D. E. Kohan, M. A. Magnuson, R. Redha, Y. Zhang, and M. D. Breyer, “Thiazolidinediones expand body fluid volume through PPARgamma stimulation of ENaC-mediated renal salt absorption,” *Nat. Med.*, vol. 11, no. 8, pp. 861–866, Aug. 2005.
[183] T. S. Pavlov, J. D. Imig, and A. Staruschenko, “Regulation of ENaC-Mediated Sodium Reabsorption by Peroxisome Proliferator-Activated Receptors,” *PPAR Res*, vol. 2010, p. 703735, 2010.
[184] S. Moreno, S. Farioli-Vecchioli, and M. P. Cerù, “Immunolocalization of peroxisome proliferator-activated receptors and retinoid X receptors in the adult rat CNS,” *Neuroscience*, vol. 123, no. 1, pp. 131–145, 2004.

[185] D. A. Sarruf, F. Yu, H. T. Nguyen, D. L. Williams, R. L. Printz, K. D. Niswender, and M. W. Schwartz, “Expression of peroxisome proliferator-activated receptor-gamma in key neuronal subsets regulating glucose metabolism and energy homeostasis,” *Endocrinology*, vol. 150, no. 2, pp. 707–712, Feb. 2009.

[186] M. Lu, D. A. Sarruf, S. Talukdar, S. Sharma, P. Li, G. Bandyopadhyay, S. Nalbandian, W. Fan, J. R. Gayen, S. K. Mahata, N. J. Webster, M. W. Schwartz, and J. M. Olefsky, “Brain PPAR-γ promotes obesity and is required for the insulin-sensitizing effect of thiazolidinediones,” *Nat. Med.*, vol. 17, no. 5, pp. 618–622, May 2011.

[187] K. K. Ryan, B. Li, B. E. Grayson, E. K. Matter, S. C. Woods, and R. J. Seeley, “A role for central nervous system PPAR-γ in the regulation of energy balance,” *Nat. Med.*, vol. 17, no. 5, pp. 623–626, May 2011.

[188] J. H. Choi, A. S. Banks, J. L. Estall, S. Kajimura, P. Boström, D. Laznik, J. L. Ruas, M. J. Chalmers, T. M. Kamenecka, M. Blüher, P. R. Griffin, and B. M. Spiegelman, “Anti-diabetic drugs inhibit obesity-linked phosphorylation of PPARgamma by Cdk5,” *Nature*, vol. 466, no. 7305, pp. 451–456, Jul. 2010.

[189] J. H. Choi, A. S. Banks, T. M. Kamenecka, S. A. Busby, M. J. Chalmers, N. Kumar, D. S. Kuruvilla, Y. Shin, Y. He, J. B. Bruning, D. P. Marciano, M. D. Cameron, D. Laznik, M. J. Jurczak, S. C. Schürer, D. Vidović, G. I. Shulman, B. M. Spiegelman, and P. R. Griffin, “Antidiabetic actions of a non-agonist PPARγ ligand blocking Cdk5-mediated phosphorylation,” *Nature*, vol. 477, no. 7365, pp. 477–481, Sep. 2011.

[190] Y. Lamotte, P. Martres, N. Faucher, A. Laroze, D. Grillot, N. Ancellin, Y. Saintillan, V. Beneton, and R. T. Gampe Jr, “Synthesis and biological activities of novel indole derivatives as potent and selective PPARgamma modulators,” *Bioorg. Med. Chem. Lett.*, vol. 20, no. 4, pp. 1399–1404, Feb. 2010.

[191] K. J. McClellan and A. Markham, “Telmisartan,” *Drugs*, vol. 56, no. 6, pp. 1039–1044; discussion 1045–1046, Dec. 1998.

[192] C. Vitale, G. Mercuro, C. Castiglioni, A. Cornoldi, A. Tulli, M. Fini, M. Volterrani, and G. M. C. Rosano, “Metabolic effect of telmisartan and losartan in hypertensive patients with metabolic syndrome,” *Cardiovasc Diabetol*, vol. 4, p. 6, May 2005.

[193] I.-N. Bähr, P. Tretter, J. Krüger, R. G. Stark, J. Schimkus, T. Unger, K. Kappert, J. Scholze, K. G. Parhofer, and U. Kintscher, “High-dose treatment with telmisartan induces monocytic peroxisome proliferator-activated receptor-γ target genes in patients with the metabolic syndrome,” *Hypertension*, vol. 58, no. 4, pp. 725–732, Oct. 2011.

[194] A. Casimiro-Garcia, G. F. Filzen, D. Flynn, C. F. Bigge, J. Chen, J. A. Davis, D. A. Dudley, J. J. Edmunds, N. Esmaeil, A. Geyer, R. J. Heemstra, M. Jalaie, J. F. Ohren, R. Ostroski, T. Ellis, R. P. Schaum, and C. Stoner, “Discovery of a series of imidazo[4,5-b]pyridines with dual activity at angiotensin II type 1 receptor and peroxisome proliferator-activated receptor-γ,” *J. Med. Chem.*, vol. 54, no. 12, pp. 4219–4233, Jun. 2011.

[195] S. Takai, D. Jin, M. Kimura, K. Kirimura, H. Sakonjo, K. Tanaka, and M. Miyazaki, “Inhibition of vascular angiotensin-converting enzyme by telmisartan via the peroxisome proliferator-activated receptor gamma agonistic property in rats,” *Hypertens. Res.*, vol. 30, no. 12, pp. 1231–1237, Dec. 2007.

[196] K. Takeda, T. Ichiki, T. Tokunou, Y. Funakoshi, N. Iino, K. Hirano, H. Kanaide, and A. Takeshita, “Peroxisome proliferator-activated receptor gamma activators downregulate angiotensin II type 1 receptor in vascular smooth muscle cells,” *Circulation*, vol. 102, no. 15, pp. 1834–1839, Oct. 2000.

[197] I. Imayama, T. Ichiki, K. Inanaga, H. Ohtsubo, K. Fukuyama, H. Ono, Y. Hashiguchi, and K. Sunagawa, “Telmisartan downregulates angiotensin II type 1 receptor through activation of peroxisome proliferator-activated receptor gamma,” *Cardiovasc. Res.*, vol. 72, no. 1, pp. 184–190, Oct. 2006.

[198] J. S. Welch, M. Ricote, T. E. Akiyama, F. J. Gonzalez, and C. K. Glass, “PPARgamma and PPARdelta negatively regulate specific subsets of lipopolysaccharide and IFN-gamma target genes in macrophages,” *Proc. Natl. Acad. Sci. U.S.A.*, vol. 100, no. 11, pp. 6712–6717, May 2003.

[199] R. Genolet, W. Wahli, and L. Michalik, “PPARs as drug targets to modulate inflammatory responses?,” *Curr Drug Targets Inflamm Allergy*, vol. 3, no. 4, pp. 361–375, Dec. 2004.

[200] M. Ricote, A. C. Li, T. M. Willson, C. J. Kelly, and C. K. Glass, “The peroxisome proliferator-activated receptor-gamma is a negative regulator of macrophage activation,” *Nature*, vol. 391, no. 6662, pp. 79–82, Jan. 1998.

[201] R. Luna-Medina, M. Cortes-Canteli, M. Alonso, A. Santos, A. Martínez, and A. Perez-Castillo, “Regulation of inflammatory response in neural cells in vitro by thiadiazolidinones derivatives through peroxisome proliferator-activated receptor gamma activation,” *J. Biol. Chem.*, vol. 280, no. 22, pp. 21453–21462, Jun. 2005.

[202] E. Mueller, P. Sarraf, P. Tontonoz, R. M. Evans, K. J. Martin, M. Zhang, C. Fletcher, S. Singer, and B. M. Spiegelman, “Terminal differentiation of human breast cancer through PPAR gamma,” *Mol. Cell*, vol. 1, no. 3, pp. 465–470, Feb. 1998.

[203] E. Mueller, M. Smith, P. Sarraf, T. Kroll, A. Aiyer, D. S. Kaufman, W. Oh, G. Demetri, W. D. Figg, X. P. Zhou, C. Eng, B. M. Spiegelman, and P. W. Kantoff, “Effects of ligand activation of peroxisome proliferator-activated receptor gamma in human prostate cancer,” *Proc. Natl. Acad. Sci. U.S.A.*, vol. 97, no. 20, pp. 10990–10995, Sep. 2000.

[204] G. Vitale, S. Zappavigna, M. Marra, A. Dicitore, S. Meschini, M. Condello, G. Arancia, S. Castiglioni, P. Maroni, P. Bendinelli, R. Piccoletti, P. M. van Koetsveld, F. Cavagnini, A. Budillon, A. Abbruzzese, L. J. Hofland, and M. Caraglia, “The PPAR-γ agonist troglitazone antagonizes survival pathways induced by STAT-3 in recombinant interferon-β treated pancreatic cancer cells,” *Biotechnol. Adv.*, vol. 30, no. 1, pp. 169–184, Jan. 2012.

Appendix A - List of publications and poster presentations

Publication:

Herbst L, Goebel M, Bandholtz S, Gust R, Kintscher U. Telmisartan-derived new PPARγ agonists with modifications at position 5 and 6 of the Central 1-(biphenyl-4-ylmethyl)-1H-benzimidazole structure act like selective PPARγ modulators. 2012, submitted to ChemMedChem

Poster:

Herbst L, Goebel M, Bandholtz S, Gust R, Kintscher U. Benzimidazole-derived new PPARgamma agonists act like selective modulators. 77. Jahrestagung der Deutschen Gesellschaft für Experimentelle und Klinische Pharmakologie und Toxikologie; Frankfurt; 2011

Herbst L, Goebel M, Bandholtz S, Gust R, Kintscher U. Benzimidazole-derived new PPARgamma agonists act like selective modulators. Spetses Summer School on Nuclear Receptor Signalling in Physiology and Disease; Greece; 2011

Herbst L, Goebel M, Bandholtz S, Gust R, Kintscher U. Benzimidazole-derived new PPARgamma agonists act like selective modulators. 35. Wissenschaftlicher Kongress der Deutschen Hochdruckliga e.V. DHL® - Deutschen Gesellschaft für Hypertonie und Prävention; Köln; 2011

Appendix B - Acknowledgment

In the first place I would like to record my gratitude to Prof. Dr. Ulrich Kintscher for his supervision, advice and guidance, and for providing me the chance to go to Houston.

My further gratitude goes to Prof. Dr. Matthias Melzig for his willingness to be my doctoral advisor.

Furthermore, I like to express my thanks to the Tumortargeting group – Charité Virchow Klinikum for providing me access to the EnVision Plate Reader for TR-FRET measurements. And I like to thank the group of Prof. Hübner – MDC/ Berlin-Buch for assistance with the microarray, especially Gabi Born for hybridization of my samples.

I like to say a special “thank you” to Dr. Michael Schupp for many constructive discussions and stimulating ideas. I appreciate all his advice for my personal growth as a scientist.

I thank Daniela and Jenny for all kind of assistance during the progression of this thesis.

Mein groesster Dank geht an meine Familie für unendliche Unterstützung! In aller Liebe.